Advanced Thermo-Structural Materials Summer School
International Center for Materials Research
University of California, Santa Barbara; August 17th, 2006

Interface Compatibility Issues in SOFCs

Degradation Modes and Materials Design

Daniel R. Mumm

Chemical Engineering and Materials Science
National Fuel Cell Research Center
Henry Samueli School of Engineering
University of California, Irvine
mumm@uci.edu

Solid Oxide Fuel Cells – Overview

Drivers for SOFC Technology

Requirements of Constituents

Materials Basis of Performance

Degradation - Time Domain

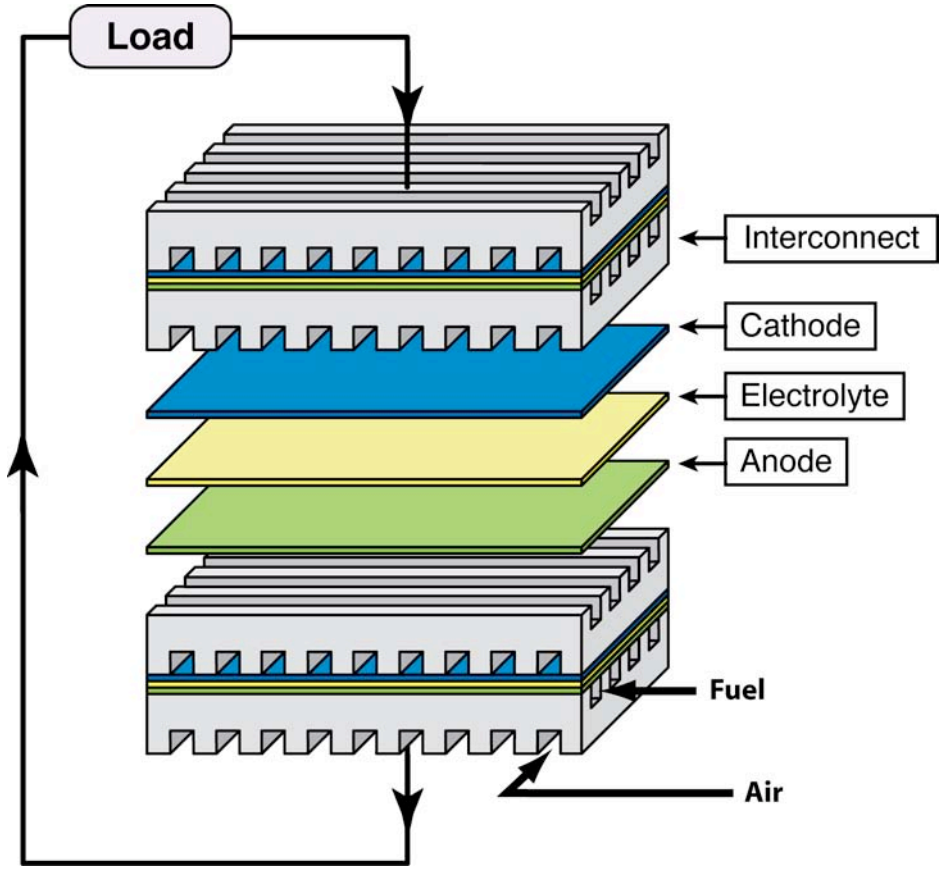

Current Electricity Production - 'Unsustainable'

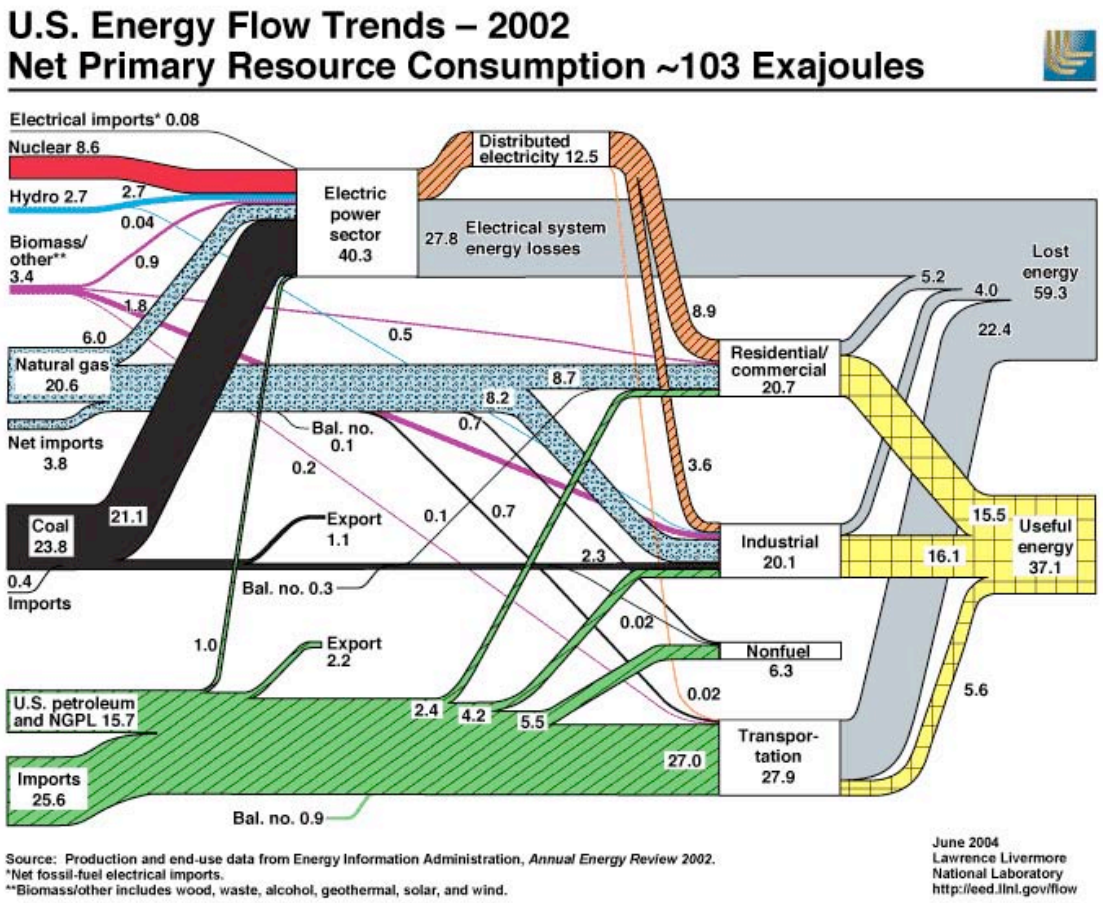

- Annual US energy production: $\sim 3.97 \ \textit{Trillion} \ \ kW \cdot hr$
- At an average deliverable cost of $\$0.10 \ kW \cdot hr$ the industry is: $\$400 \ \textit{Billion Annually}$

- Tremendous need for more efficient energy systems
- Distributed power (with waste heat recovery) can significant reduce losses

Electrochemical Processes & Carnot Limitations

- A Fuel Cell is an Electrochemical Energy Conversion Device

$$H_2 + \tfrac{1}{2}O_2 \rightarrow H_2O \qquad CO + \tfrac{1}{2}O_2 \rightarrow CO_2$$

- Greatly Improved Conversion Efficiencies
- Significantly Reduced Environmental Impact/Emissions
- Potential For Cogeneration and Hybrid Power Systems

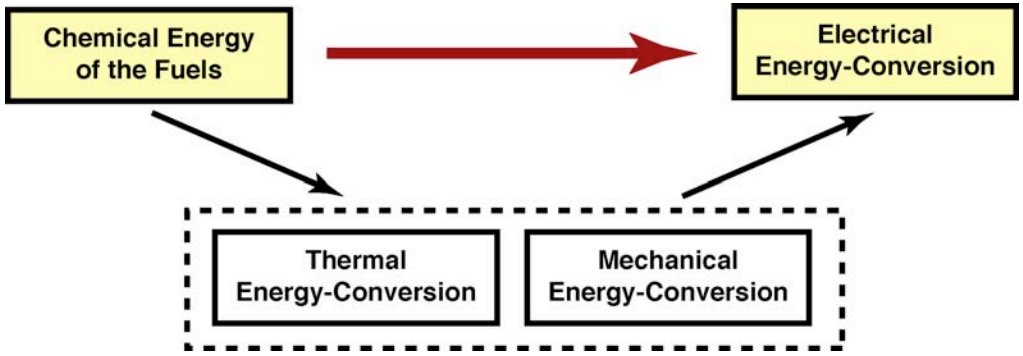

- Benefits of 'Distributed Power'

Fuel Cell Systems - Different Types for Different Applications

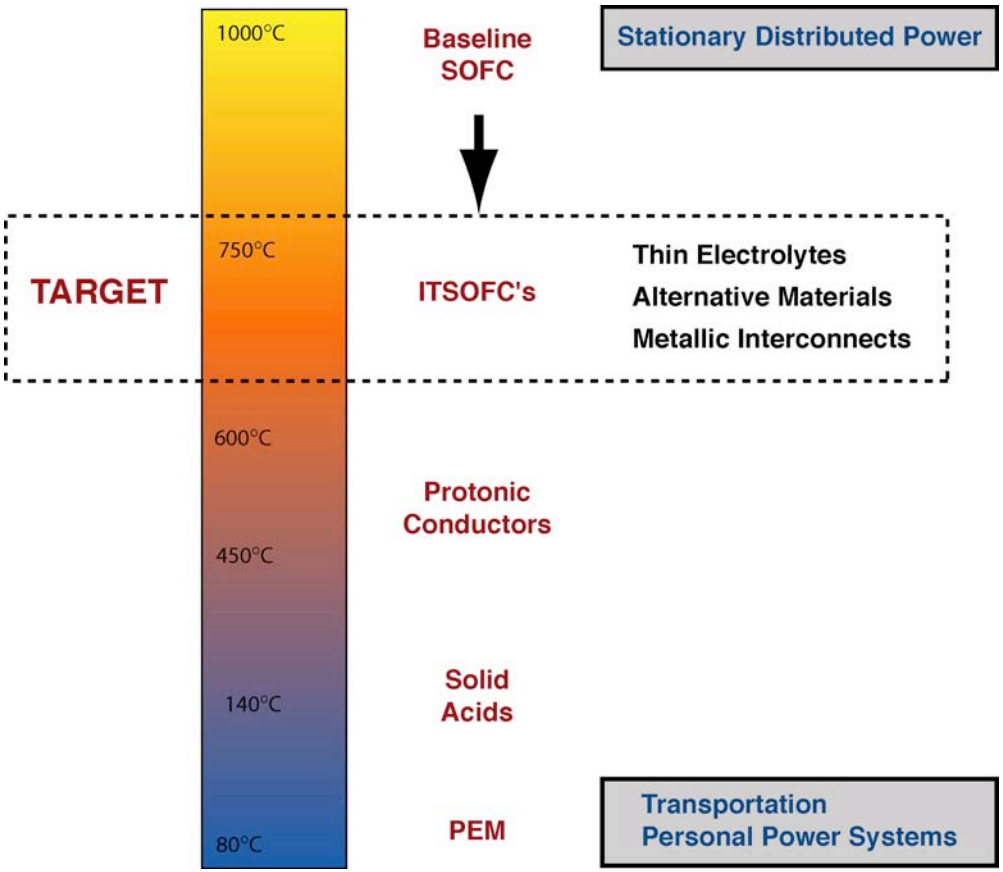

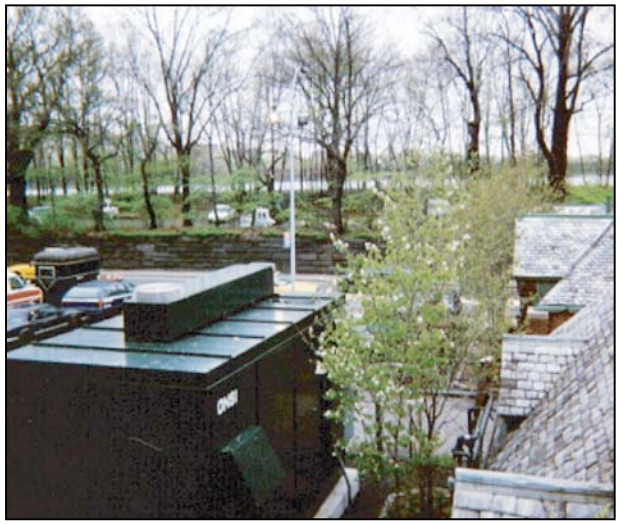

Potential Impact of Fuel Cell Systems - Efficiency:

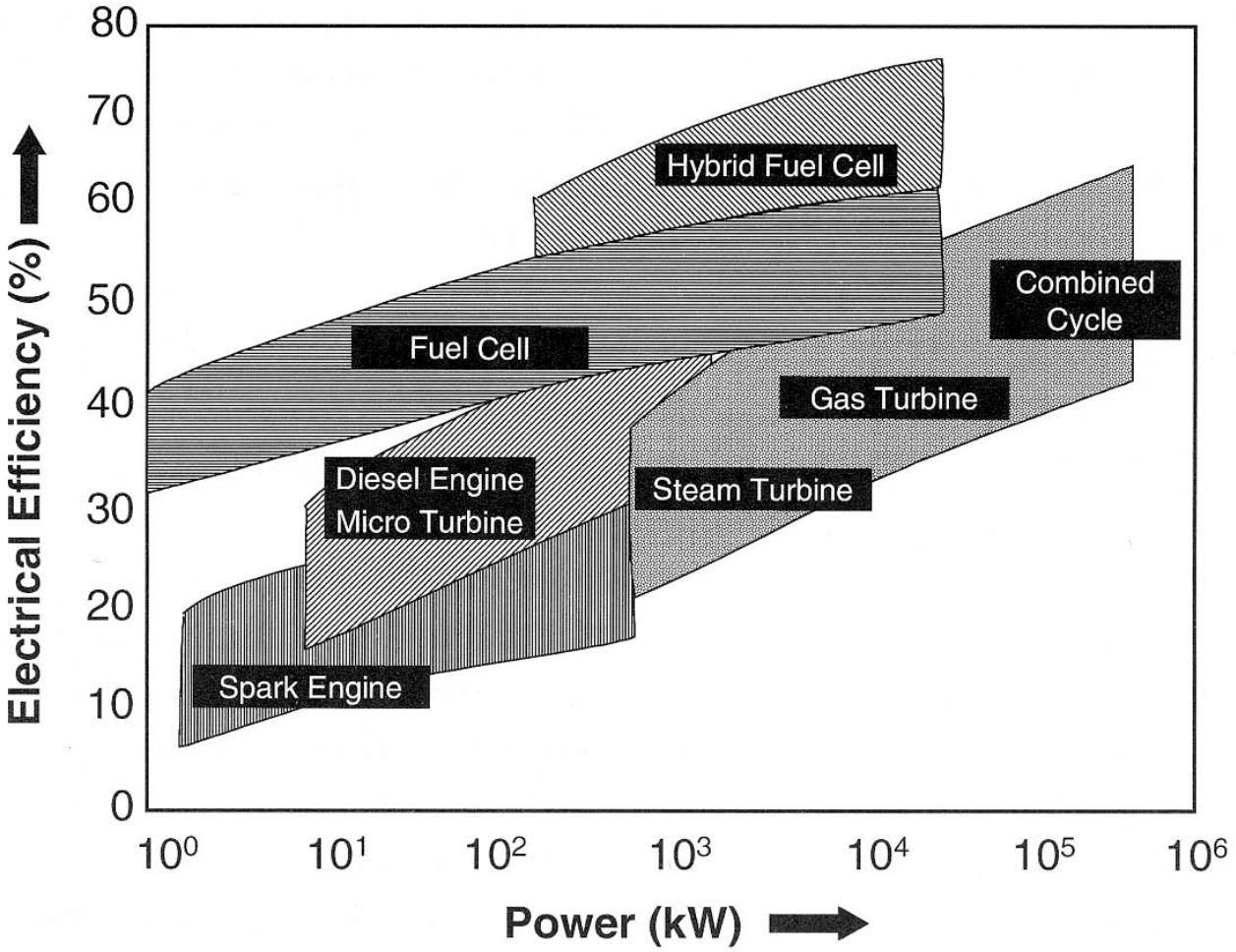

Stationary Hybrid Systems

- 220 kW HYBRID FUEL CELL GAS TURBINE SYSTEM:
  - Southern California Edison, Siemens-Westinghouse - SOFC with IRES micro-turbine
  - Over 2880 hours of operation
  - World Record Efficiency (53%)

Targets for Commercial Viability – SECA Guidelines

Cost, Cost, Cost…. $400/kW

Lifetime…. 40,000 Hours Service Lifetime

Stability…. < 0.1% degradation per 1000 hours

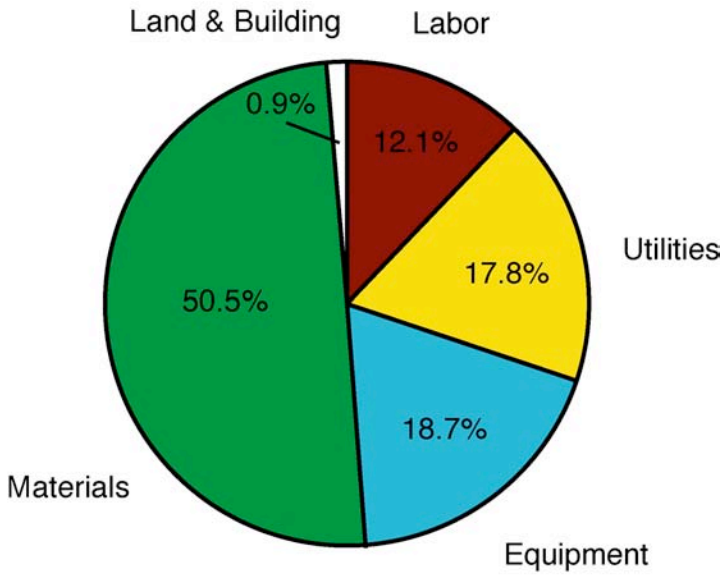

Materials Developments Hold Significant Promise for Driving System Costs Down

Outline – SOFC Materials: Challenges and Opportunities

- Review of Stack Materials and Requirements

  Stack materials and functionality requirements
  Synthesis and fabrication techniques

- Performance I-V Curves and the Materials Basis for Polarizations

  Intrinsic properties of constituents
  Extrinsic characteristics (microstructural topology)

- Materials Innovations Aimed at Improving Performance

- General Overview of In-Service Degradation and its Materials Basis

- Specific Examples of Degradation Modes and Mechanisms

  Interdiffusion at oxide/oxide interfaces
  Reaction at oxide/oxide interfaces
  Interconnect oxidation
  Redox of electrodes
  Cr Poisoning
  Thermo-Mechanical Issues

Range of Applications and Service Environments

No Single Power Source for All Platforms and Applications

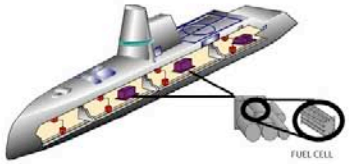

1 MWatt

100 KWatt

1 KWatt

100 Watts

1 Watt

Military systems power requirements often follow a "step-function", and so, different power sources technologies may be better suited for certain applications over others.

Energy Harvesting/Renewable

Batteries/Energy Storage

Fuel cells

Stirling Engines

Turbines

Nuclear Power

Systems integration

Stack Unit Cells - Constituent Functionality

Anode
- Ni/8YSZ cermets
- Good electronic conductivity
- Adequate porosity
- High concentration of **T**riple **P**hase **B**oundaries
- Durability (Ni coarsening and CTE mismatch)

Electrolyte
- 8YSZ
- Good ionic conductivity
- Stable in both oxidizing and reducing environments

Cathode
- LaSrMnO3 (LSM)
- Stable with regards to oxygen potential gradients

Interconnect
- LaCrO3
- Electrical connection between cells
- Gas separation between cells
- Chemical stability in both fuel and air

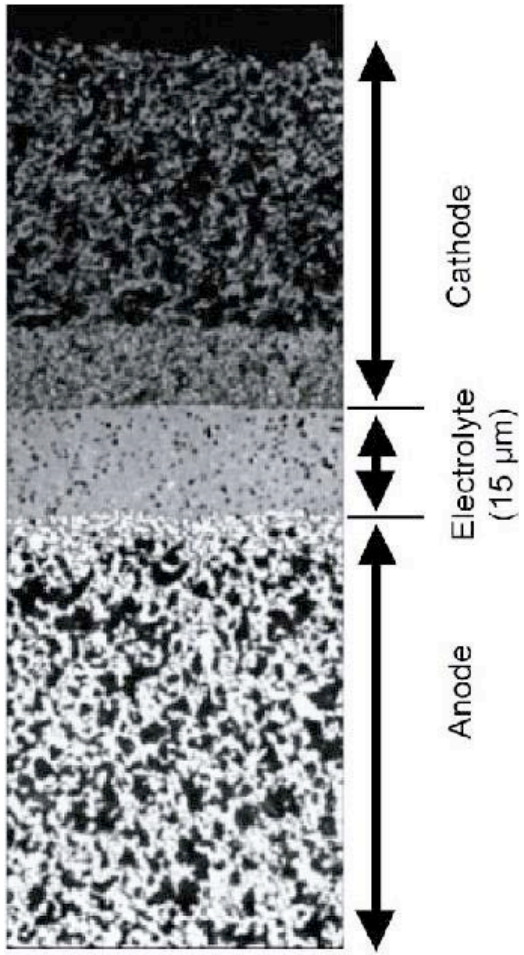

Teitz et al.

Stack Design and Materials Integration:

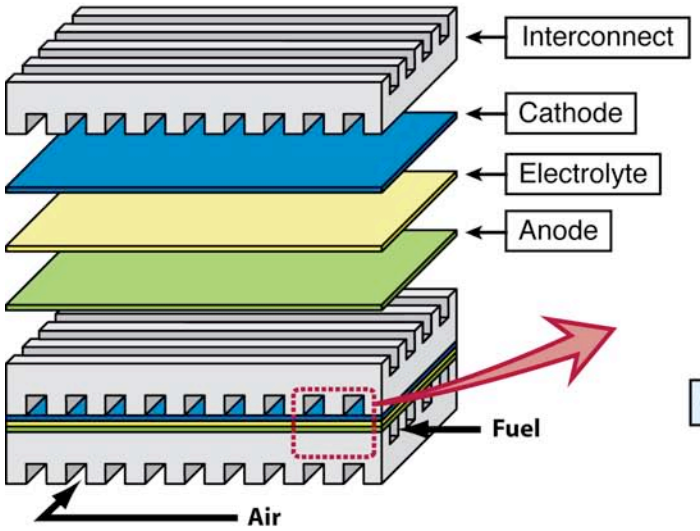

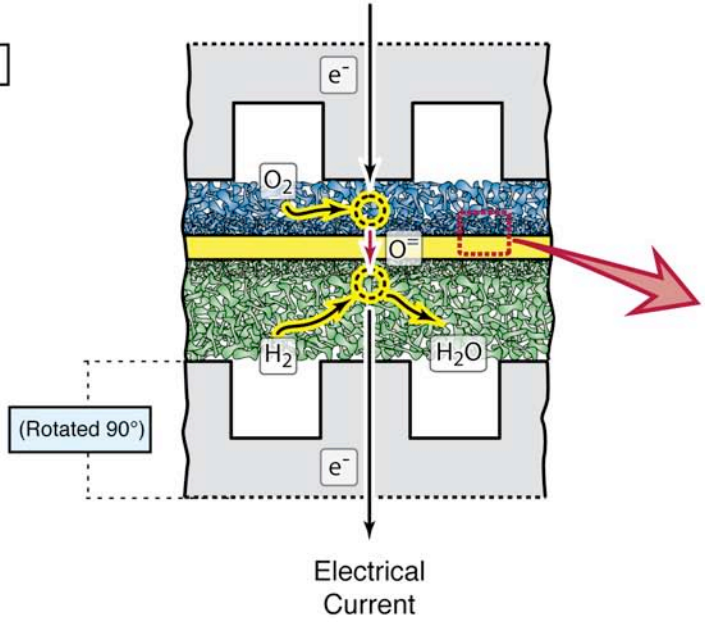

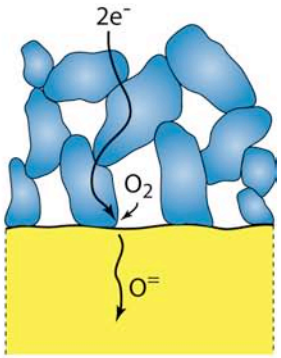

Oxygen Reducation
in Cathode

Solid Oxide Fuel Cell Functionality:

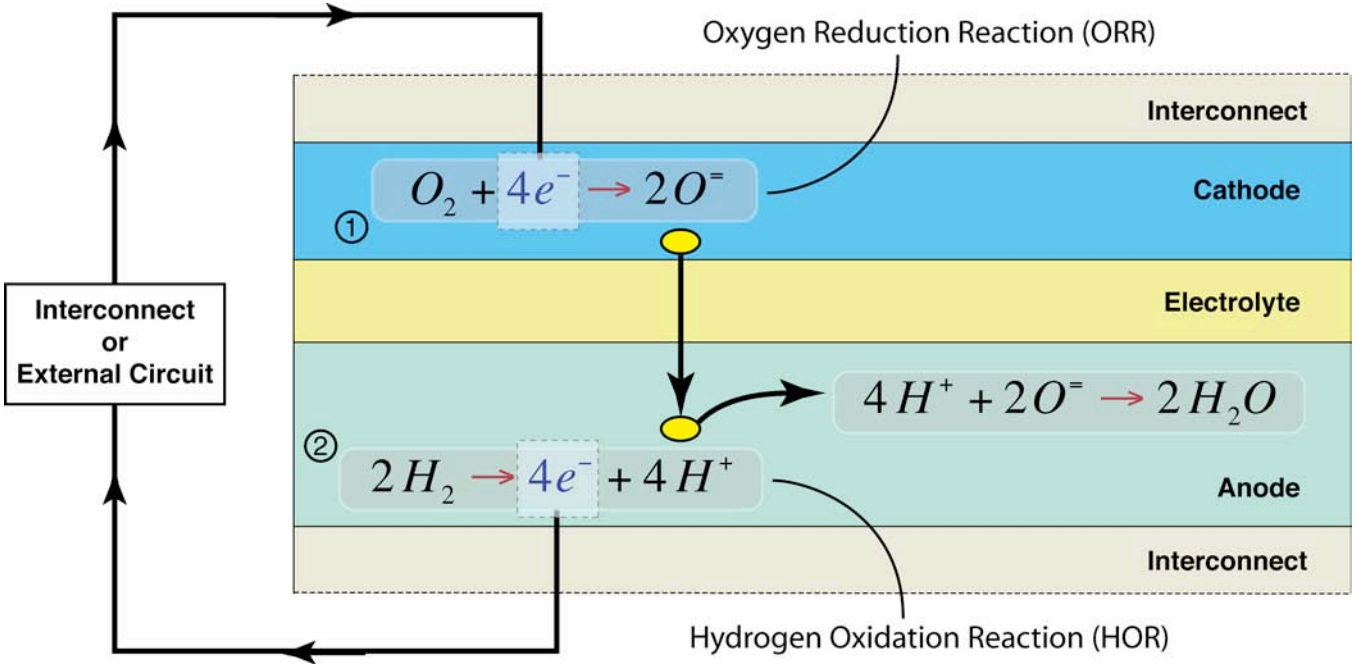

System Performance Metrics and Relation to Materials Design:

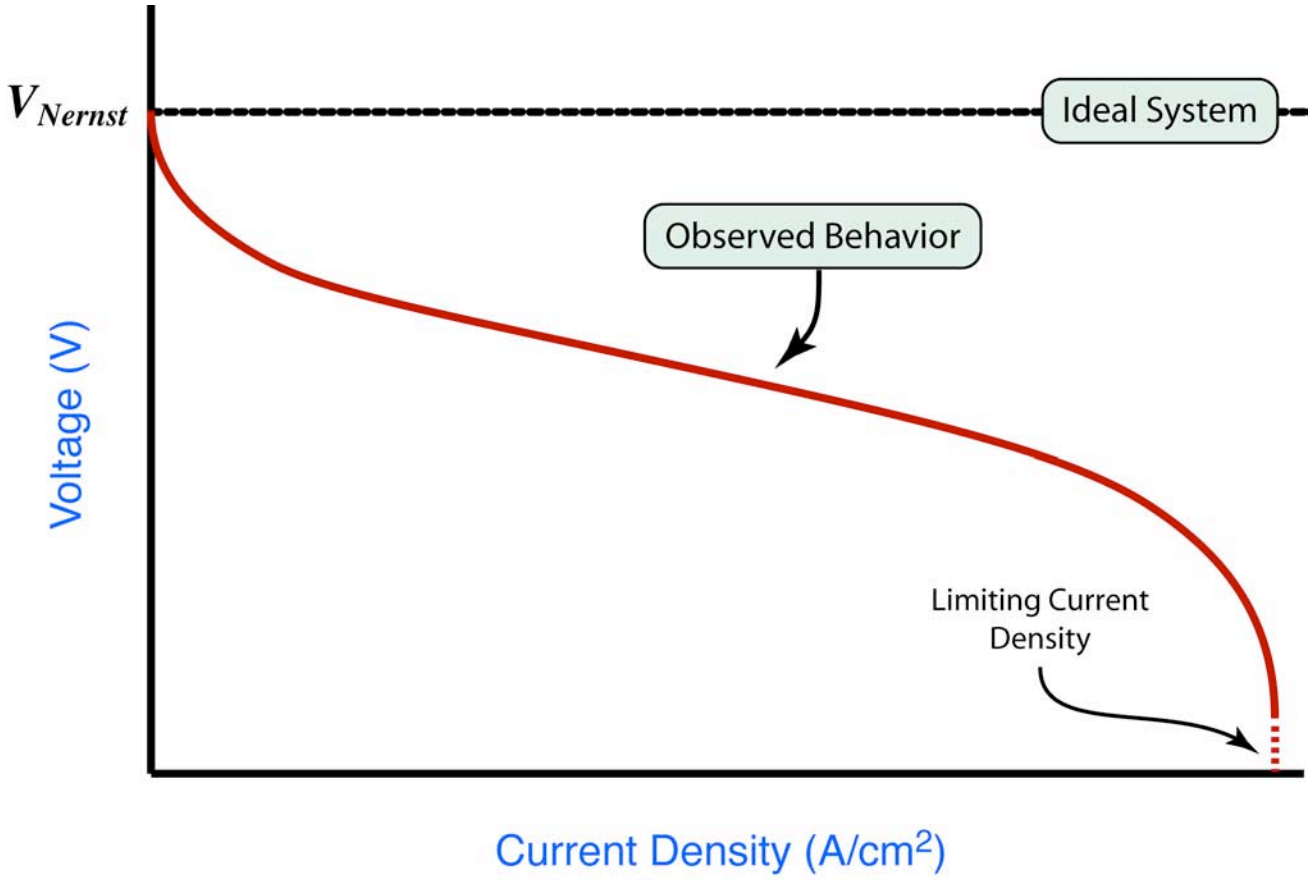

System Performance Metrics and Relation to Materials Design:

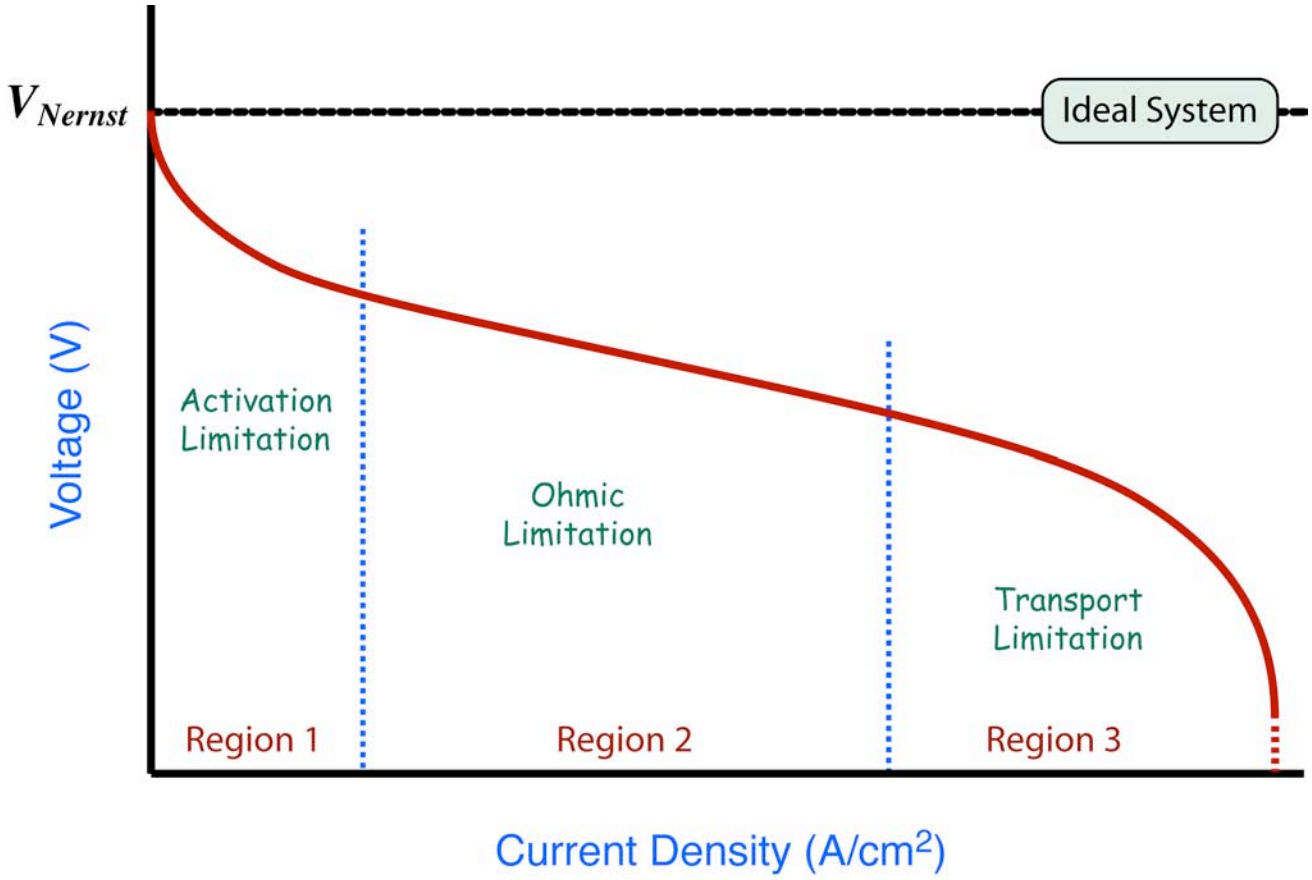

System Performance Metrics and Relation to Materials Design:

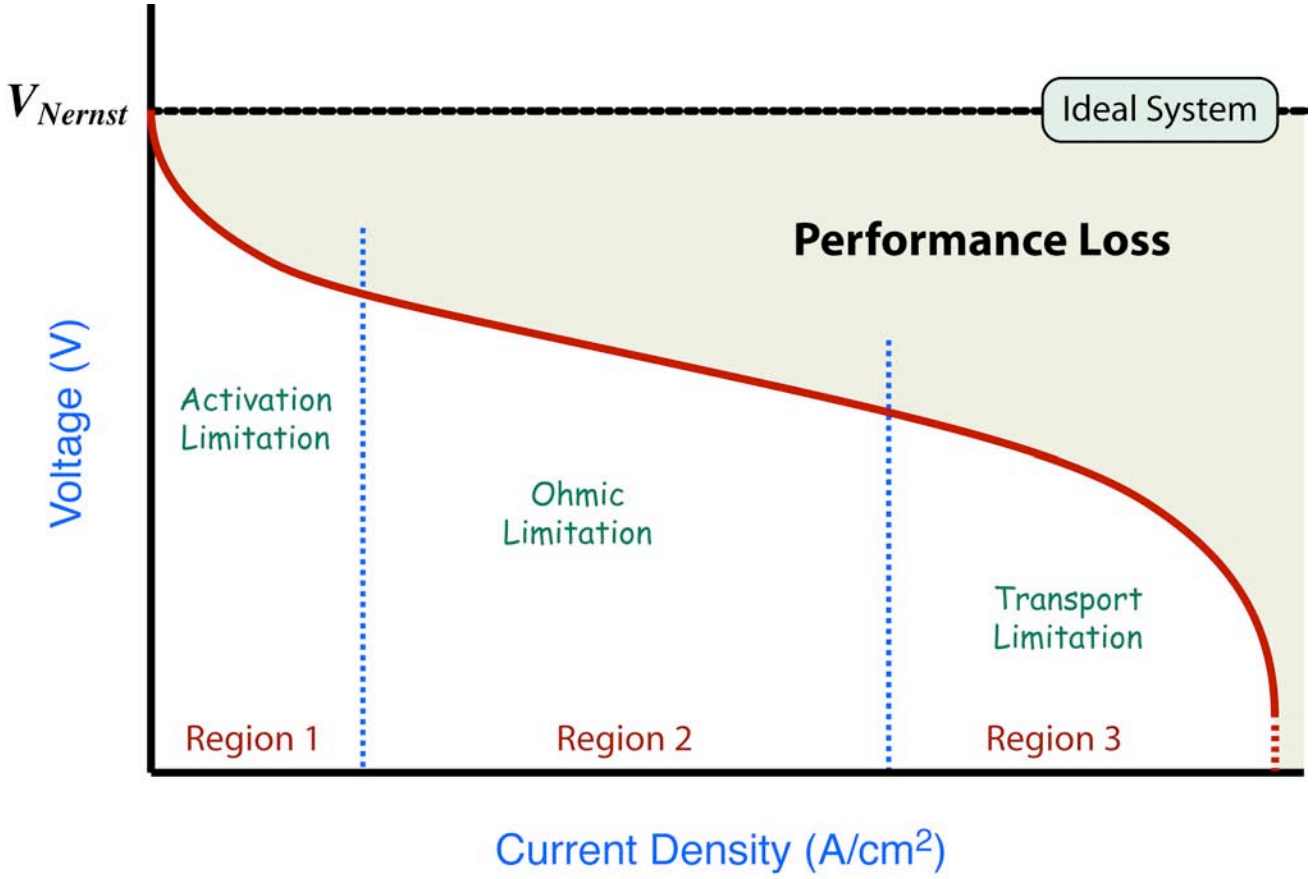

Contributions to Performance Losses

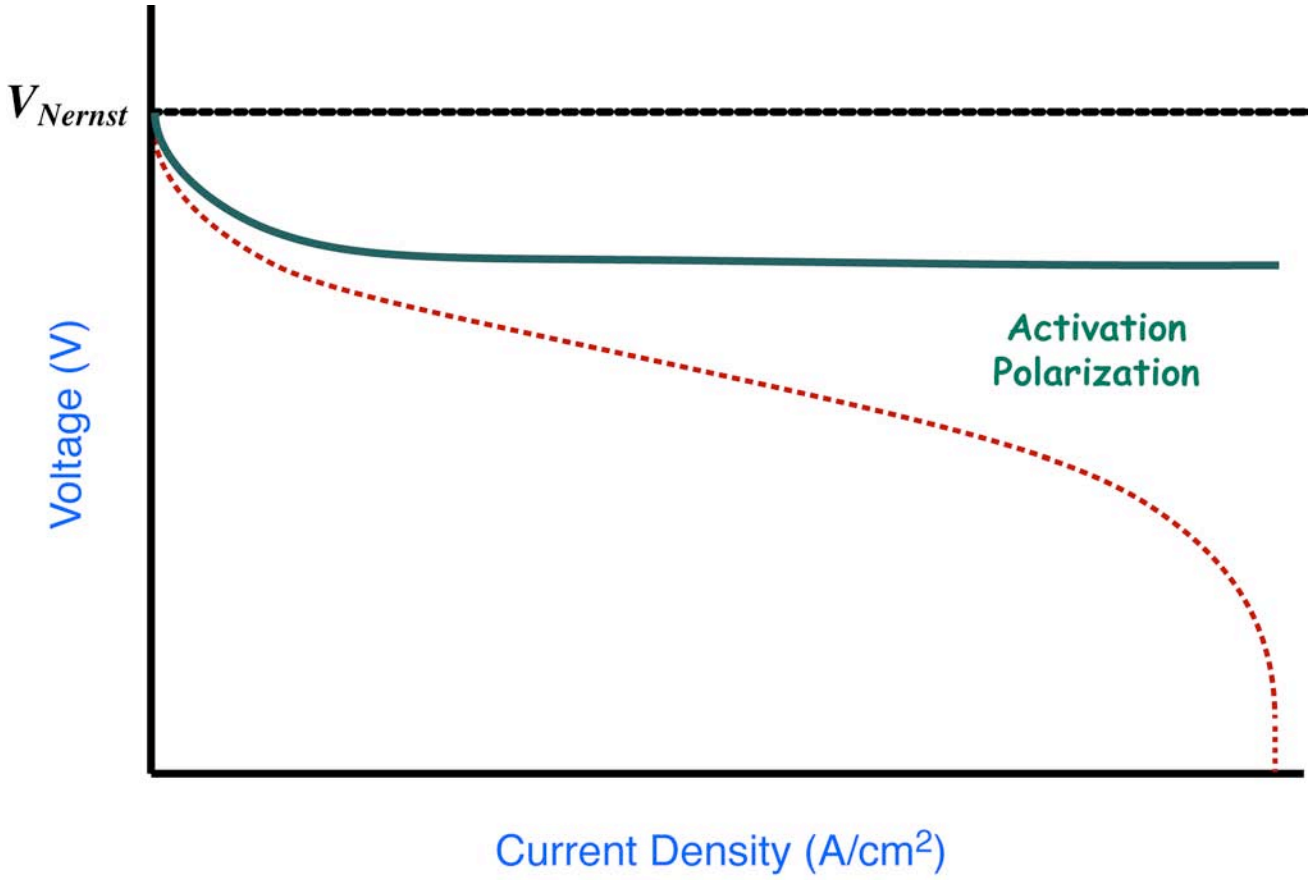

Activation Polarization

S.B. Adler (2004),Chemical Reviews, ***104****,4791*

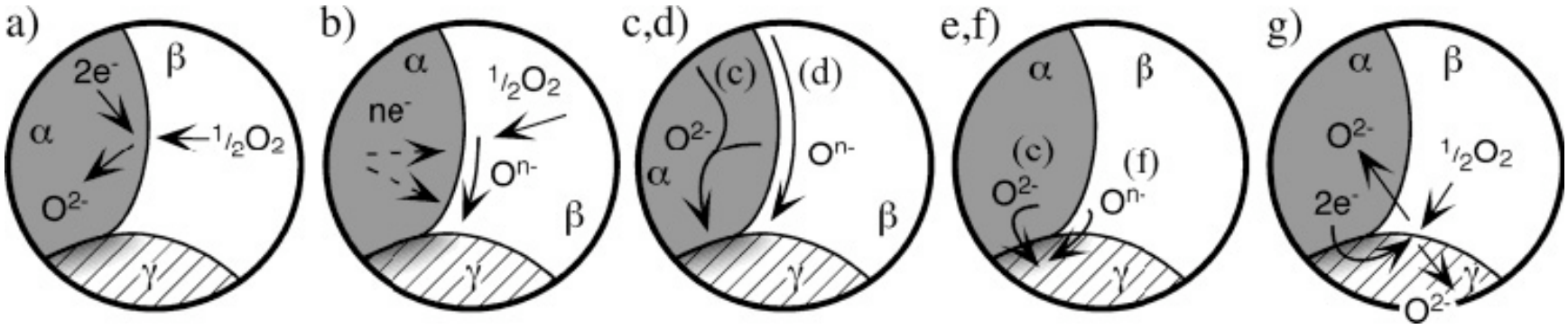

Some mechanisms thought to govern oxygen reduction in SOFC cathodes. Phases α, β, and γ refer to the electronic phase, gas phase, and ionic phase, respectively: (a) Incorporation of oxygen into the bulk of the electronic phase (if mixed conducting); (b) adsorption and/or partial reduction of oxygen on the surface of the electronic phase; (c) bulk or (d) surface transport of O^{2-} or O^{n-}, respectively, to the R/ç interface, (e) Electrochemical charge transfer of O^{2-} or (f) combinations of O^{n-} and e-, respectively, across the R/ç interface, and (g) rates of one or more of these mechanisms wherein the electrolyte itself is active for generation and transport of electroactive oxygen species.

$$j = j^{o}\left[\exp\left(\frac{\alpha n F \eta}{RT}\right) - \exp\left(\frac{-(1-\alpha) n F \eta}{RT}\right)\right]$$

Butler-Volmer Equation

Contributions to Performance Losses

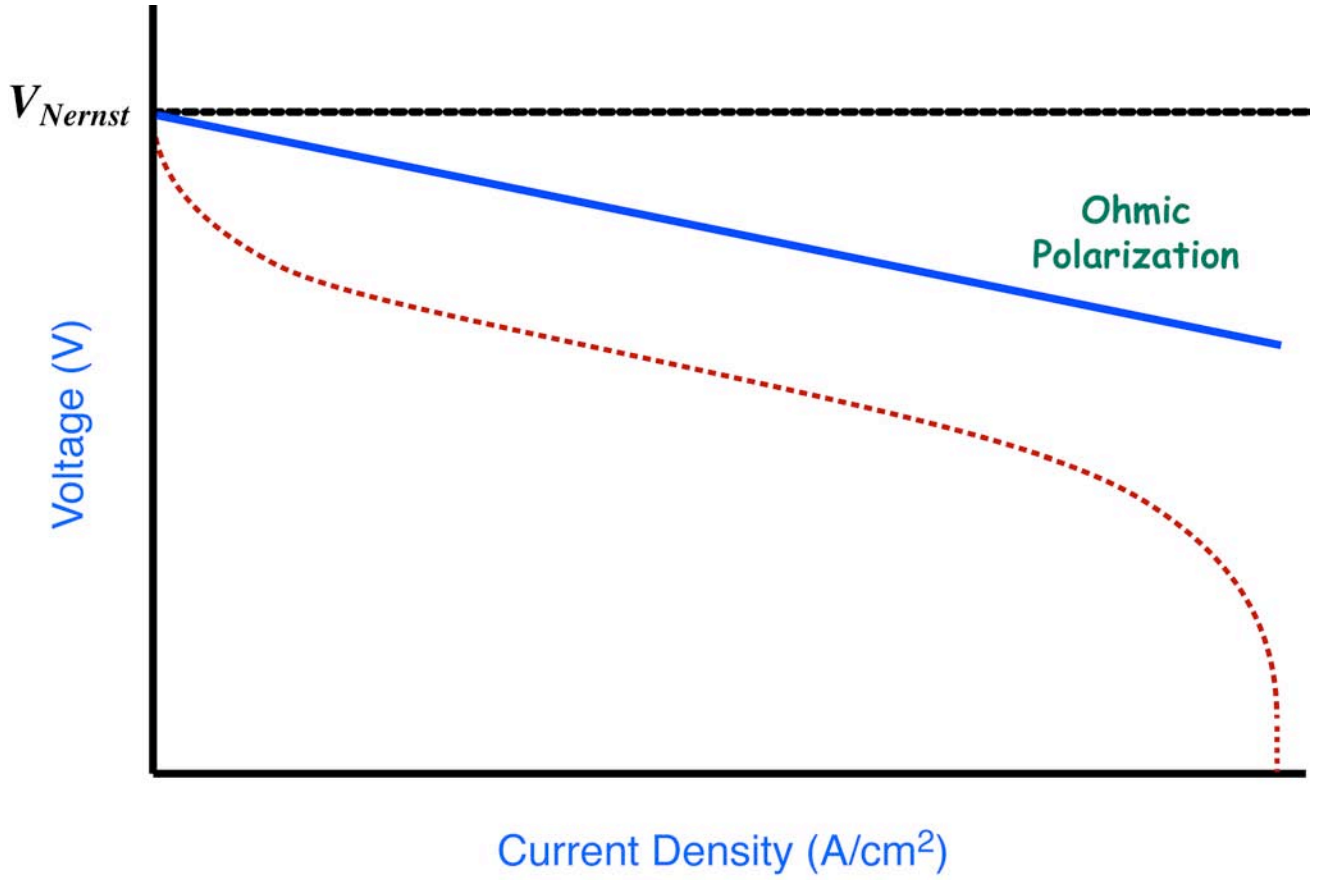

Equivalent Circuit and Materials Design:

$R \equiv f(P_{O_2}, c_i, \Phi_{ext}, K)$

$C \equiv f(P_{O_2}, c_i, \Phi_{ext}, K)$

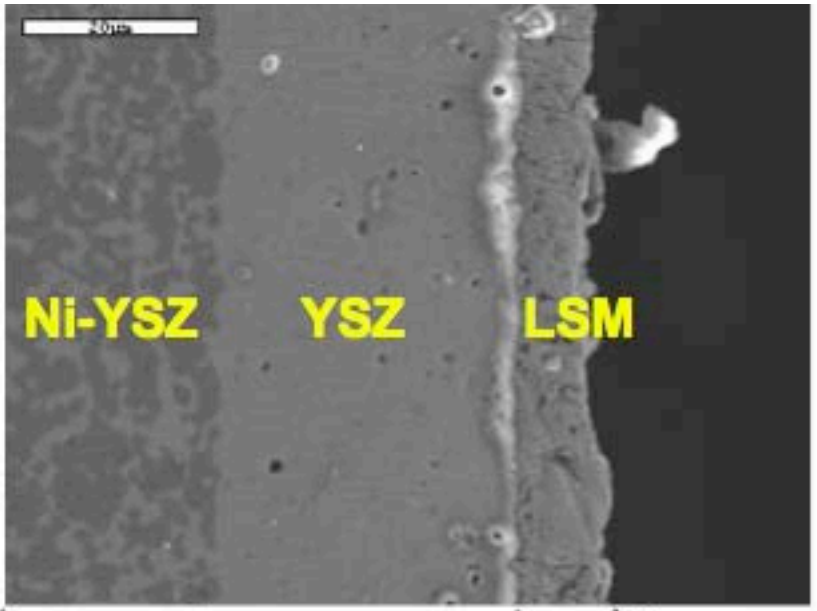

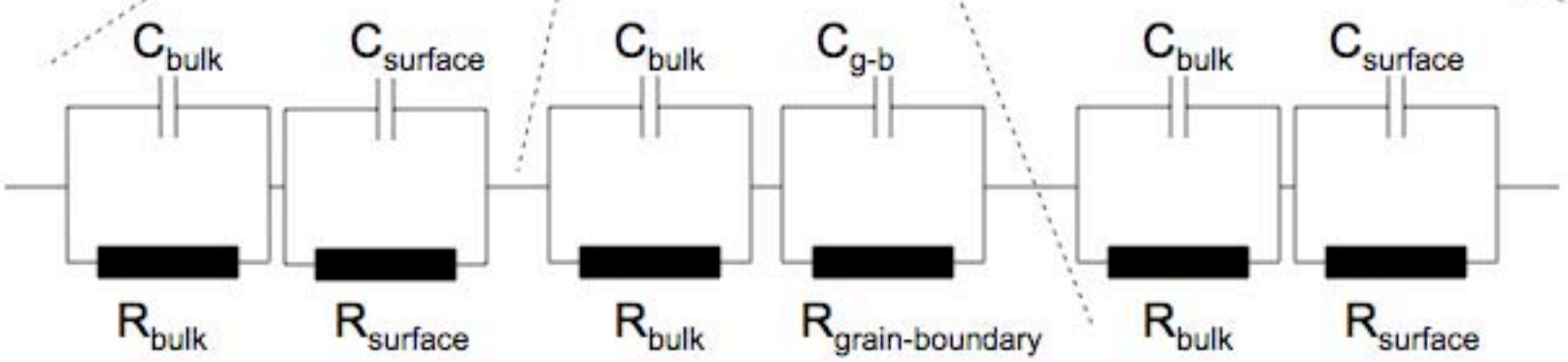

Contributions to Performance Losses

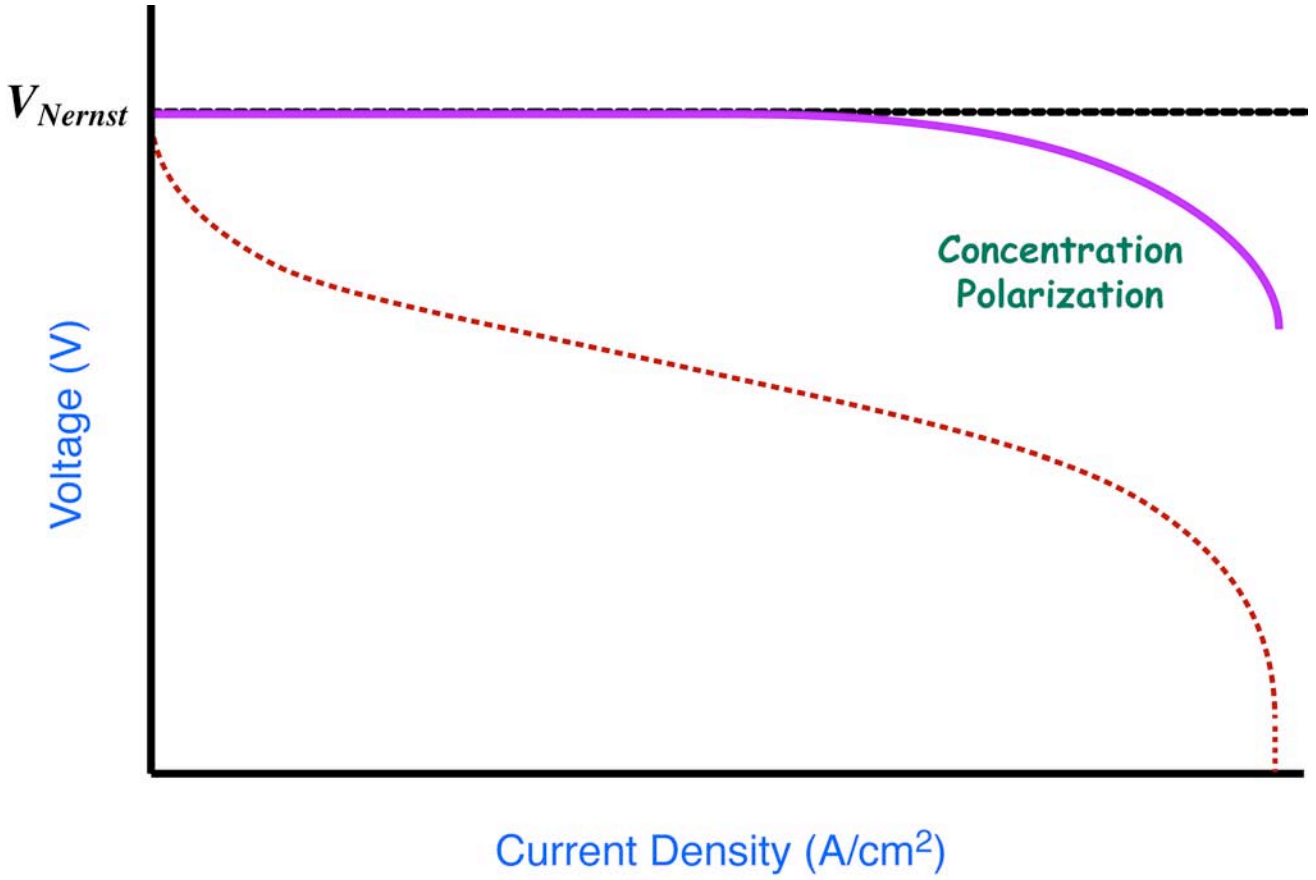

Electrode Topology and Degradation Mechanisms:

Topological optimization provides a path for reducing diffusional polarization losses

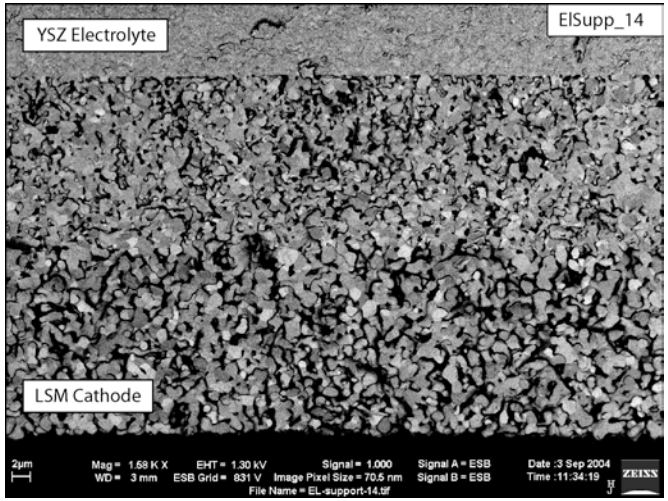

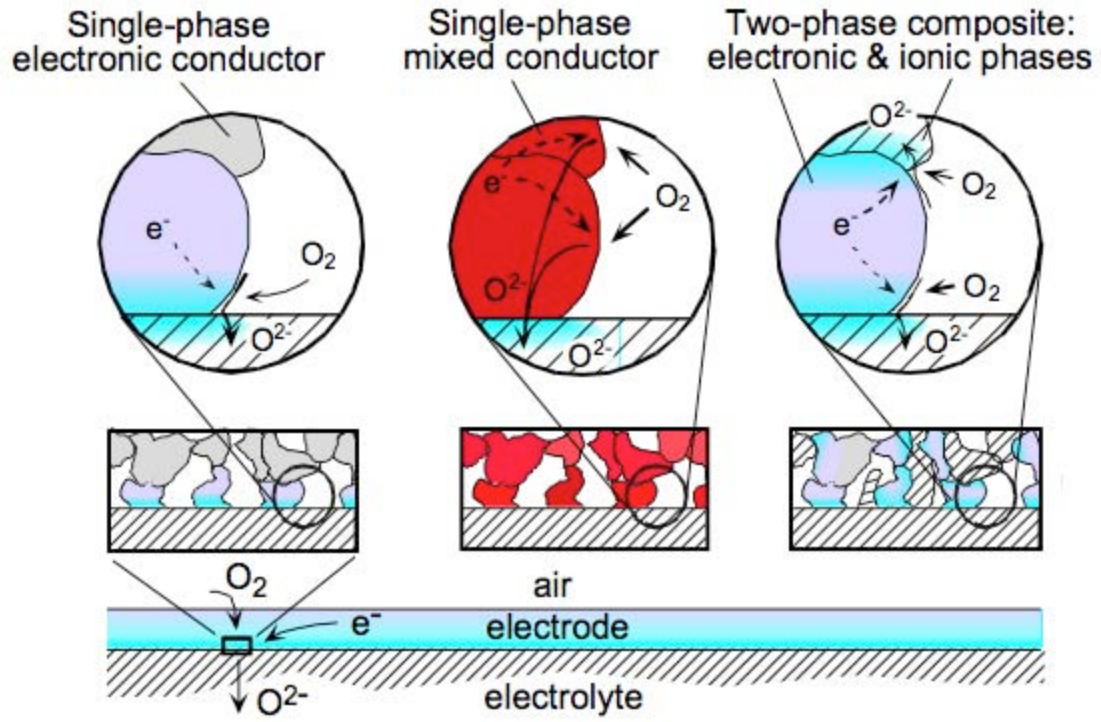

S.B. Adler (2004)

Model systems for fundamental studies of controlling physical phenomena

Summation of Polarization Losses

$$V_{Cell} = V_{Nernst} - i\,R - \eta_{Activation} - \eta_{Concentration}$$

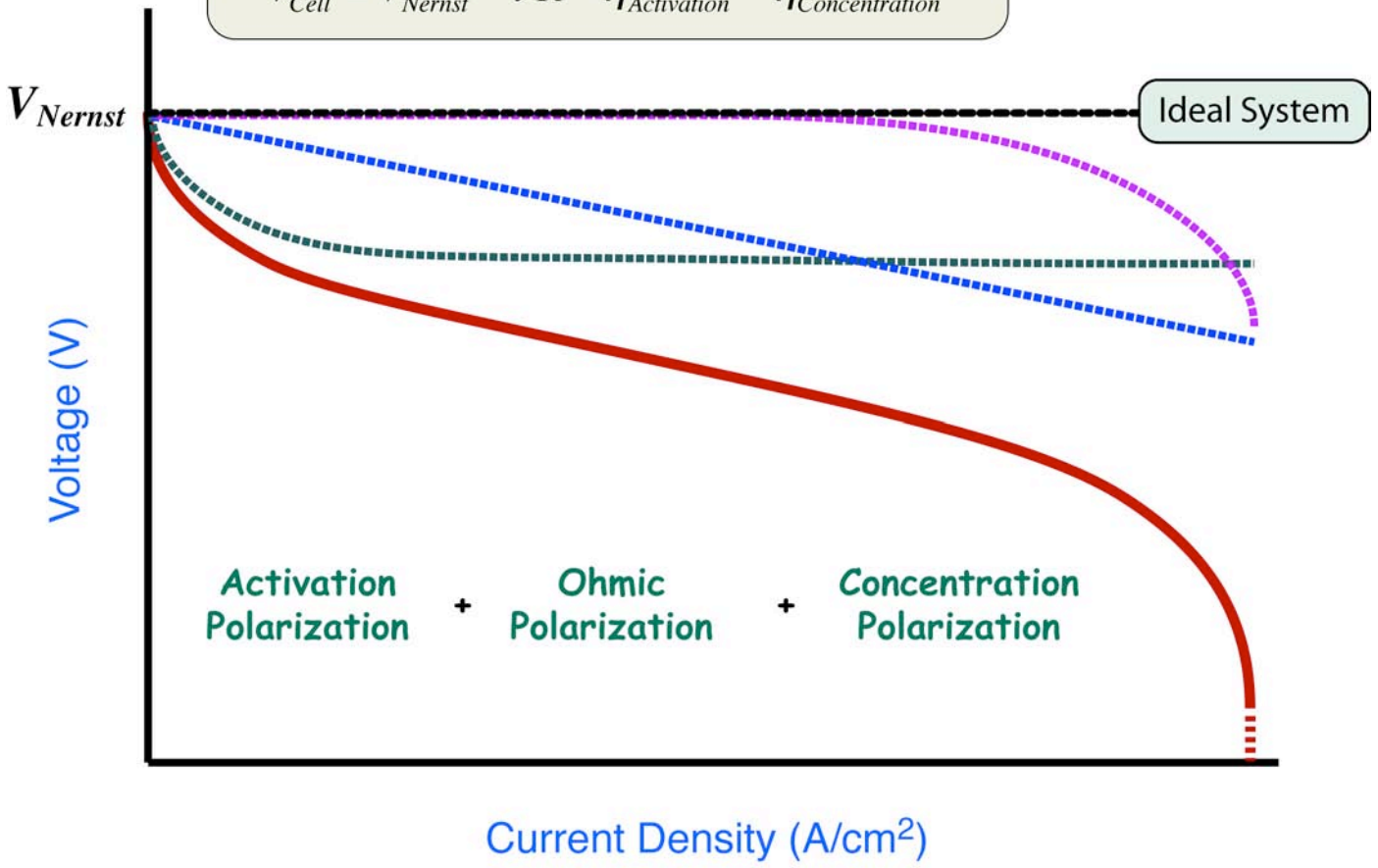

Materials Design for Improved Performance

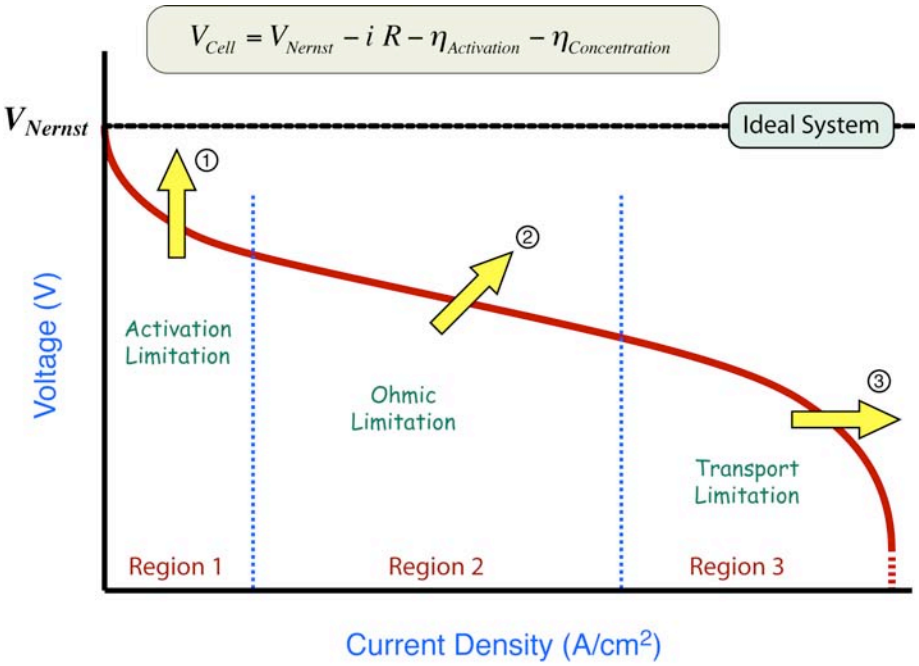

Mechanistic Approach to Improved Performance Through Materials Science and Engineering

1. **Region 1 – *Reduce Activation Polarization***

   (Move $V - i$ curve upwards)

   ⇒ Develop electrodes with improved surface reaction kinetics

   ⇒ Develop electrodes with maximum volume density of TPB

   ⇒ Develop electrode materials exhibiting ***M**ixed **I**onic and **E**lectronic **C**onductivity (MIEC)*

2. **Region 2 – *Reduce Ohmic Polarization***

   (Reduce slope of $V - i$ curve)

   ⇒ Develop thin electrolyte layers

   ⇒ Develop more conductive electrodes and interface structures

   ⇒ Develop higher conductivity contact materials, current collectors and oxide scales

3. **Region 3 – *Reduce Diffusional Polarization***

   (Extend range of the $V - i$ curve drop-off)

   ⇒ Develop electrodes with tailored porosity electrodes

   ⇒ Develop theoretical and experimental approaches for electrode topology optimization

After P. Singh, PNNL

Conductivity of Doped Chromia

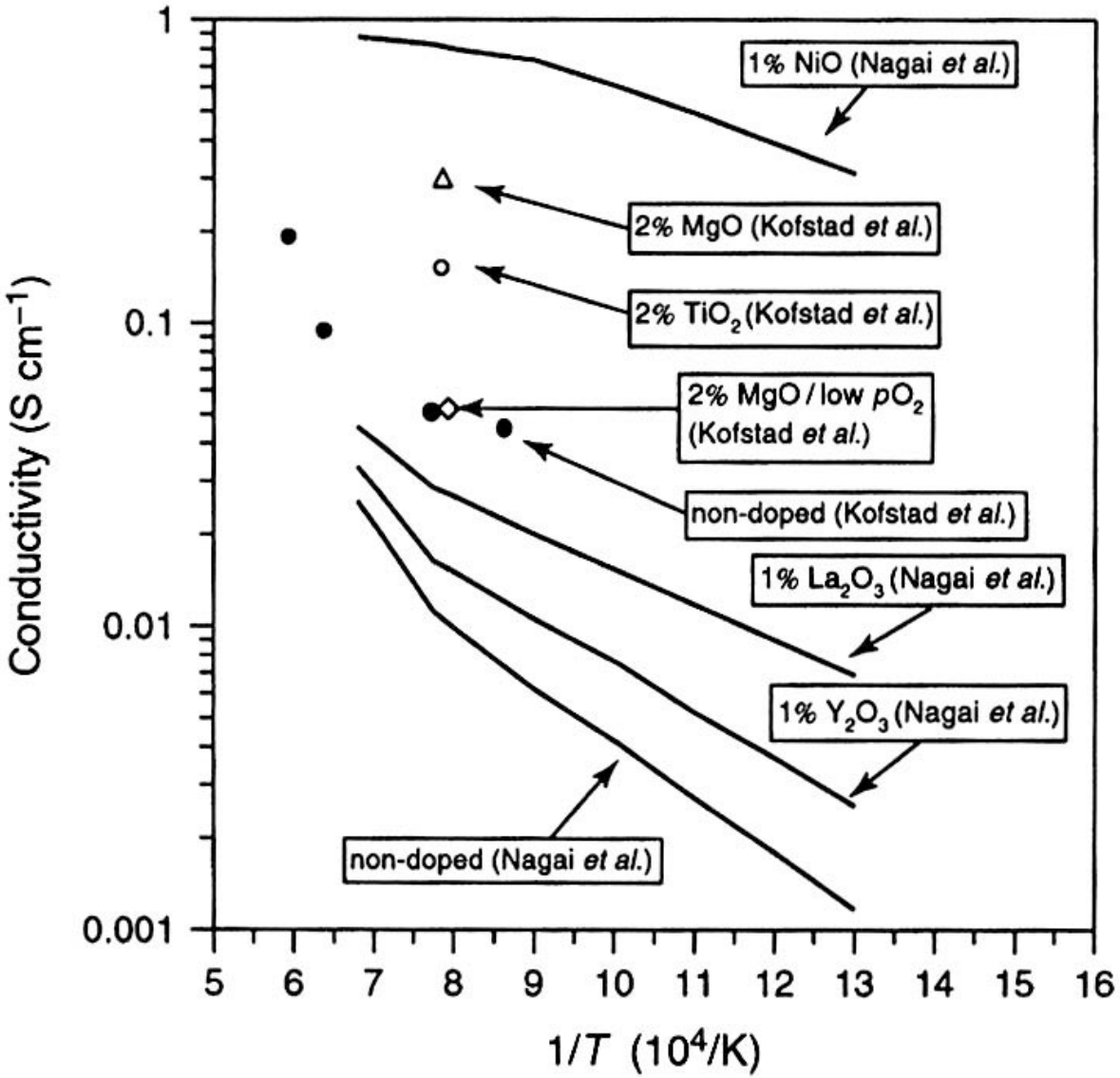

Mixed Electronic and Ionic Conductors for Electrodes

What are the potential advantages to utilizing emerging mixed conductors in the anode and cathode structures?

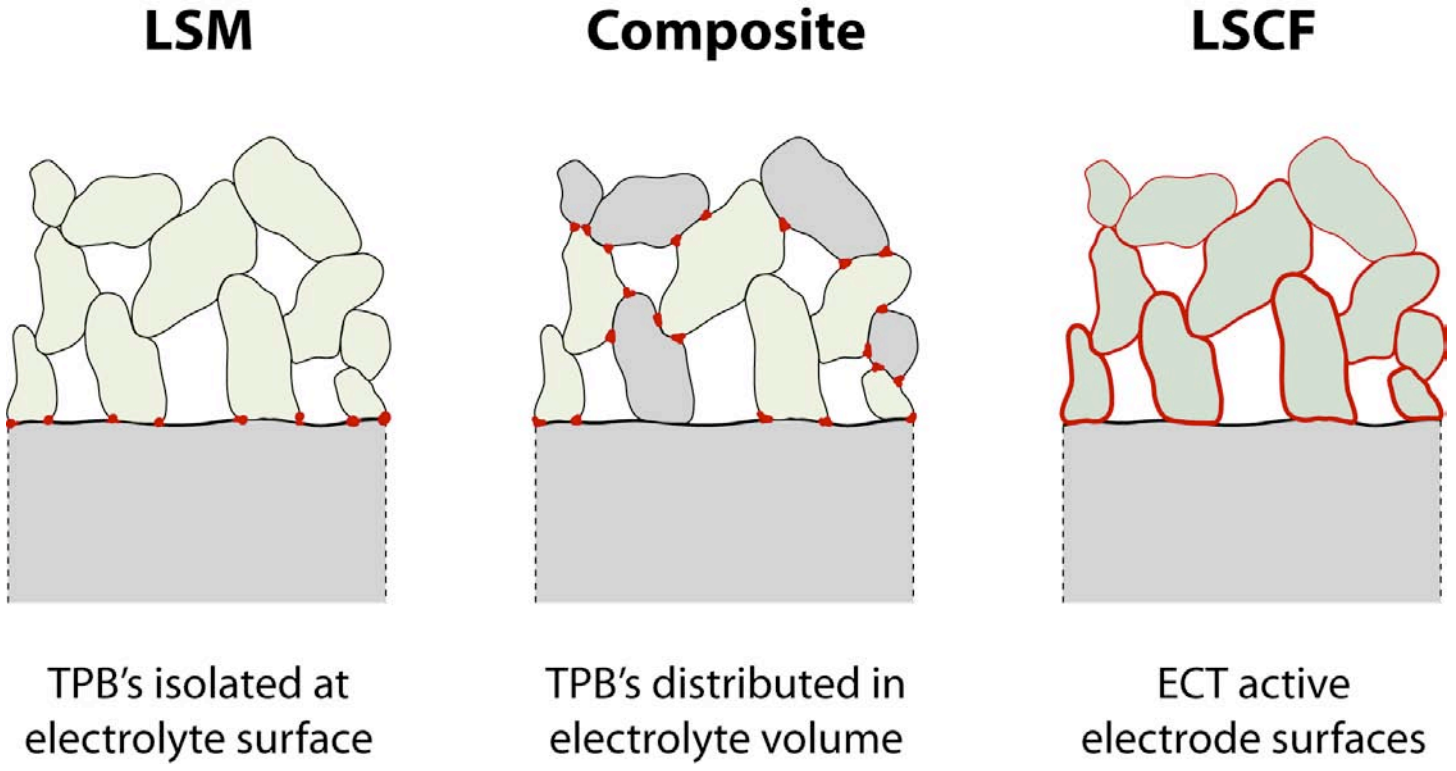

What does this mean in terms of materials integration challenges?

Sol-Gel Synthesis of Anode Materials:

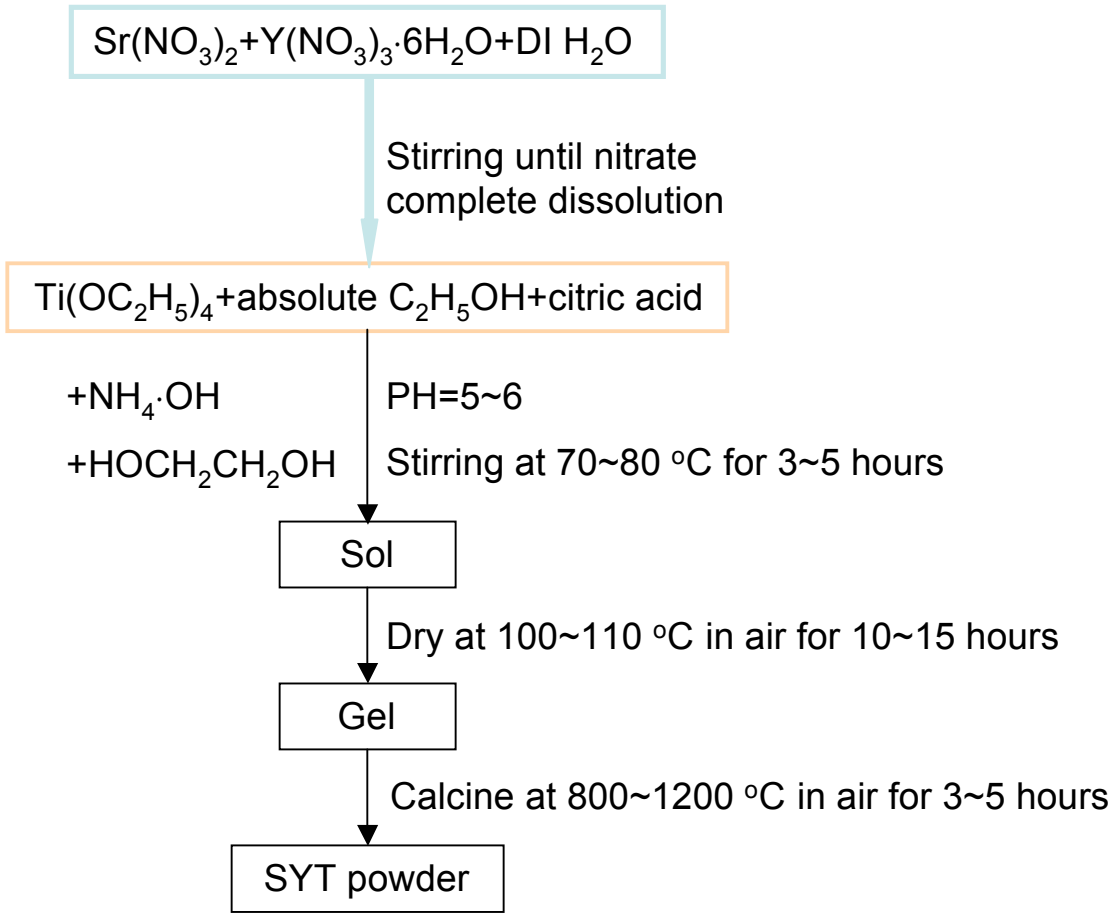

Sol-Gel Processing of Alternative Anode SYT

Sintered Pellet

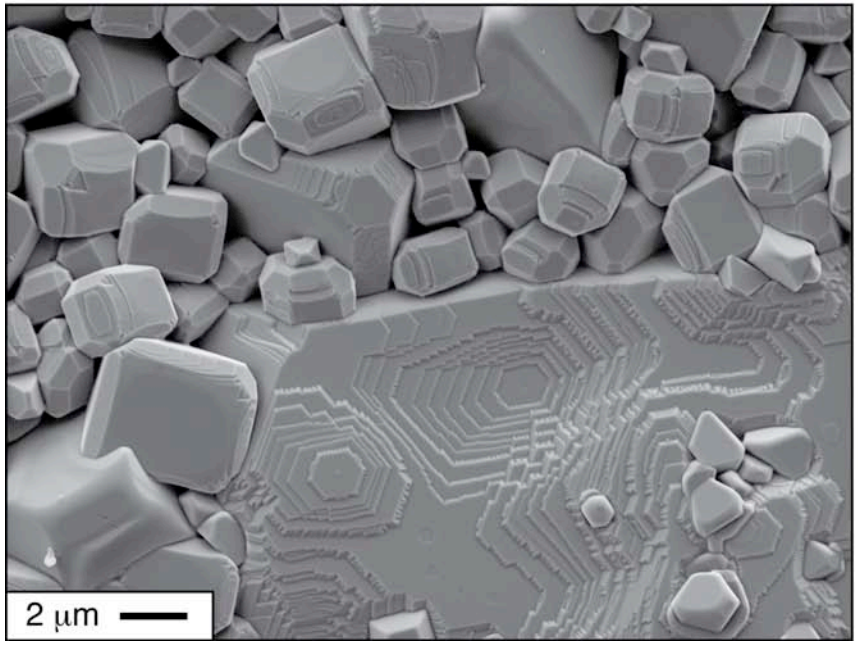

Calcined Powder

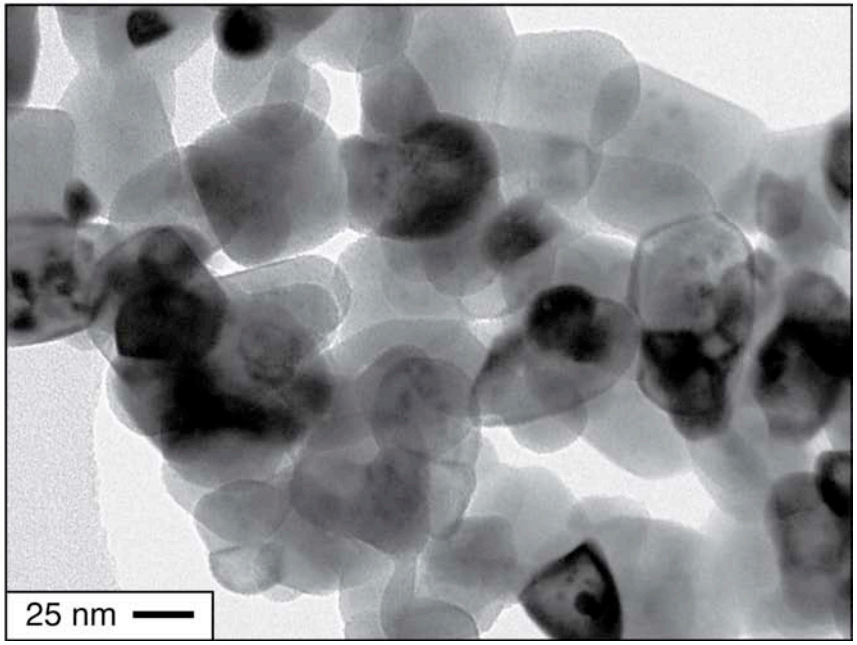

TEM Analysis of Powder after Exposure to Anode Gas Environment

Microstructure Undergoes Significant Coarsening

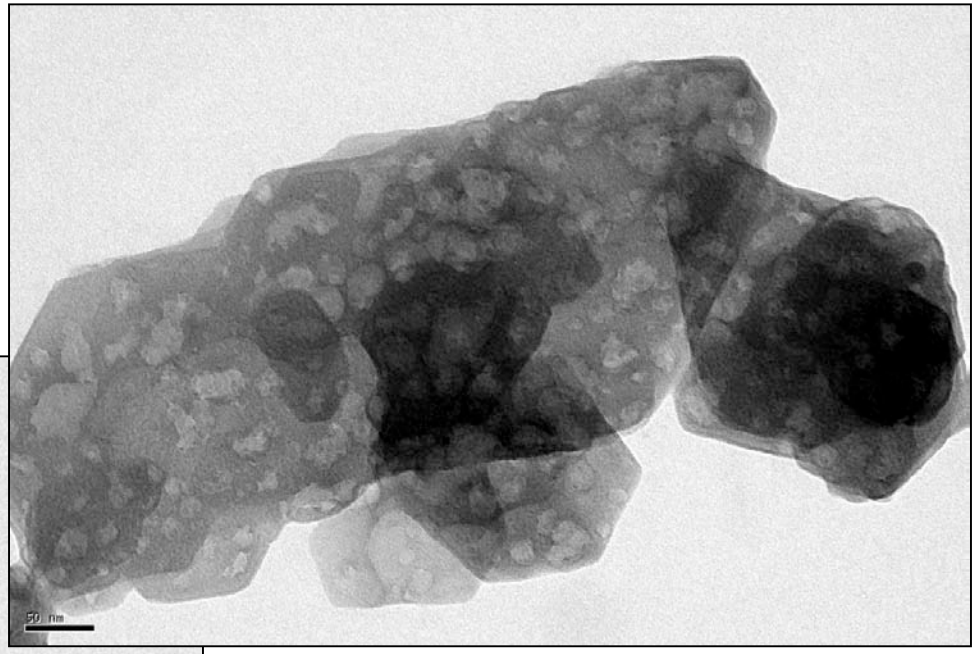

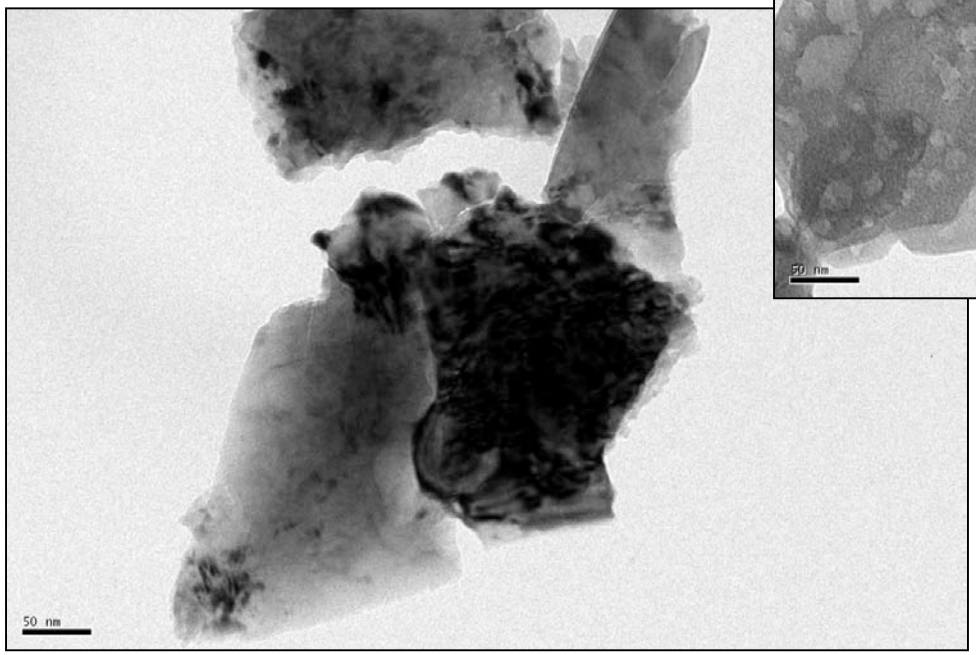

Crystallites show Heterogeneous structure as a Result of Reduction in Anode Gas environment.

Selected-Area Diffraction of As-Synthesized Powders

Indexing diffraction rings shows consistency with XRD analysis and known lattice parameters

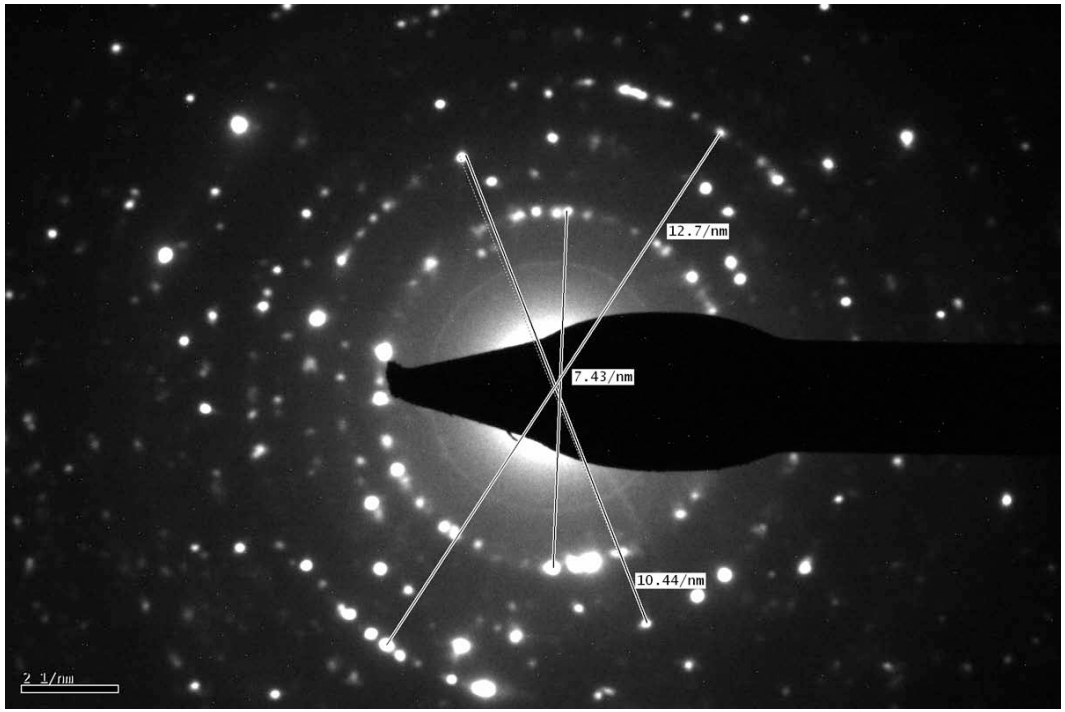

(N)	h	k	l	d(hkl)	2-Theta	Intensity	I/Imax	m(hk
1	0	0	1	3.90123	22.7743	1.04675e-04	0.1	6
2	1	1	0	2.75859	32.4272	1.62111e-01	100.0	12
3	1	1	1	2.25238	39.9942	1.13403e-01	70.0	8
4	2	0	0	1.95061	46.5164	1.50873e-01	93.1	6
5	1	0	2	1.74468	52.3972	7.48407e-04	0.5	24
6	2	1	1	1.59267	57.8444	6.51408e-02	40.2	24
8	2	0	2	1.37929	67.8957	8.03705e-02	49.6	12
9	1	2	2	1.30041	72.6427	1.04352e-03	0.6	30
10	0	3	1	1.23368	77.2694	2.87057e-02	17.7	24
11	3	1	1	1.17627	81.8130	2.85435e-02	17.6	24
12	2	2	2	1.12619	86.3053	2.59264e-02	16.0	8
13	3	0	2	1.08201	90.7748	8.03947e-04	0.5	24
14	1	3	2	1.04265	95.2491	3.85024e-02	23.8	48

Cubic perovskite material with lattice parameter a = 3.9012Å

Selected-Area Diffraction of Reduced Powders

Indexed rings show that lattice parameter has been reduced by ~ 0.8%

This is consistent with the changes expected during reduction

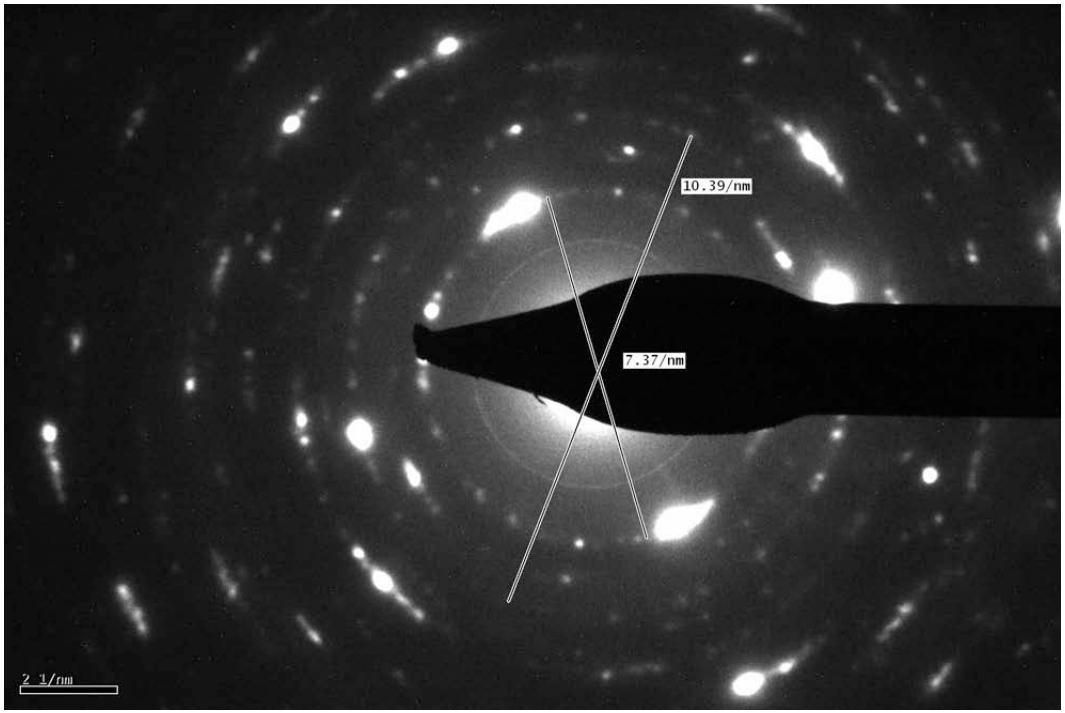

(N)	h	k	l	d(hkl)	2-Theta	Intensity	I/Imax	m(hk
1	0	0	1	3.90123	22.7743	1.04675e-04	0.1	6
2	1	1	0	2.75859	32.4272	1.62111e-01	100.0	12
3	1	1	1	2.25238	39.9942	1.13403e-01	70.0	8
4	2	0	0	1.95061	46.5164	1.50873e-01	93.1	6
5	1	0	2	1.74468	52.3972	7.48407e-04	0.5	24
6	2	1	1	1.59267	57.8444	6.51408e-02	40.2	24
8	2	0	2	1.37929	67.8957	8.03705e-02	49.6	12
9	1	2	2	1.30041	72.6427	1.04352e-03	0.6	30
10	0	3	1	1.23368	77.2694	2.87057e-02	17.7	24
11	3	1	1	1.17627	81.8130	2.85435e-02	17.6	24
12	2	2	2	1.12619	86.3053	2.59264e-02	16.0	8
13	3	0	2	1.08201	90.7748	8.03947e-04	0.5	24
14	1	3	2	1.04265	95.2491	3.85024e-02	23.8	48

Cubic perovskite material with lattice parameter $a < 3.9012$Å

Ohmic Resistance – Electrolyte Materials (YSZ)

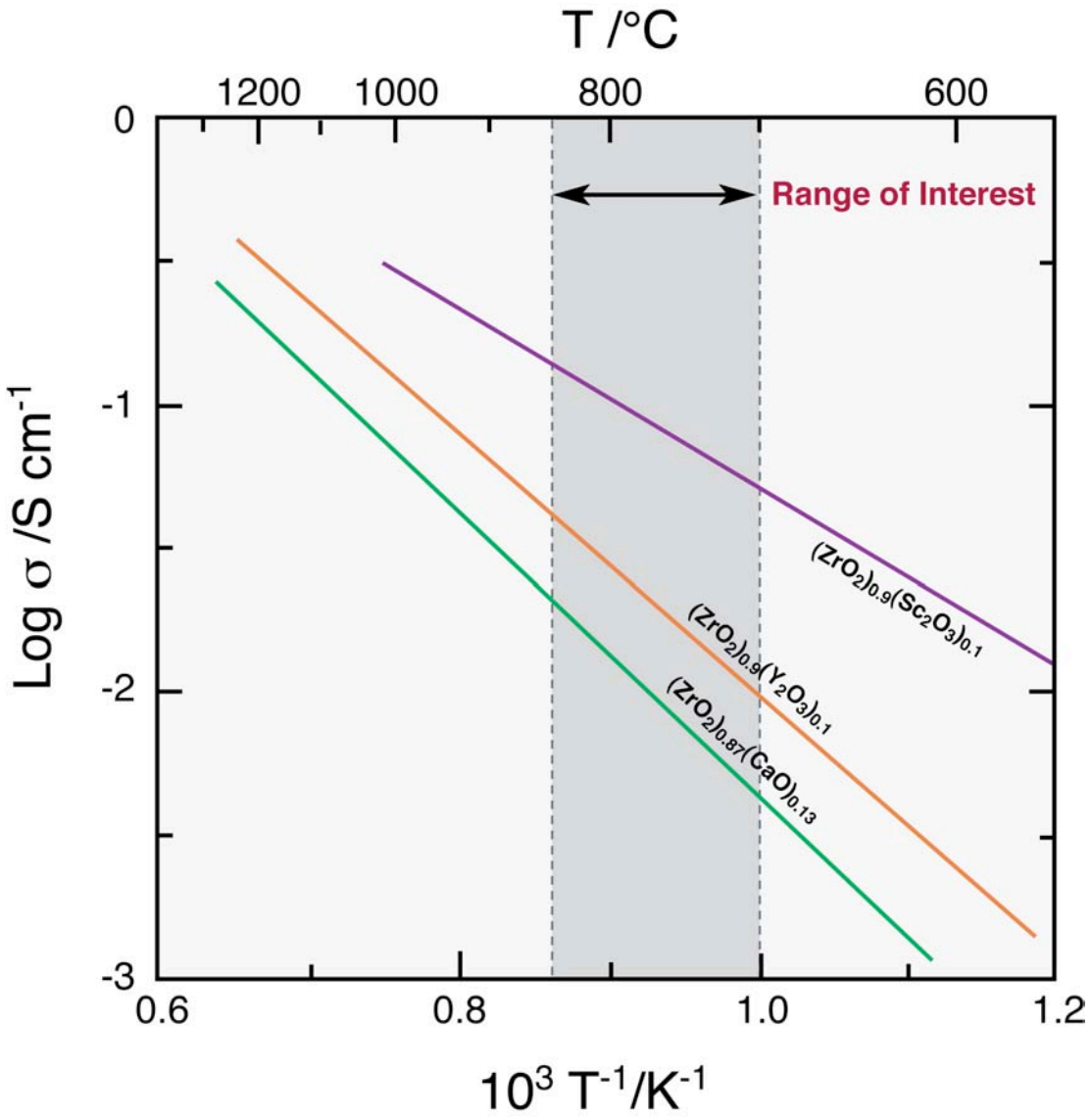

Ohmic Resistance – Electrolyte Materials (Emerging Systems)

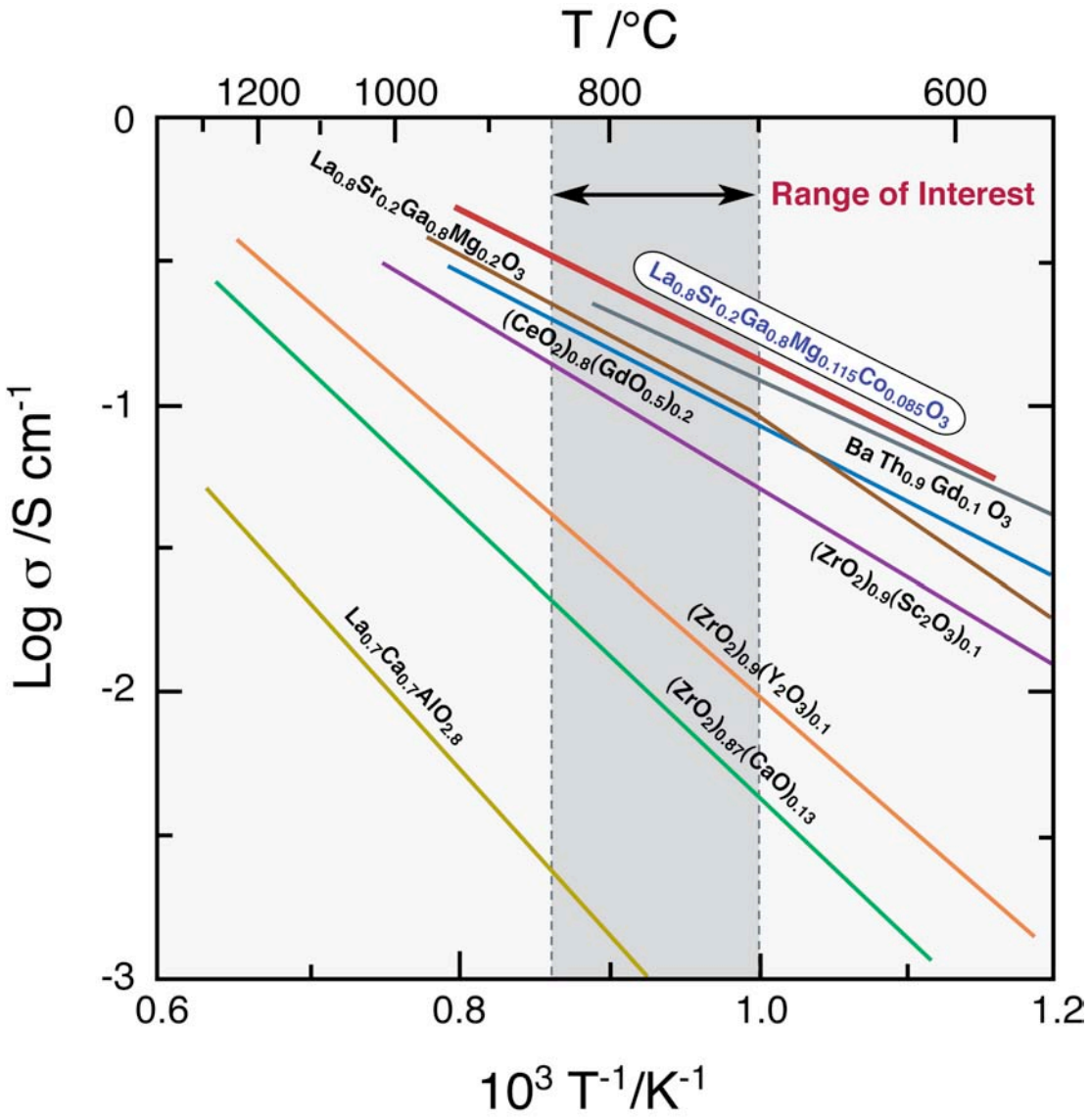

Ohmic Resistance – Electrolyte Materials (Emerging Systems)

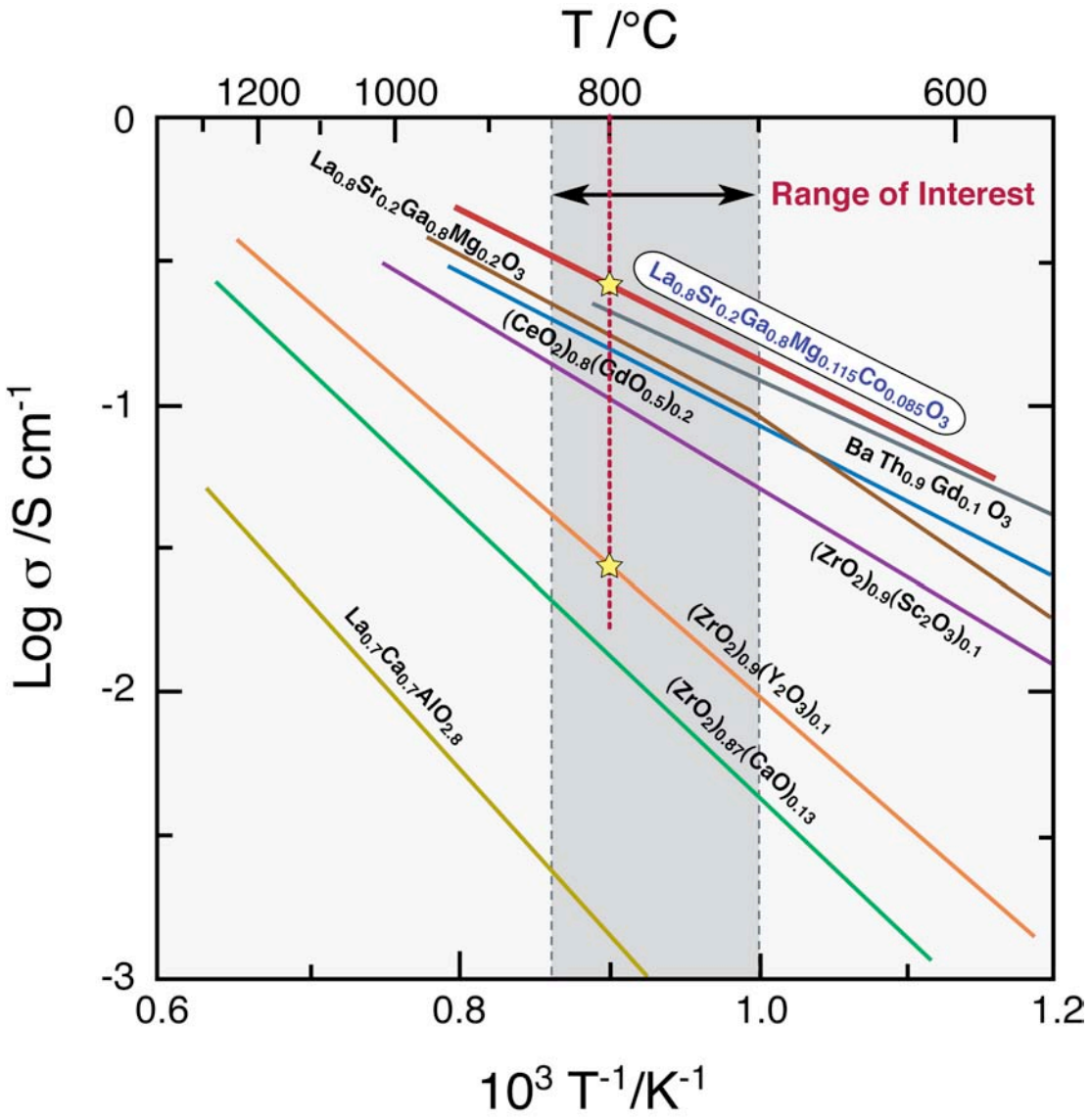

Ohmic Resistance – Electrolyte Materials (Emerging Systems)

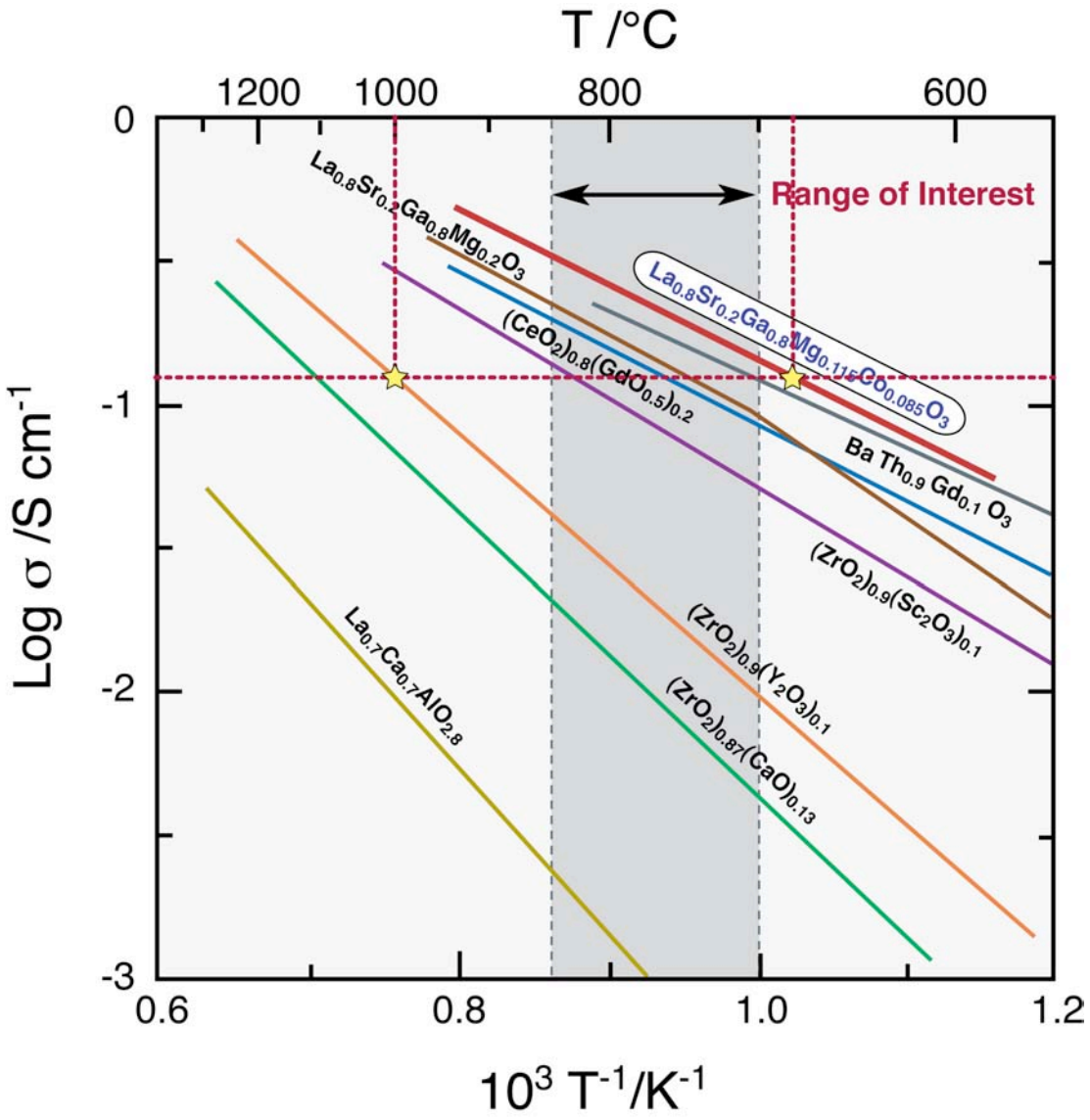

Glycine - Nitrate Combustion Synthesis Route

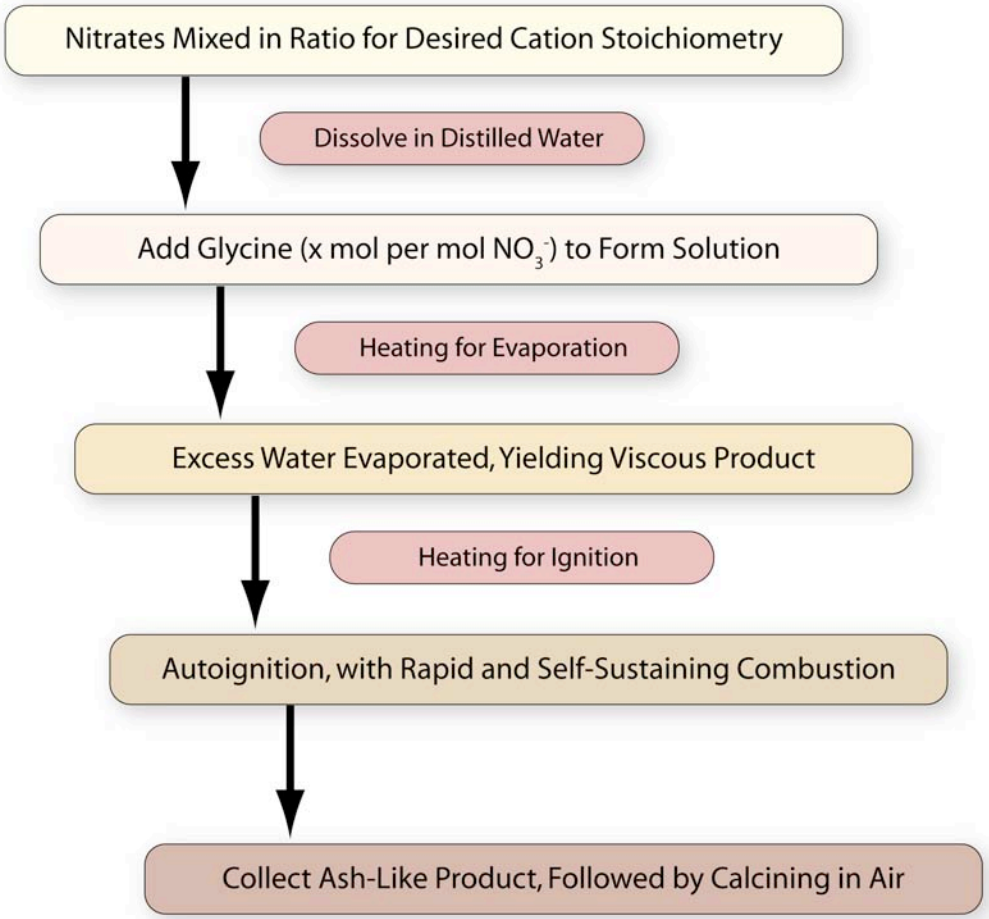

Candidate Materials

-- SSC $Sm_{0.5}Sr_{0.5}CoO_{3-\delta}$

-- LSGMC $La_{0.8}Sr_{0.2}Ga_{0.8}Mg_{0.115}Co_{0.085}O_{3-\delta}$

-- LSCF $La_{0.7}Sr_{0.3}Co_{0.2}Fe_{0.8}O_{3-\delta}$

Advantages of GNP Synthesis

- Availability of raw materials
- Good stoichiometric control
- Precise composition control
- Equipment simplicity
- Nano-scale products

X-Ray Analysis of Synthesized Materials – LSGMC Electrolytes

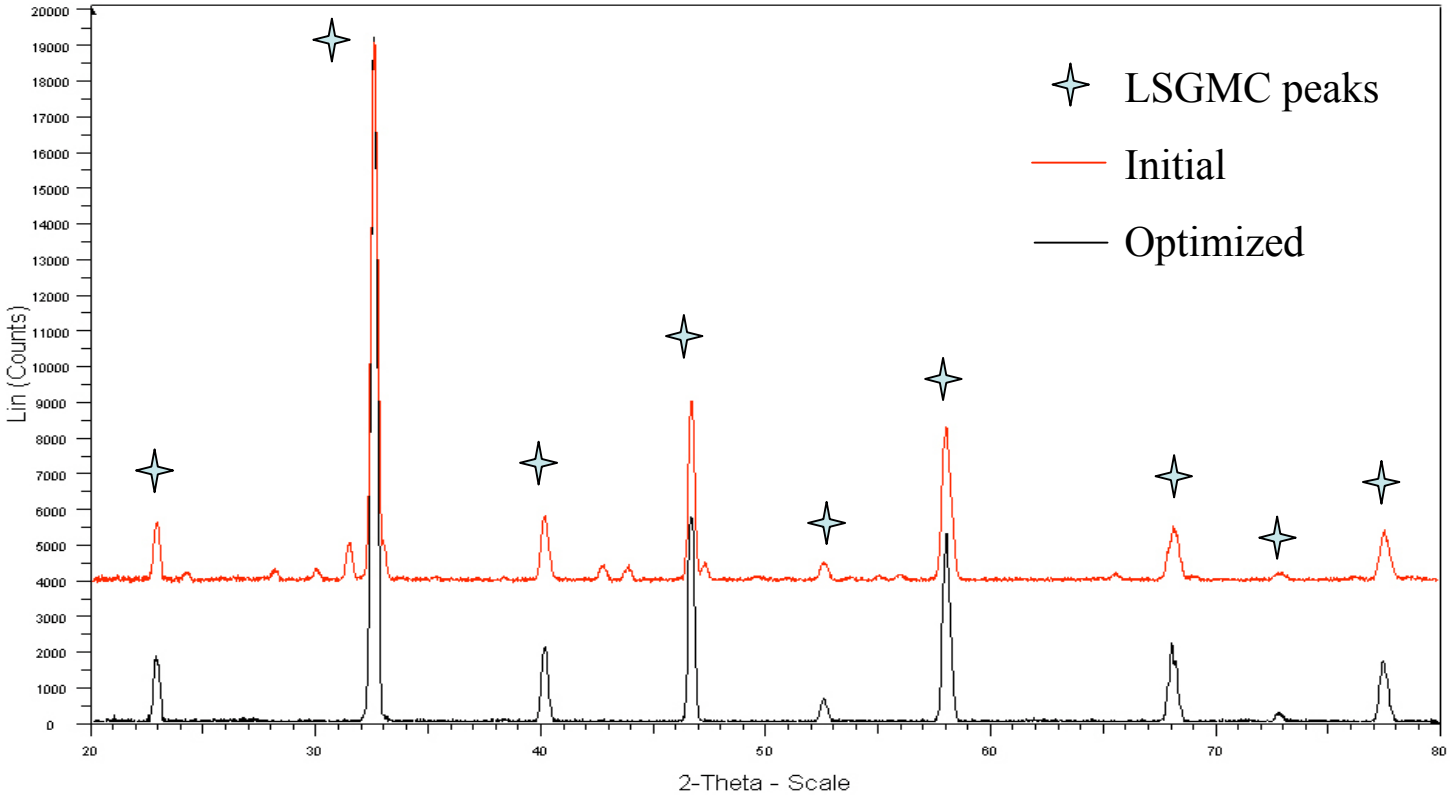

Precise control of reagent mixtures and associated lattice water content ensured phase purity

Conductivity for Synthesized LSGMC Materials

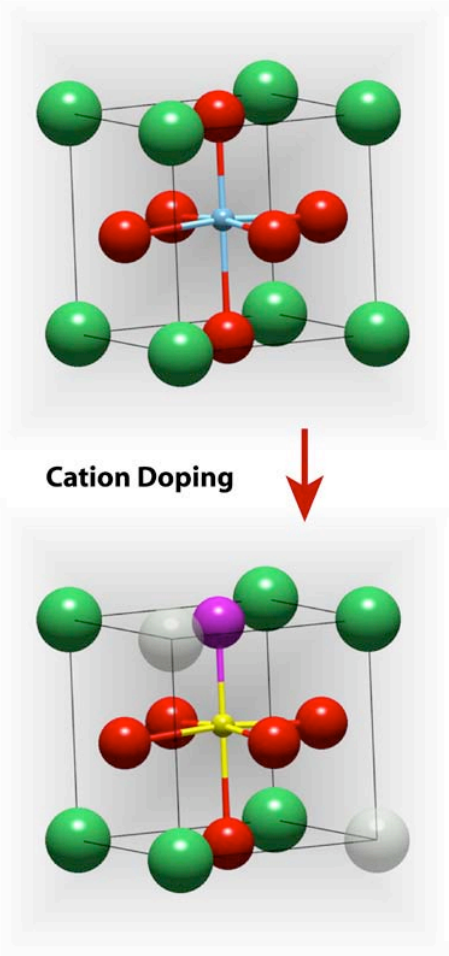

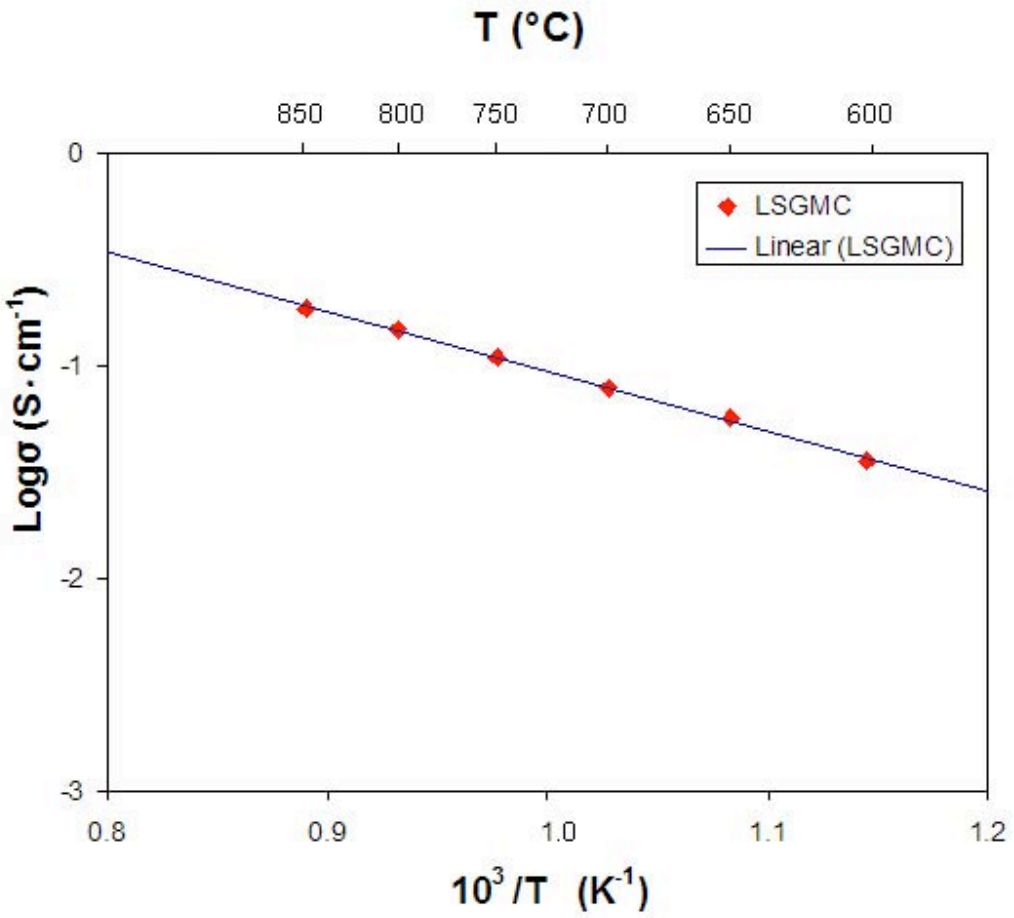

Materials Synthesis and Configuration - Perovskite Cathodes

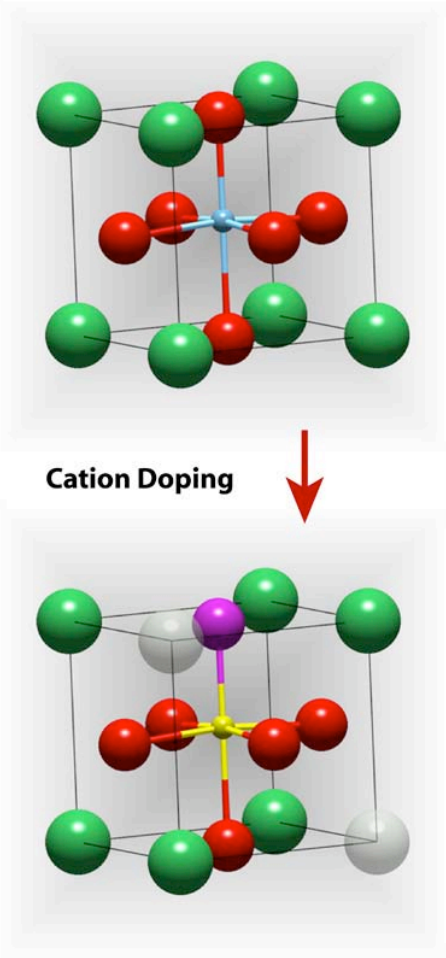

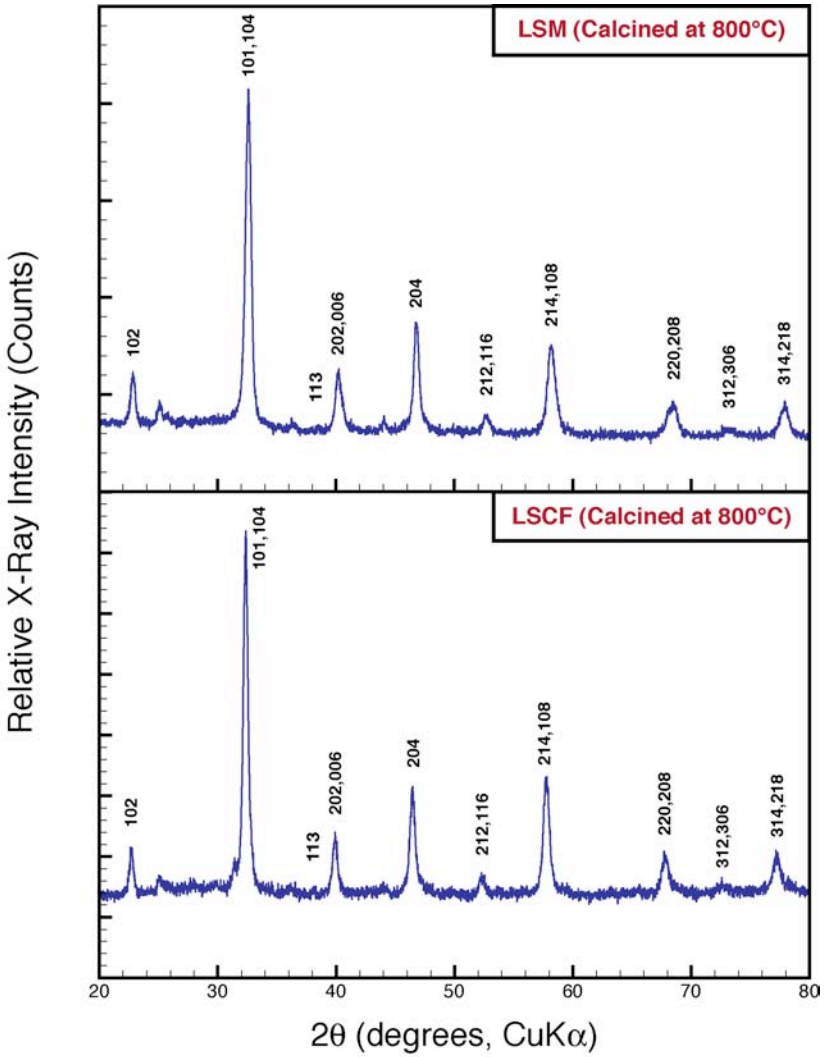

Contact Materials Synthesis - LNF:

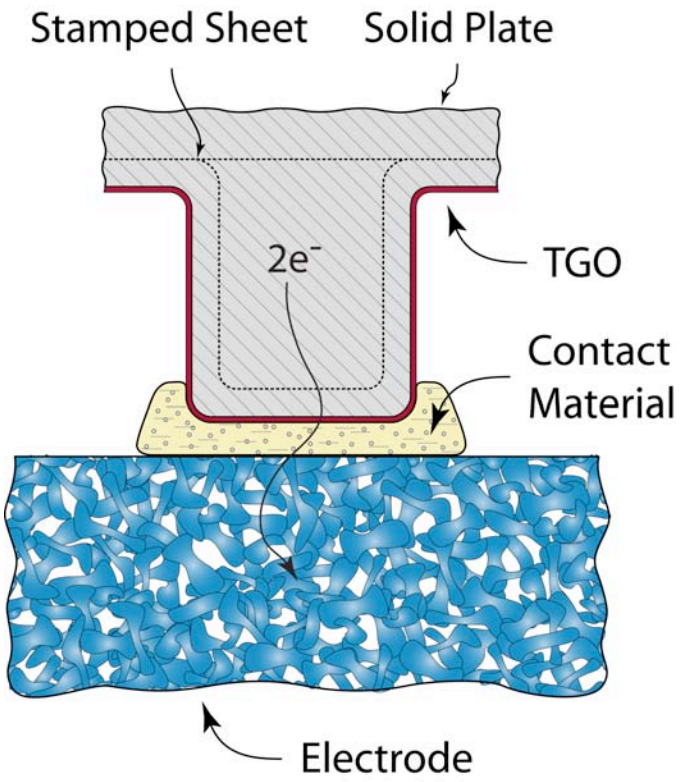

$La_{0.5}Ni_{0.5}FeO_{3-\delta}$

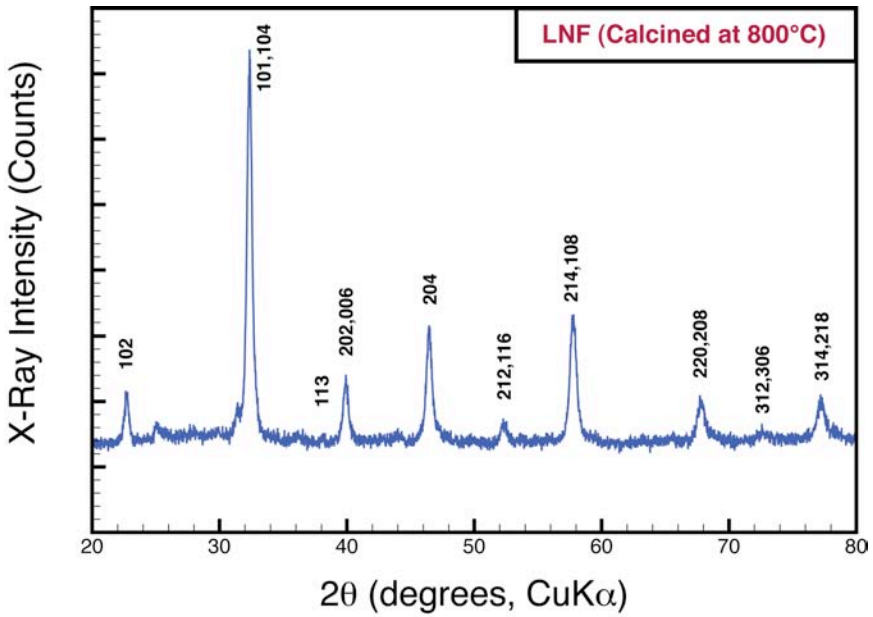

X-Ray Analysis of Synthesized Materials – SSC Cathode

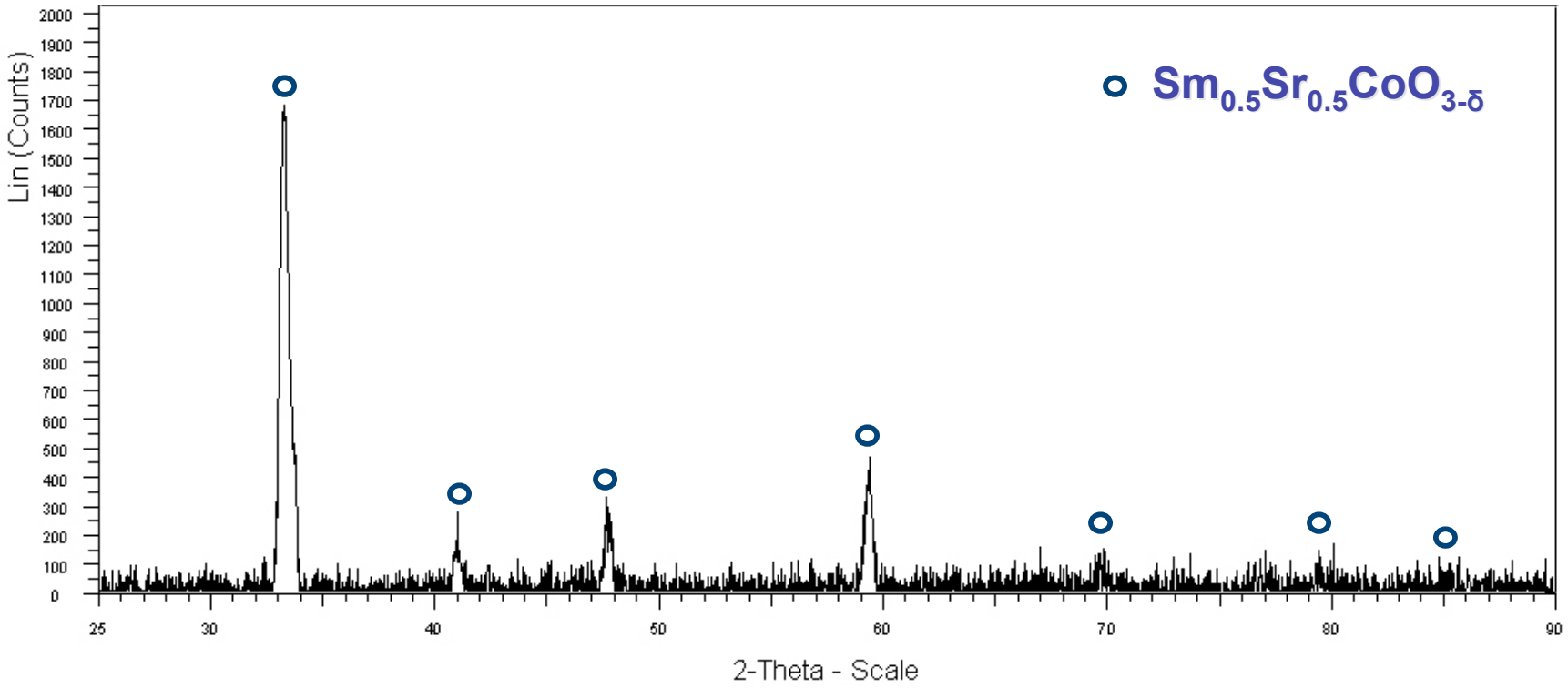

Orthorhombic Structure (space group 62:Pbnm)

a = 5.3591Å, b = 5.3927 Å, c = 7.5766 Å

Representative Microstructure of Cathode/Electrolyte Interface

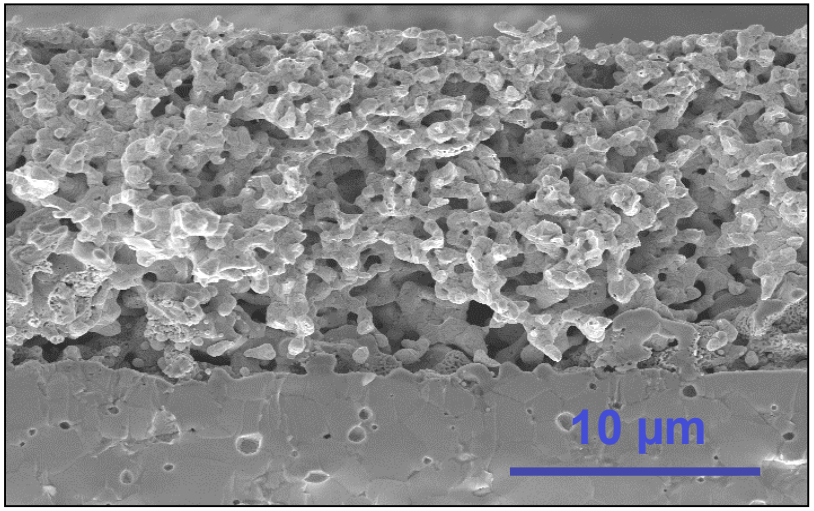

(a)

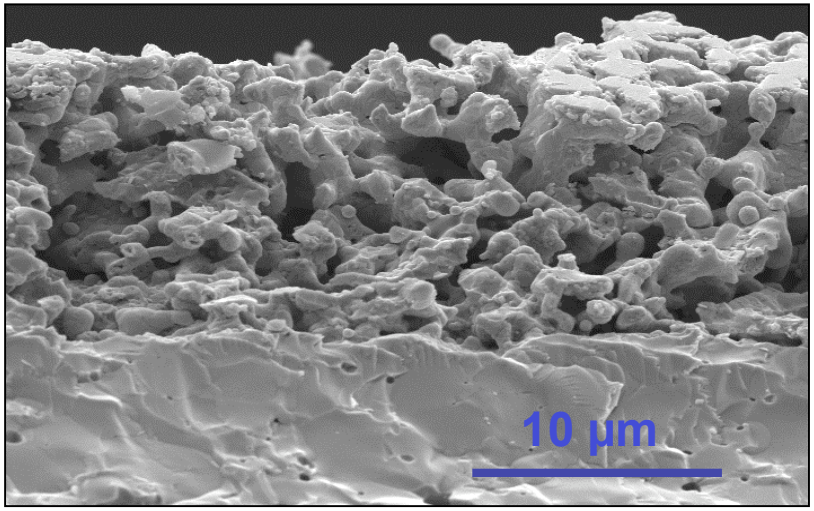

(b)

Cross-sectional views of (a) Composite SSC0.7LSGMC0.3 (b) SSC on LSGMC

Representative Microstructure of Cathode/Electrolyte Interface

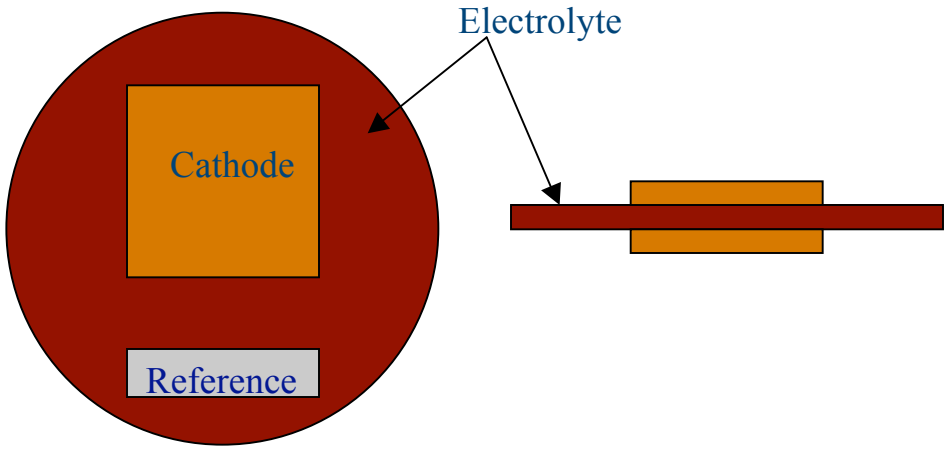

Schematic diagram of cathode/electrolyte interfacial characterization sample

Overpotential vs. Current density curves can be obtained to indicate the cathodic kinetics of investigated cathode materials base on Bulter-Volmer equation:

$$i = i_0 \left[\exp\left(\frac{\alpha_a F \eta}{RT}\right) - \exp\left(-\frac{\alpha_c F \eta}{RT}\right) \right]$$

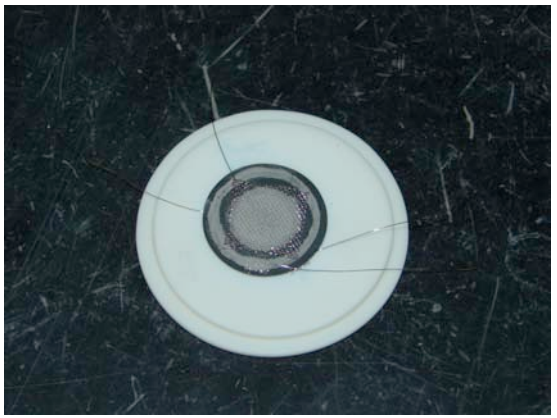

Overpotential Measurements:

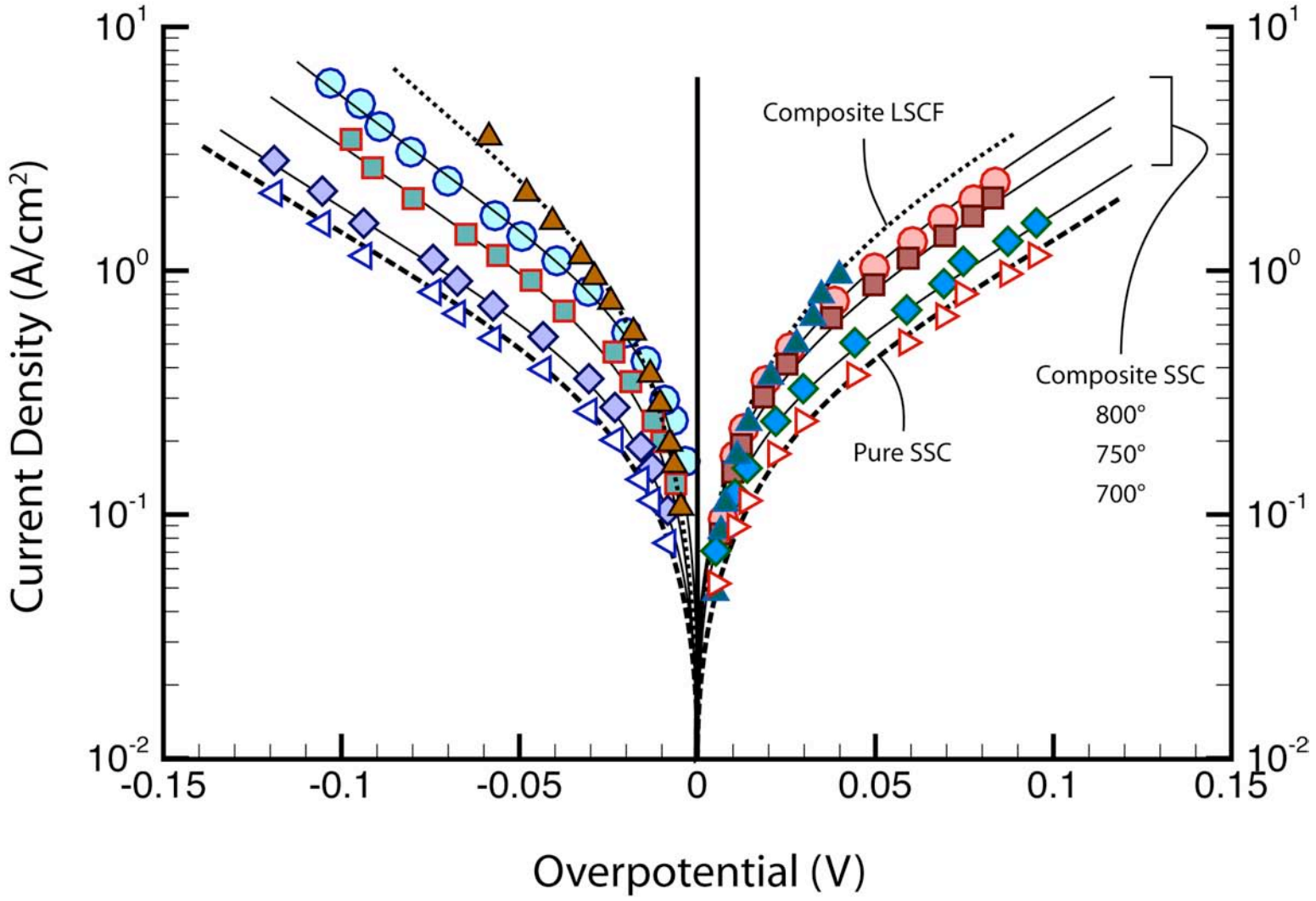

Planar Geometries

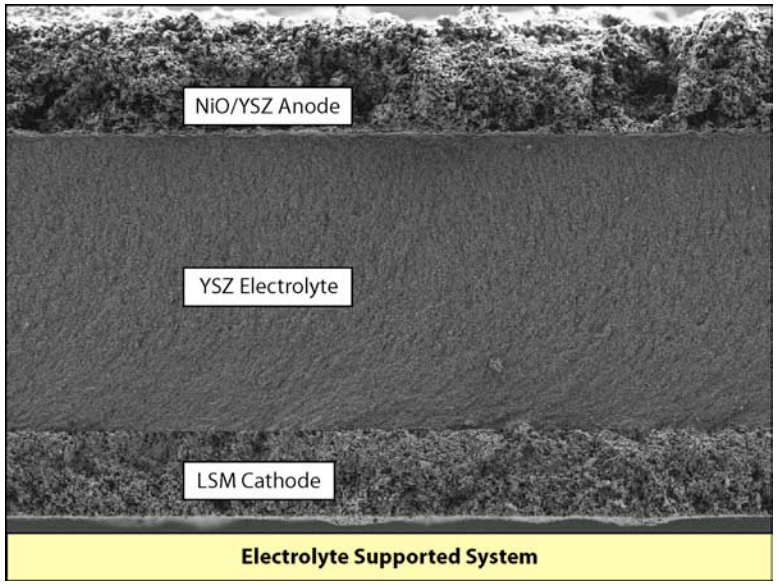

Electrolyte Supported System

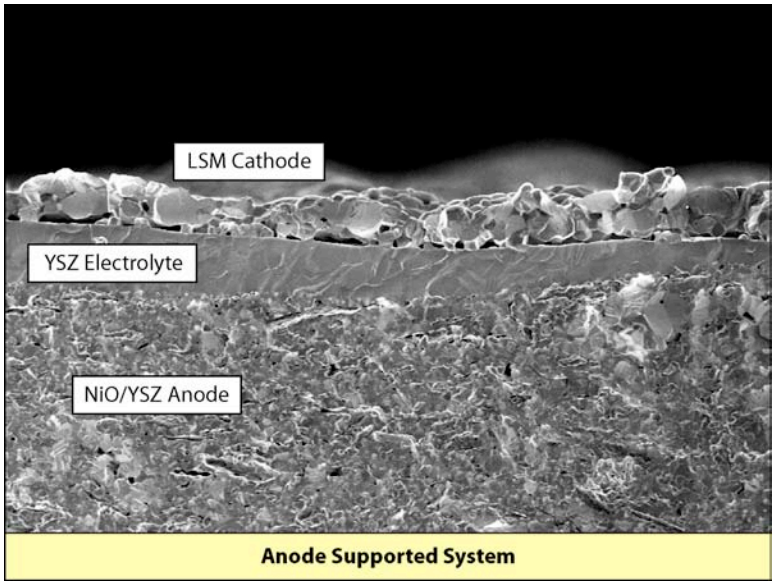

Anode Supported System

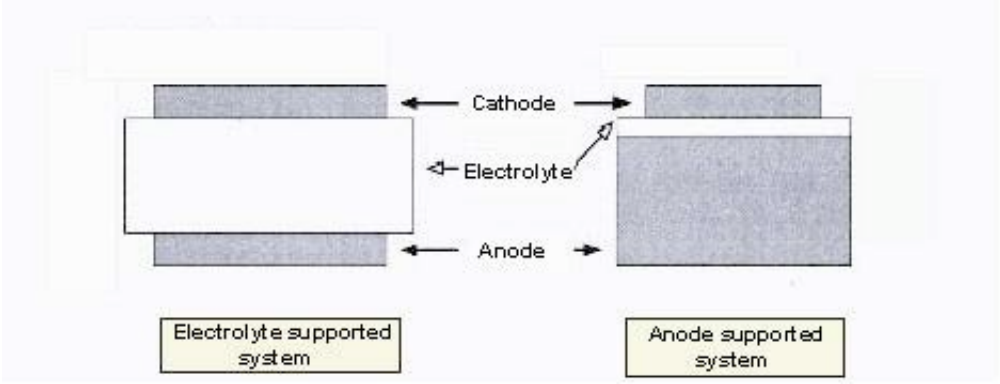

Stability (Conductivity Characteristics) of LSGMC Electrolytes

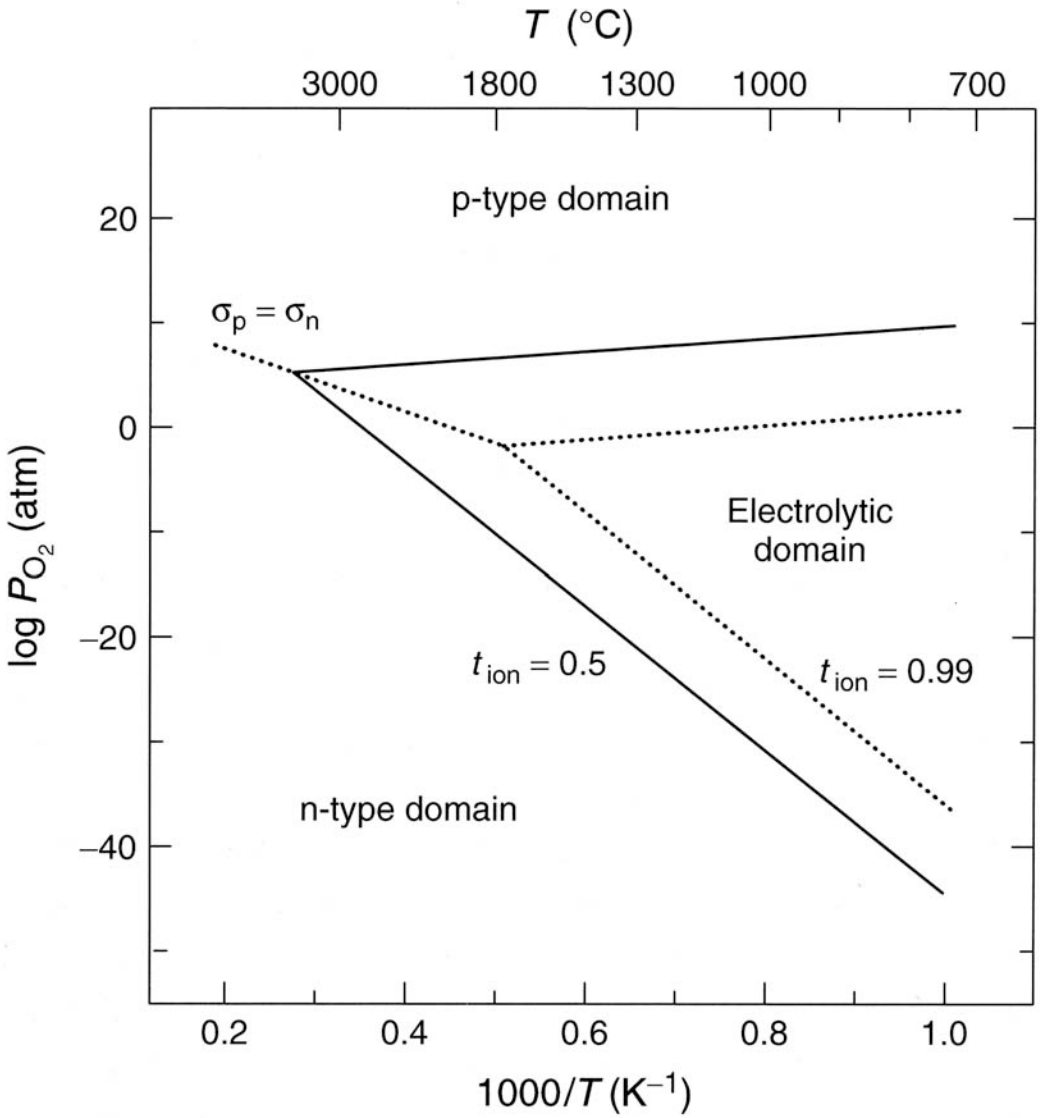

J.H. Kim and H.I. Yoo, et al.(2001) , Solid State Ionics, ***140****, 1051*

In-Service Degradation

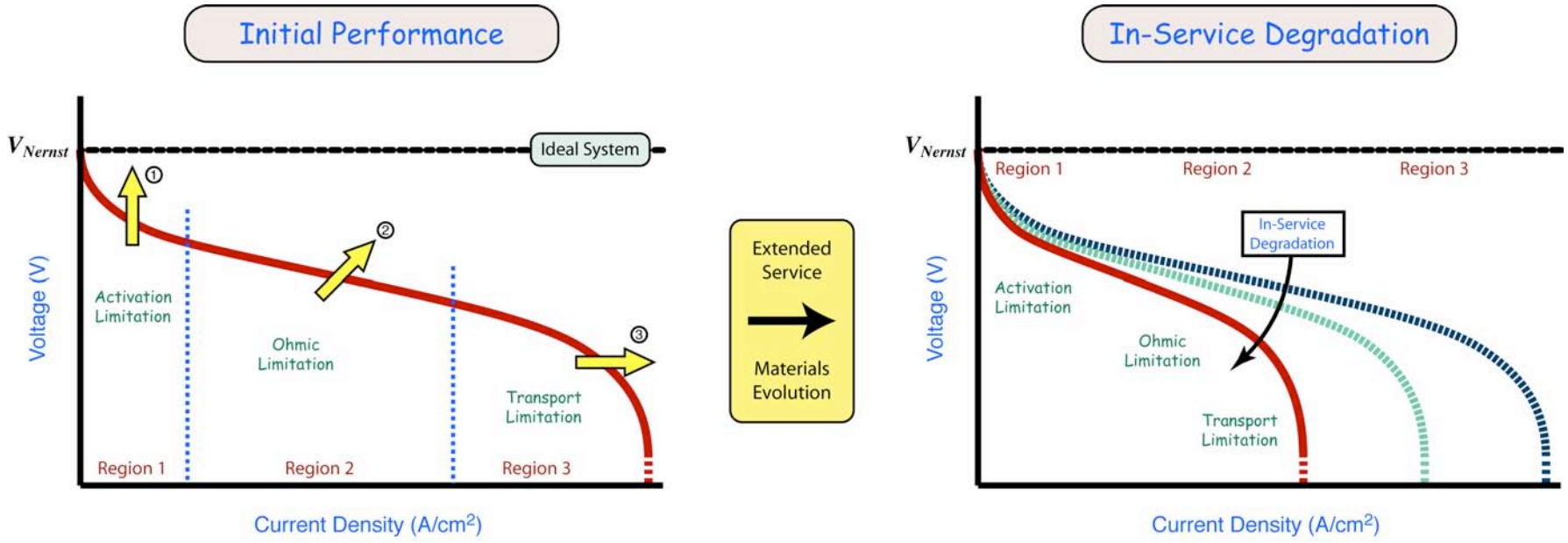

Surface Contamination and Poisoning, Coarsening, Oxidation,
Thermo-Mechanical Damage, Interdiffusion,Carbon Deposition, Void Growth,
Insulating Phase Formation, Interdiffusion,
RedOx Behavior, Vaporization,
etc.

Survey of Potential Degradation Processes - Incomplete

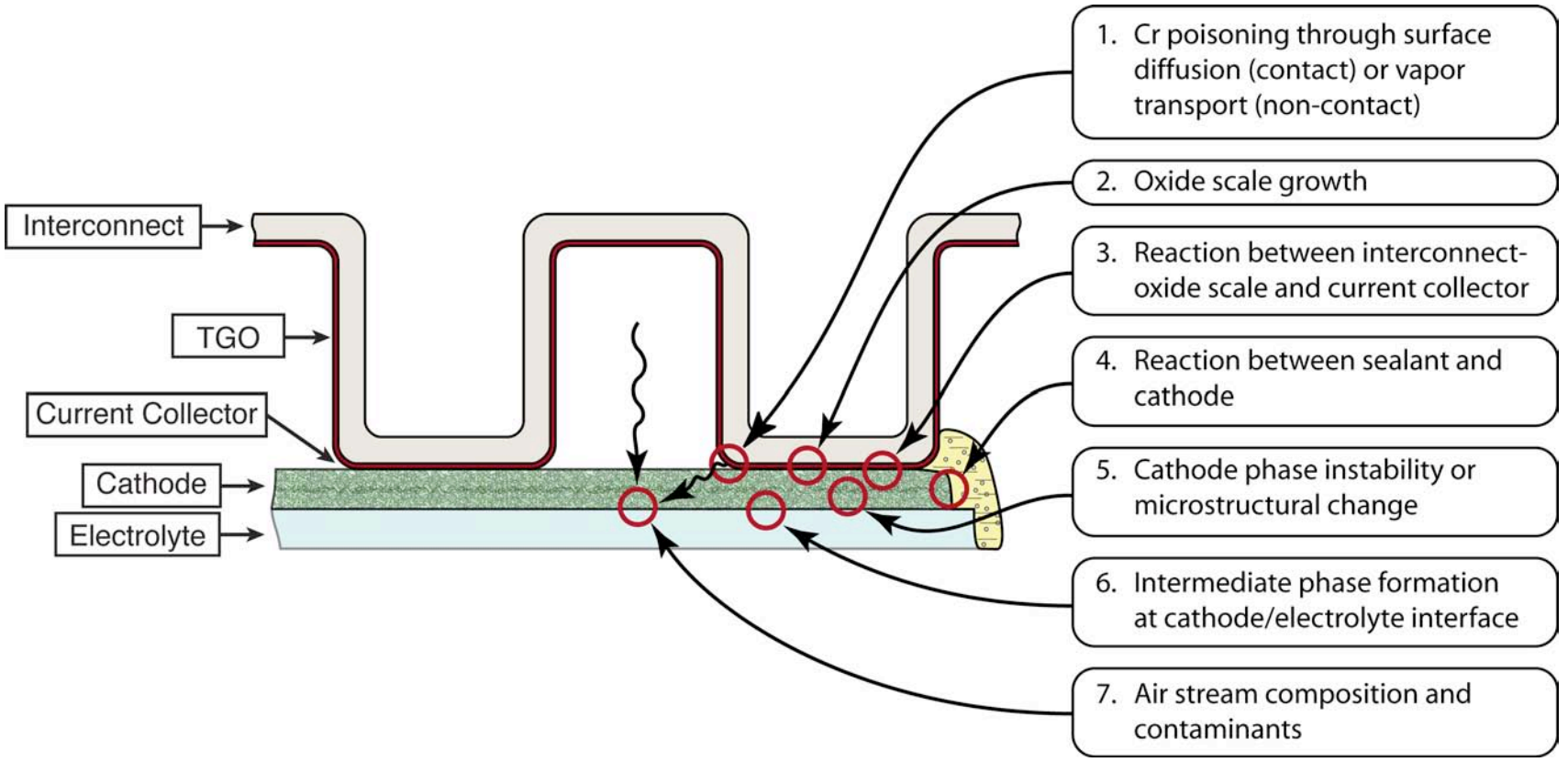

Cathode/Electrolyte Interface Reactivity

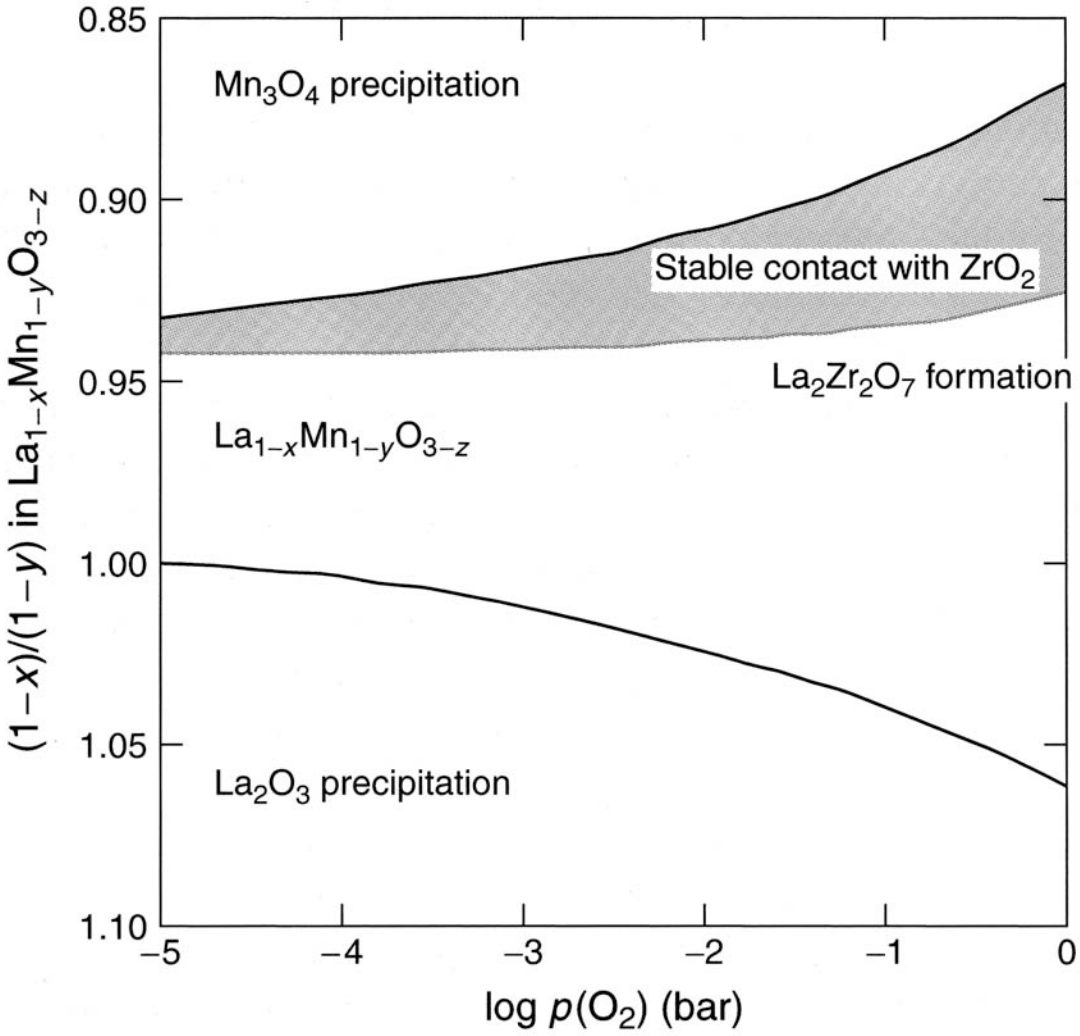

Yokokawa, et al.(1996) , Solid State Ionics, 86-88, 1161

Oxidation Under the Influence of Transverse Current - Theoretical:

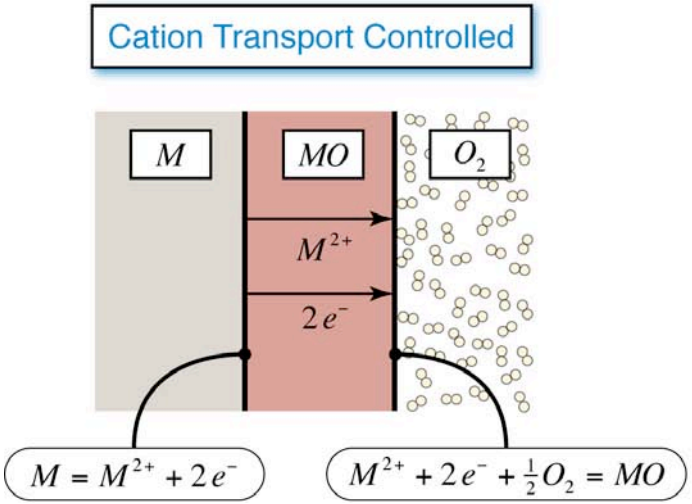

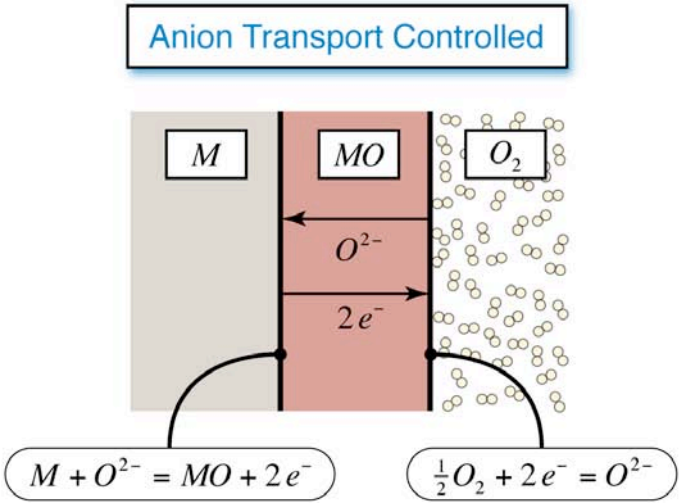

Charge Balance:

$$j_{e^-} + r\, j_{x^{z-}} + m\, j_{M^{m+}} = I_{ox}$$

Oxidation Rate:

$$\frac{dx}{dt} = \left(\frac{dx}{dt}\right)_0 - \frac{I_{ox}}{erb}\left(t_{ox} + t_x\right)$$

$$t_1 + t_2 + \ldots + t_i \ldots = 1 \qquad t_i = \frac{\sigma_i}{\sigma}$$

ASR Measurements – Independent Assessment of Current Effects:

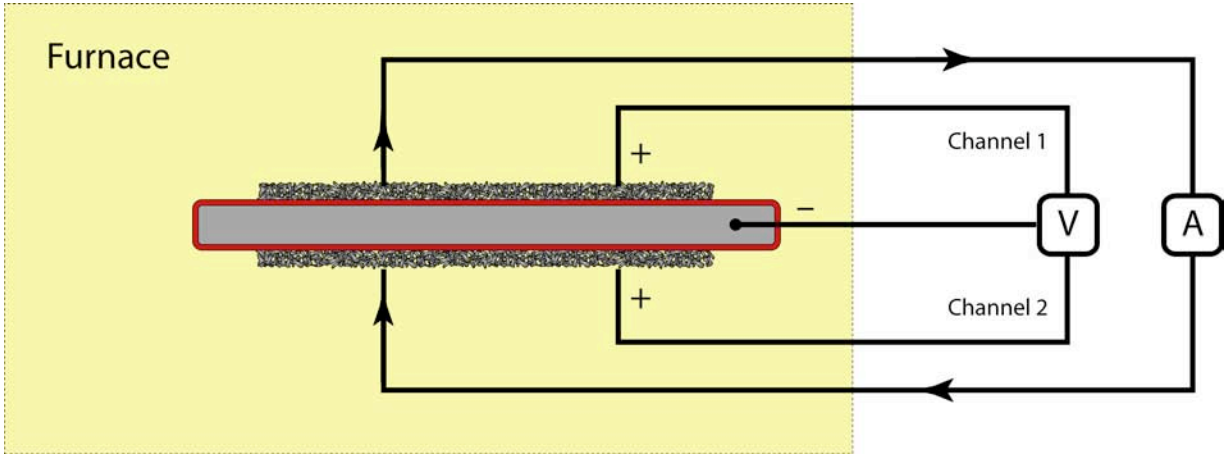

Dual channel voltage measurement

DC current sourcing

Current sourcing and resistance measurements at 10-1000mA (per square cm)

Resistance measured using current-reversal methods for error reduction

Oxidation in the Presence of LSCF Contacting Material

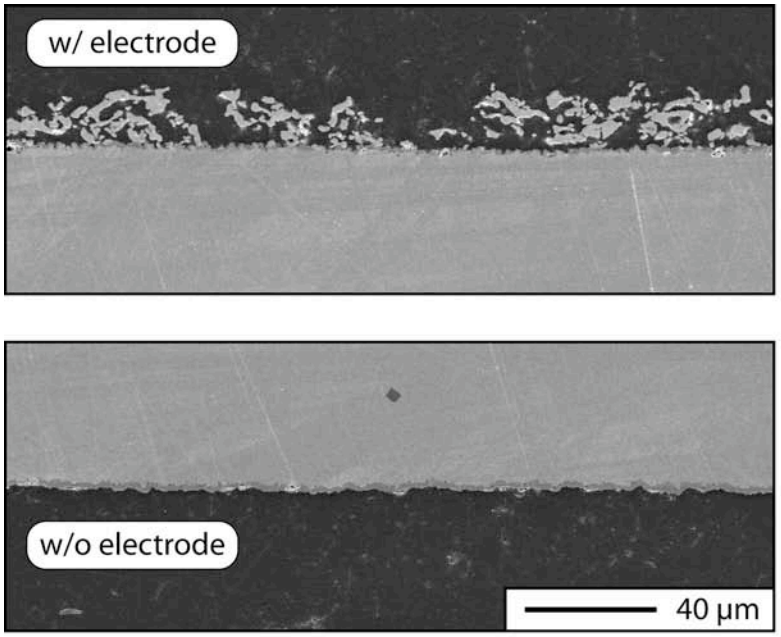

Low Magnification View

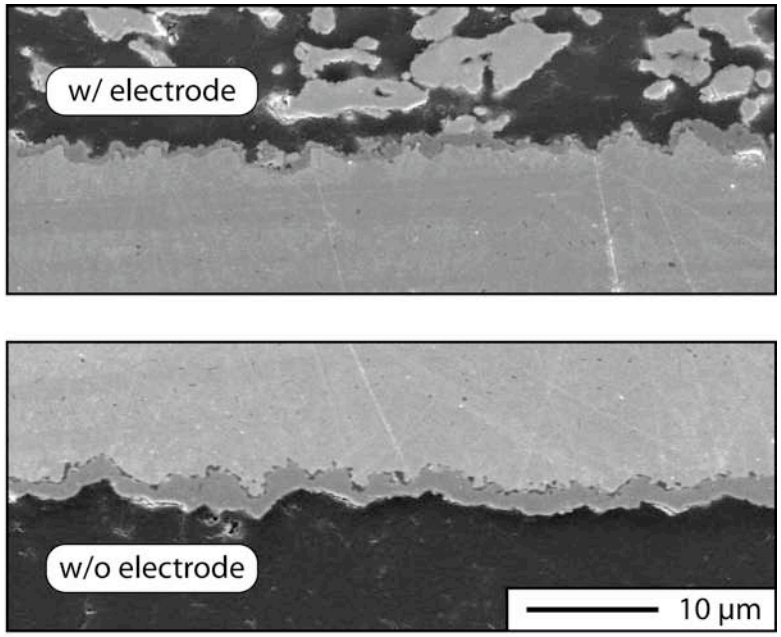

Higher Magnification View

Oxidation at 800°C – 1000 hours

Dry Air Exposure

E-Brite Alloy Substrate

Oxidation of SOFC Metal/Oxide Interfaces – Role of Current:

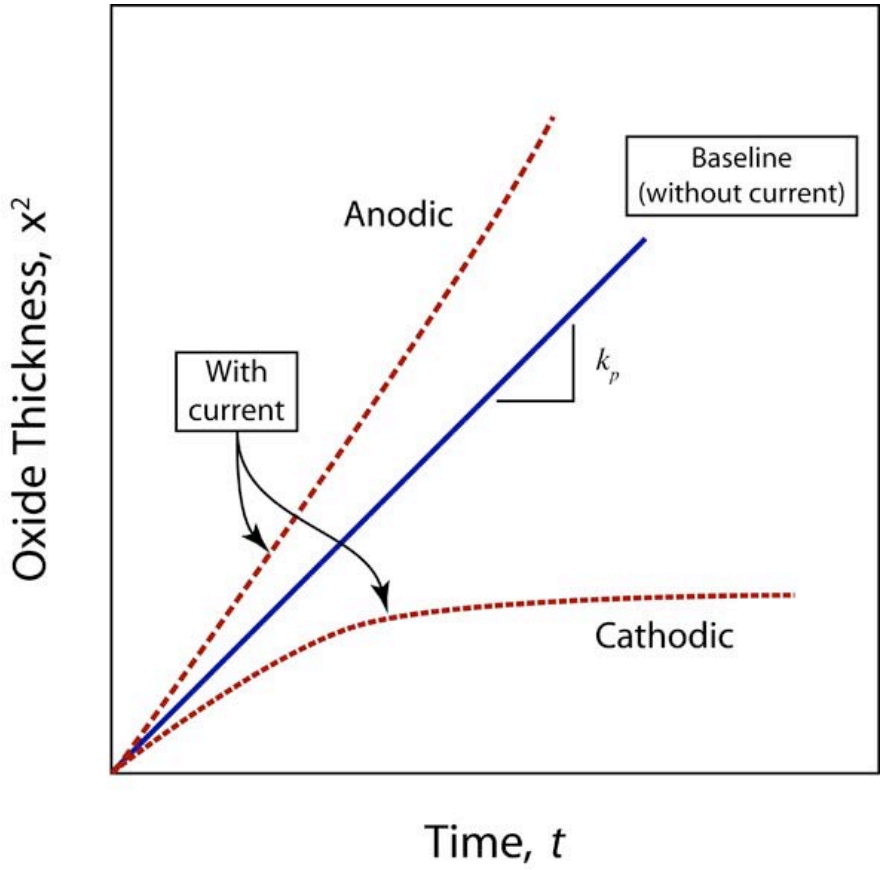

Oxidation Rate:

$$\frac{dx}{dt} = \left(\frac{dx}{dt}\right)_0 - \frac{I_{ave}}{erb}\left(t_{ox} + t_e\right)$$

Interconnect Degradation Rates
May Depend
Upon Transverse Current Density

Oxidation in the Presence of LSCF Contacting Material

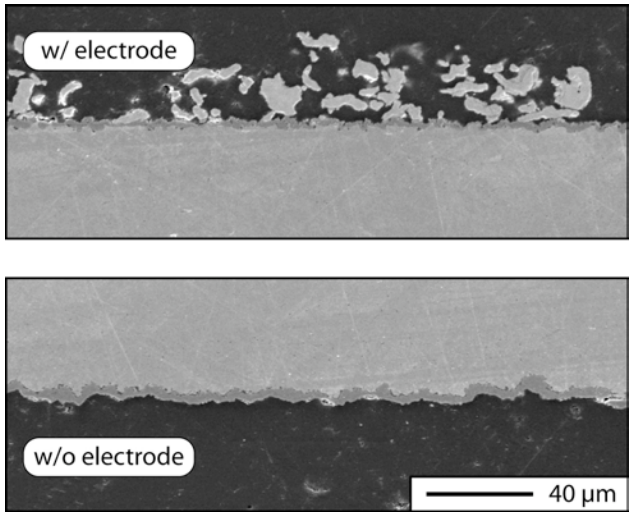

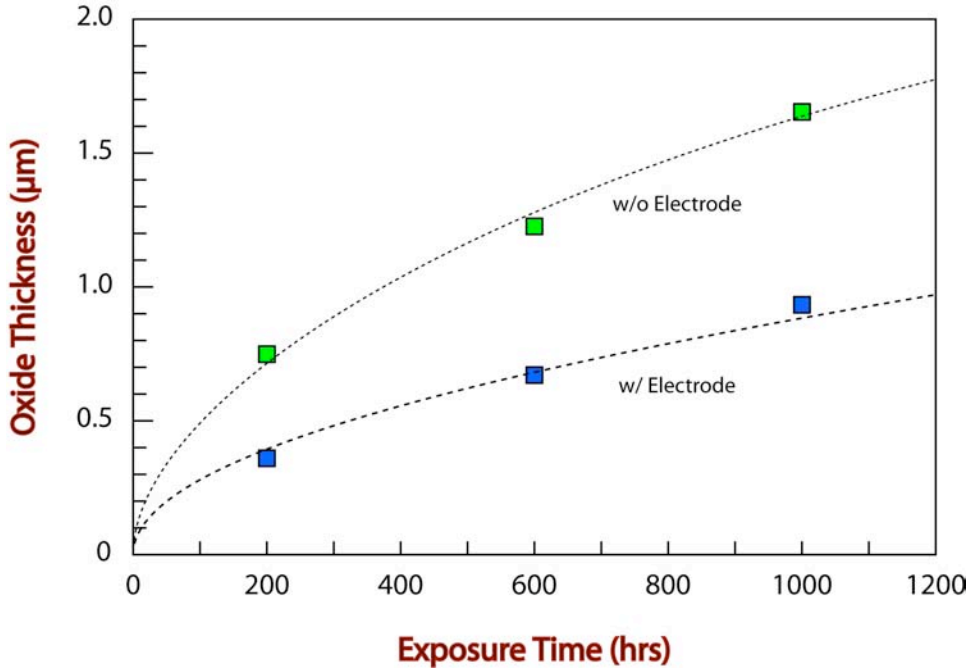

With Electrode: $K_p = 2.25 \times 10^{-15}\ cm^2\ s^{-1}$ $\left(2.8 \times 10^{-2}\ \mu m\ \sqrt{hr}\right)$

Without Electrode: $K_p = 7.47 \times 10^{-15}\ cm^2\ s^{-1}$ $\left(5.2 \times 10^{-2}\ \mu m\ \sqrt{hr}\right)$

$$K_p = f\left(Material, Temp, Environment, Contacting\ Material\right)$$

Oxidation Under the Influence of Transverse Current - Experimental

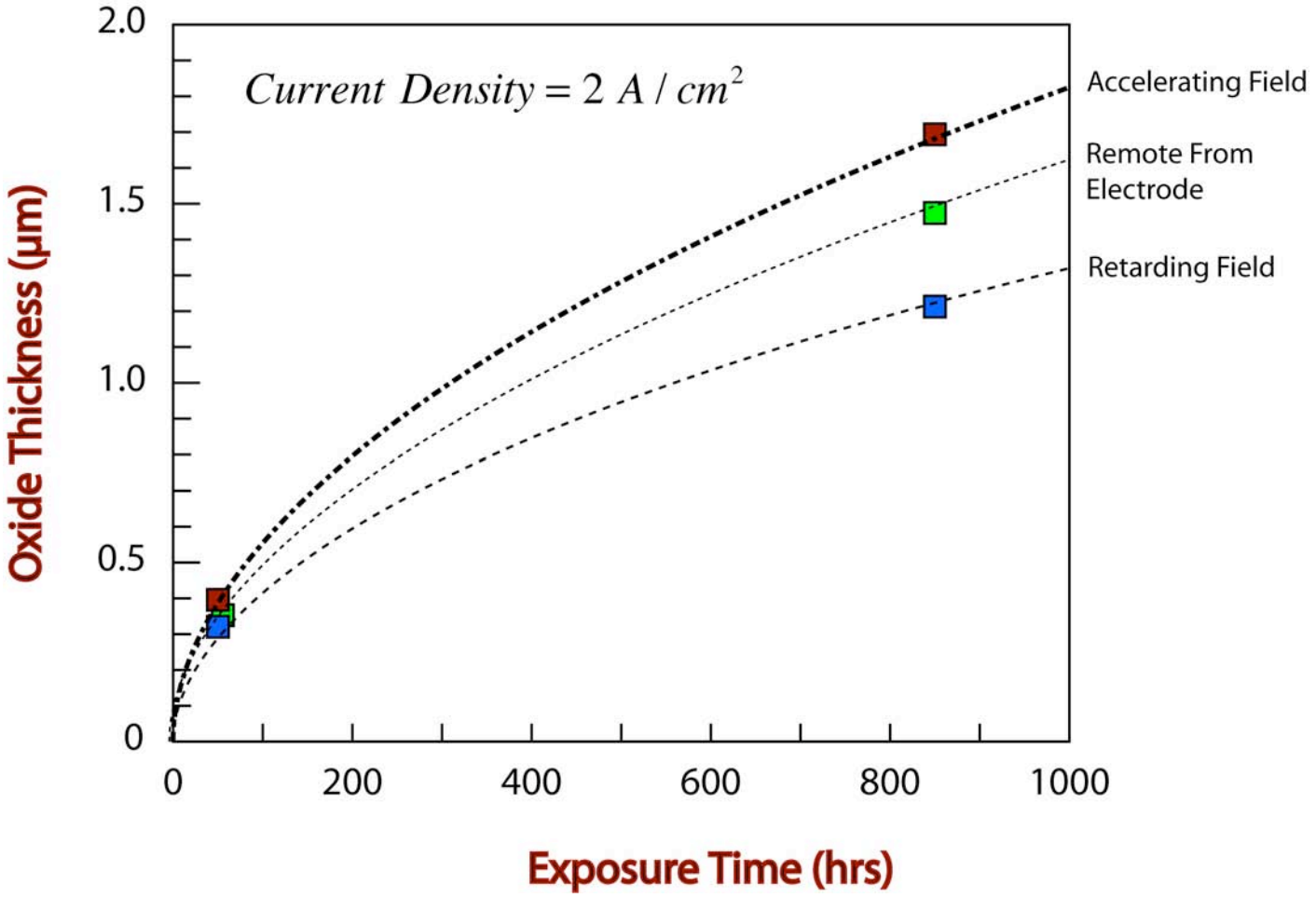

Ongoing Research - Combined Effects

Interplay between contacting materials and transverse current is possible

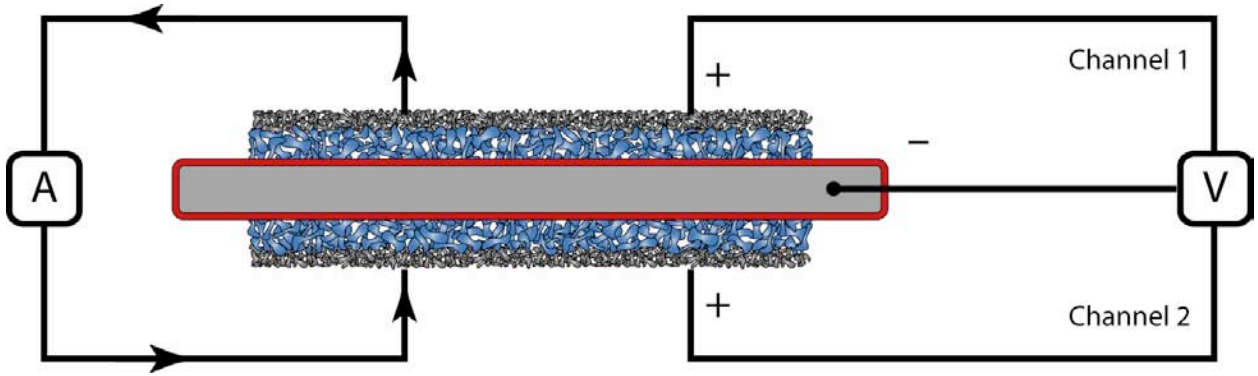

Oxidation Under the Influence of Transverse Current - Theoretical

Under normal oxidation conditions (no impressed current):

Flux of charged species:

$$j_i = -\frac{\kappa_i}{Z_i^2 F^2}\left(\frac{\partial \mu_i}{\partial x} + Z_i F \frac{\partial \phi}{\partial x}\right)$$

For transport of cations:

$$j_c = -\frac{\kappa_c}{Z_c^2 F^2}\left(\frac{\partial \mu_c}{\partial x} + Z_c F \frac{\partial \phi}{\partial x}\right)$$

Charge Balance:

$$j_{c^-} + r\, j_{x^-} + m\, j_{M^-} = 0$$

$$\frac{dx}{dt} = \frac{j_{x^-}}{b} + \frac{j_{M^-}}{a} \qquad ma = rb$$

Oxidation Under the Influence of Transverse Current - Theoretical

With Impressed Current:

Charge Balance:

$$j_{e^-} + r\, j_{x^+} + m\, j_{M^{m+}} = I_{ext}$$

Potential Gradient:

$$\frac{\partial \phi}{\partial x} = \left(\frac{\partial \phi}{\partial x}\right)_0 - \frac{I_{ext}}{\sigma}$$

Oxidation Rate:

$$\frac{dx}{dt} = \left(\frac{dx}{dt}\right)_0 - \frac{I_{ext}}{erb}\left(t_{ox} + t_x\right)$$

$$t_1 + t_2 + \ldots + t_i \ldots = 1$$

$$t_i = \frac{\sigma_i}{\sigma}$$

In-Situ ASR Measurement with 'Standard' Pt-Paste Electrodes

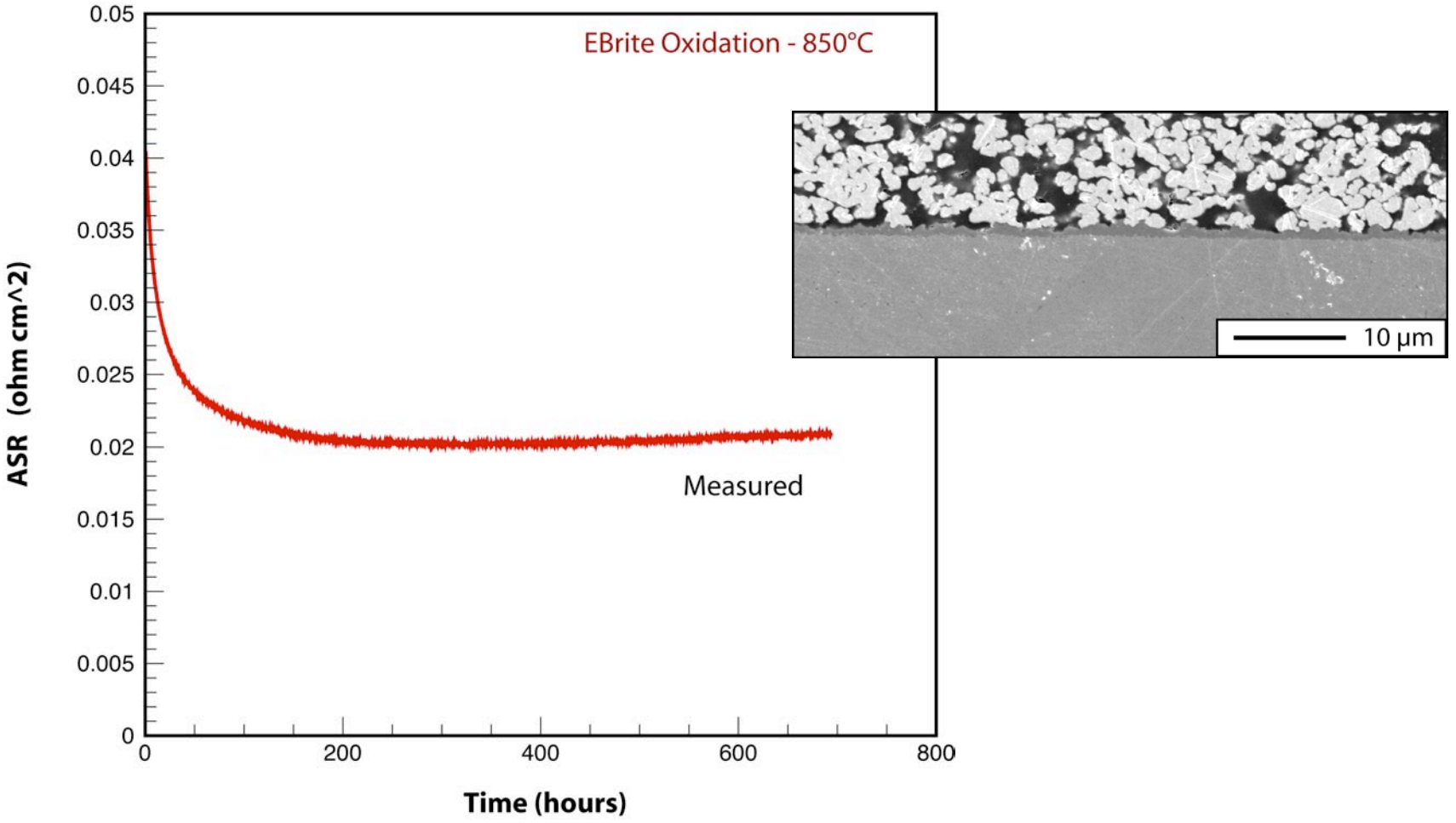

Discriminating Electrode and TGO Effects

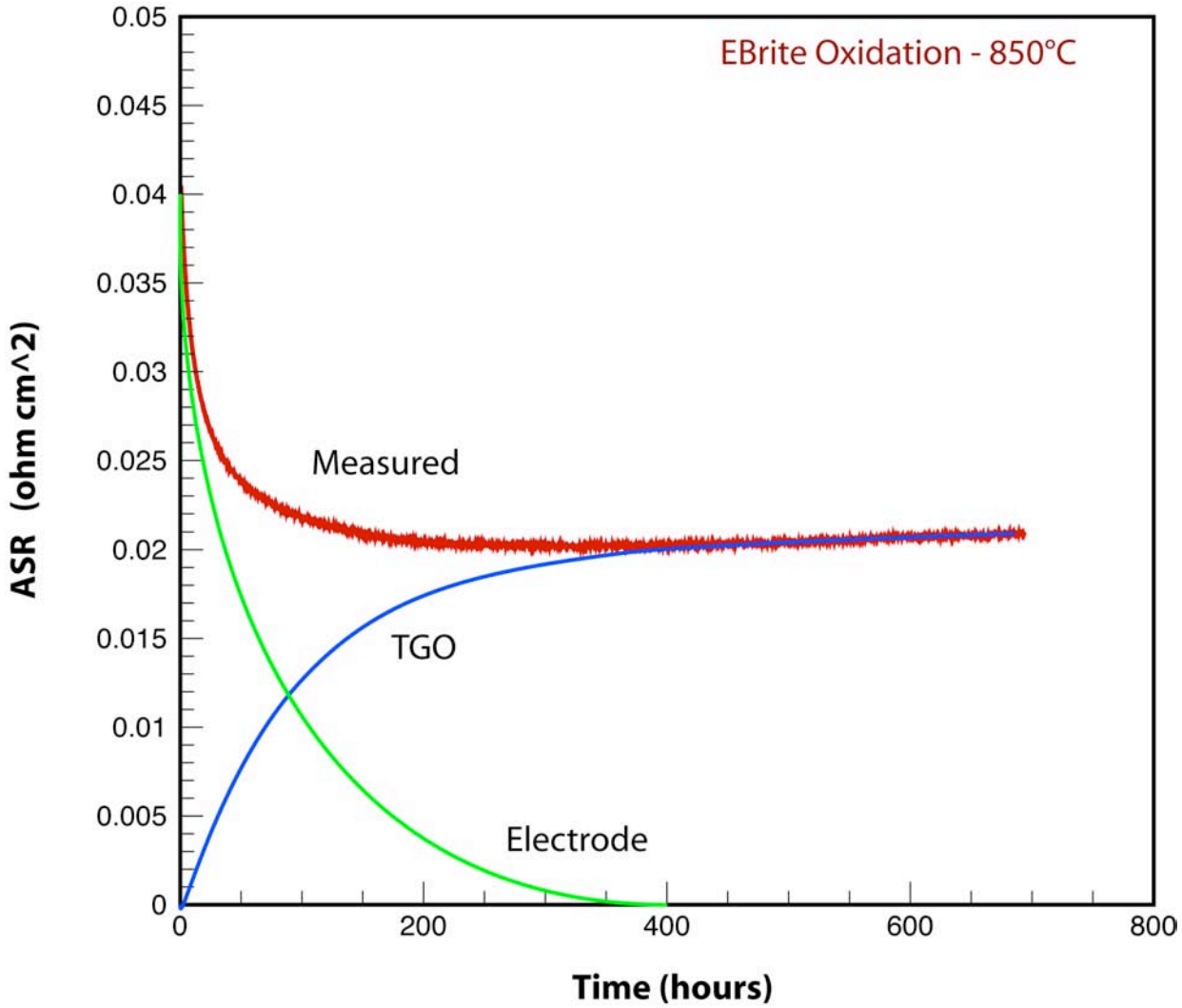

Discriminating Electrode and TGO Effects

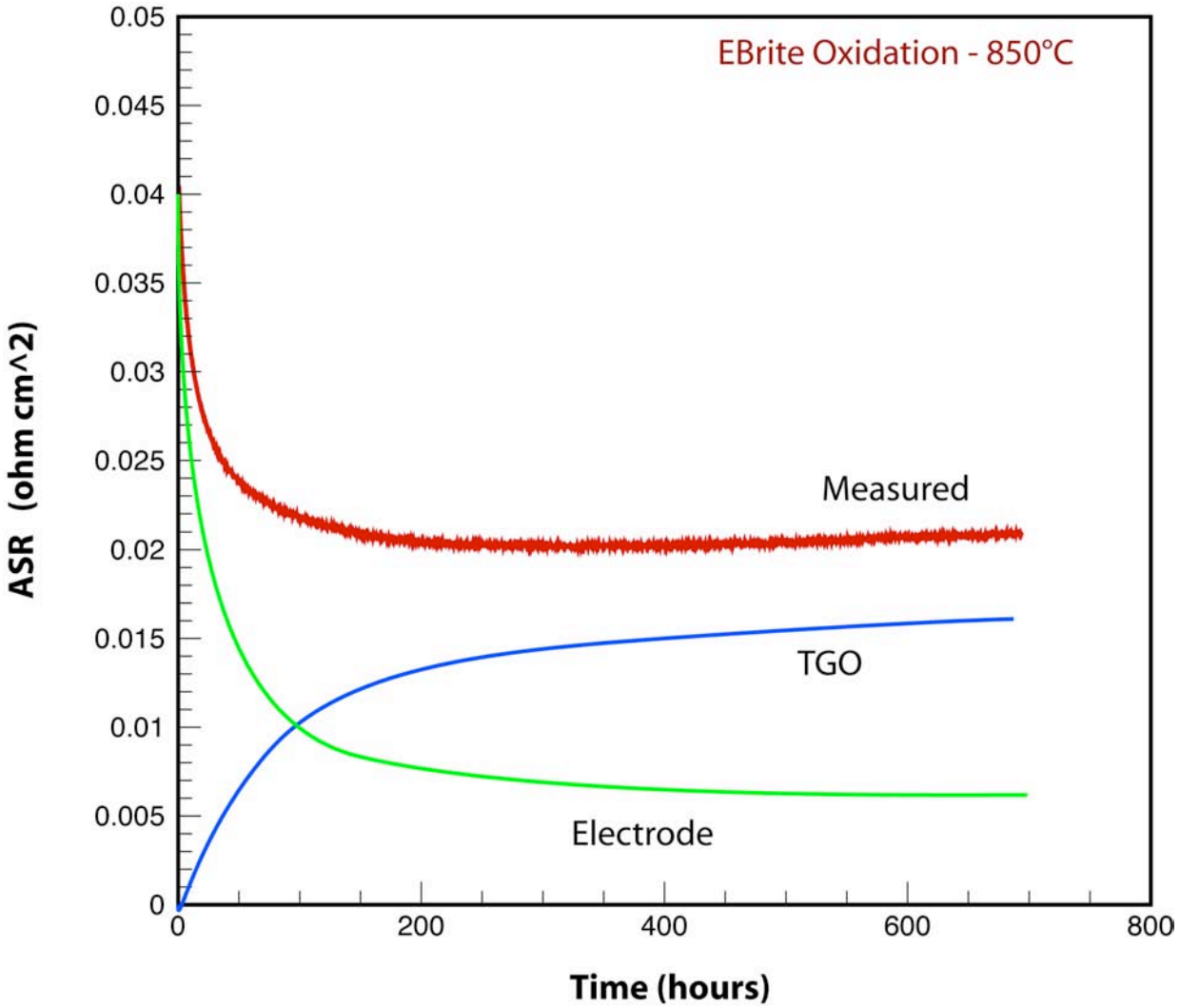

Composition and Evolution of Pt-Paste Electrodes

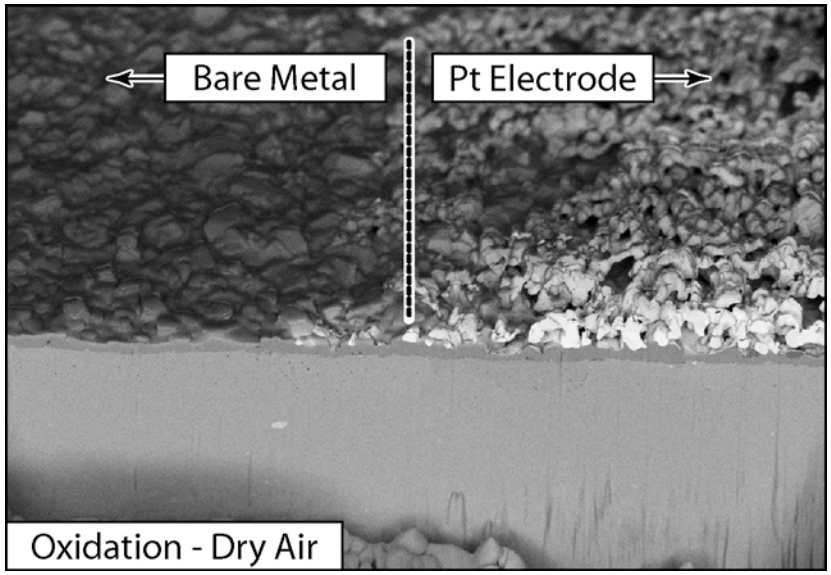

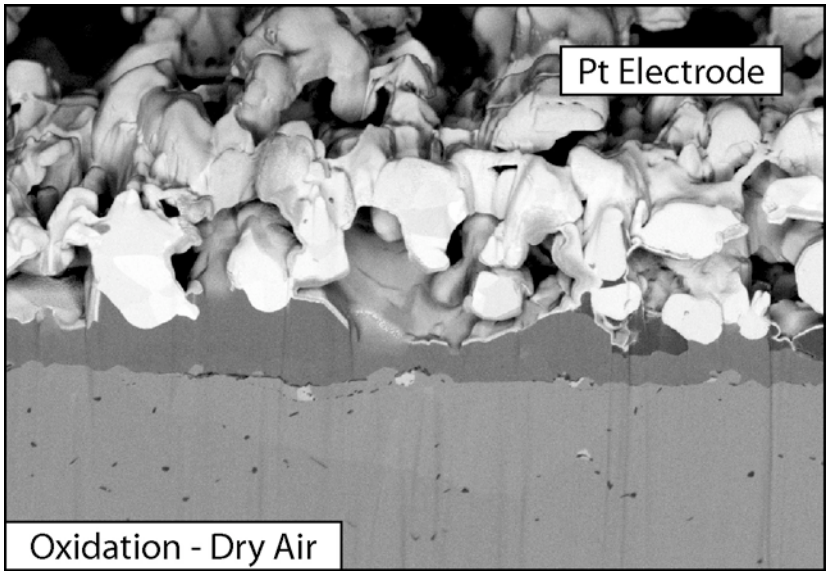

Bismuth fluxing agent and microstructural evolution contribute to overall ASR measurements

Oxidation Under the Influence of Transverse Current - Experimental

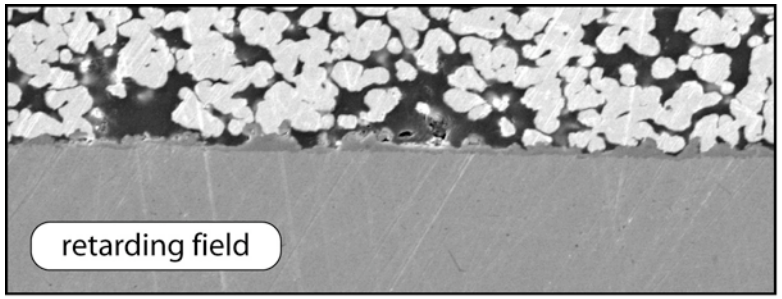

$$K_p = 4.87 \times 10^{-13}\ cm^2\ s^{-1}$$

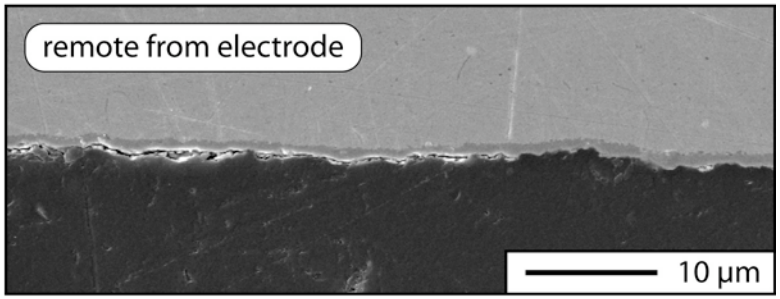

$$K_p = 7.32 \times 10^{-13}\ cm^2\ s^{-1}$$

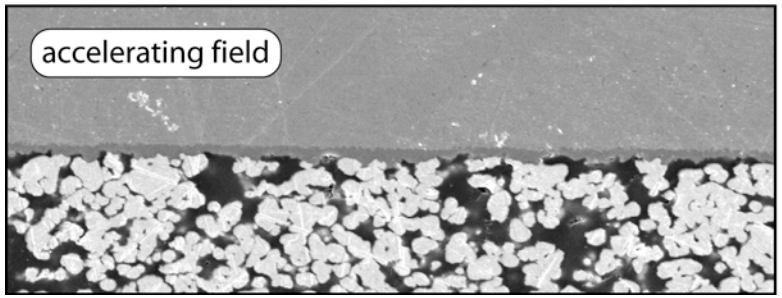

$$K_p = 9.24 \times 10^{-13}\ cm^2\ s^{-1}$$

Variation of Setup for ASR Measurement w/ Polarity Discrimination:

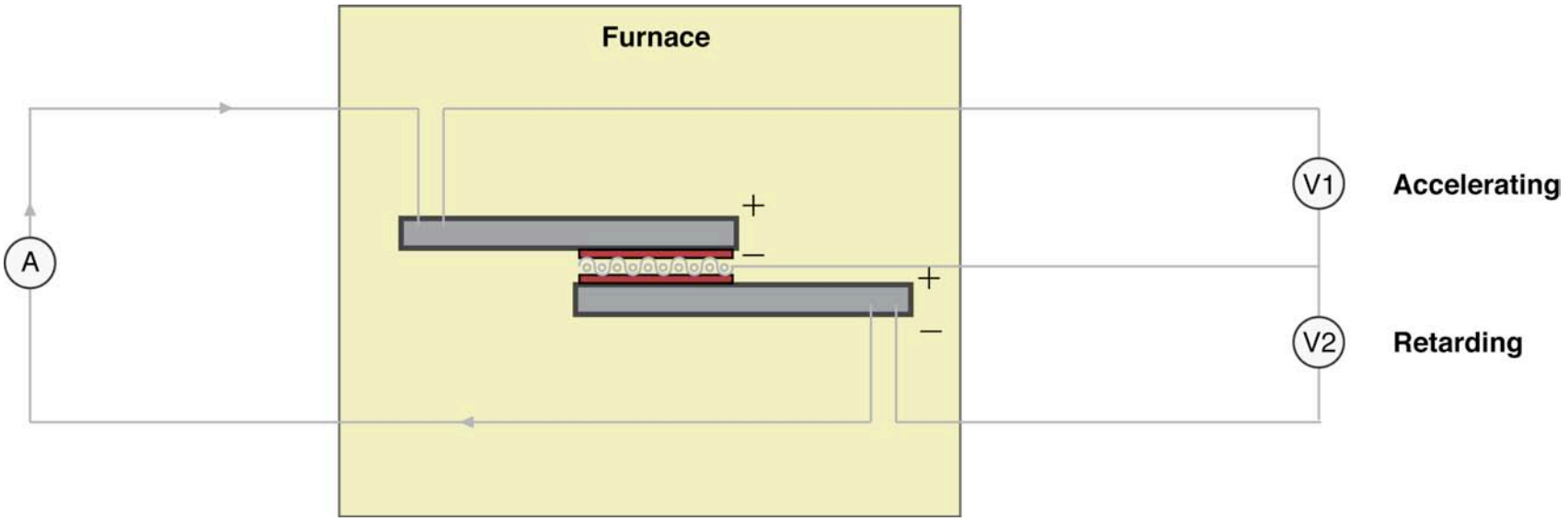

Plates are bonded with ceramic LNF contact paste
(ideally invariant with oxidizing conditions)

Variation of Setup for ASR Measurement w/ Polarity Discrimination:

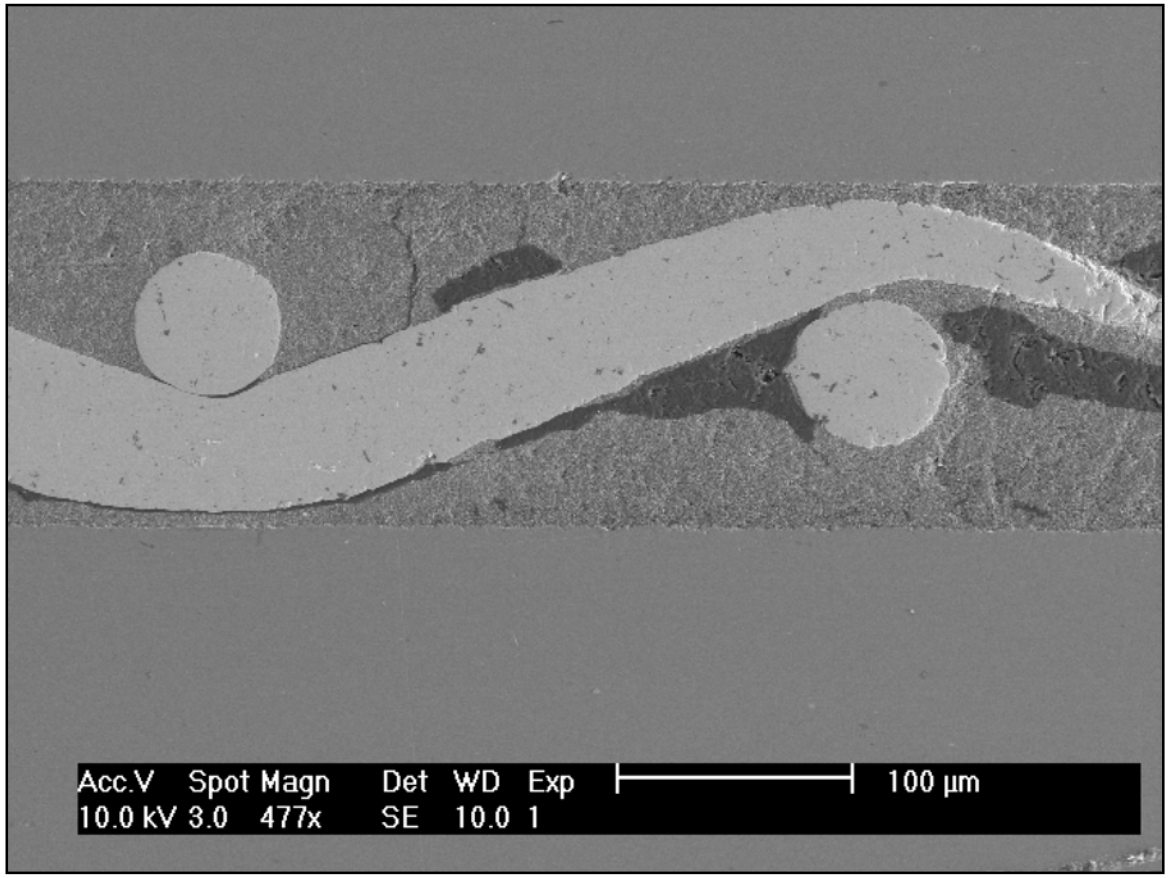

Plates are bonded with ceramic LNF contact paste (ideally invariant with oxidizing conditions)

Oxidation Under the Intermittent High-Current Exposures:

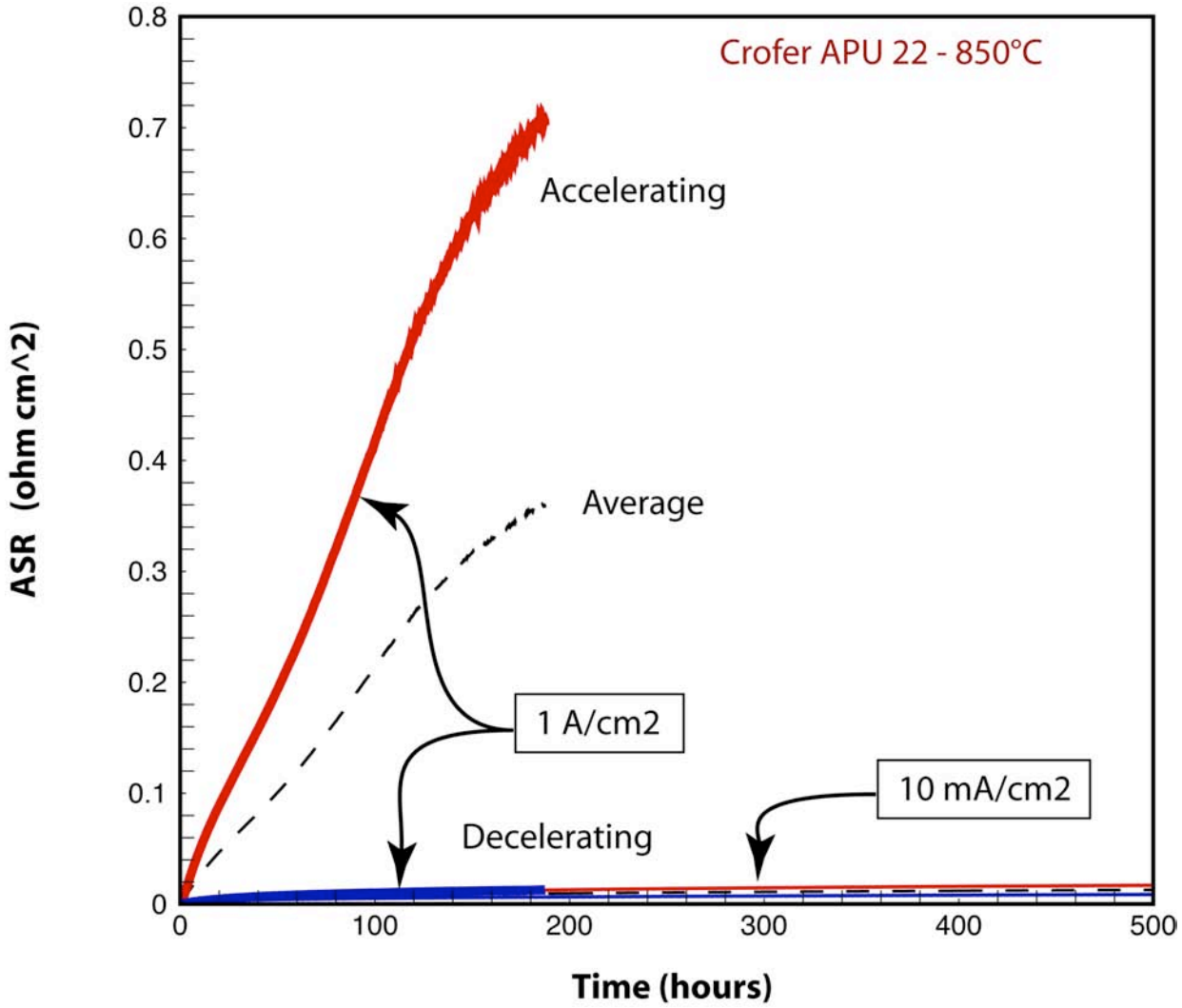

Oxidation Under the Constant Transverse Current:

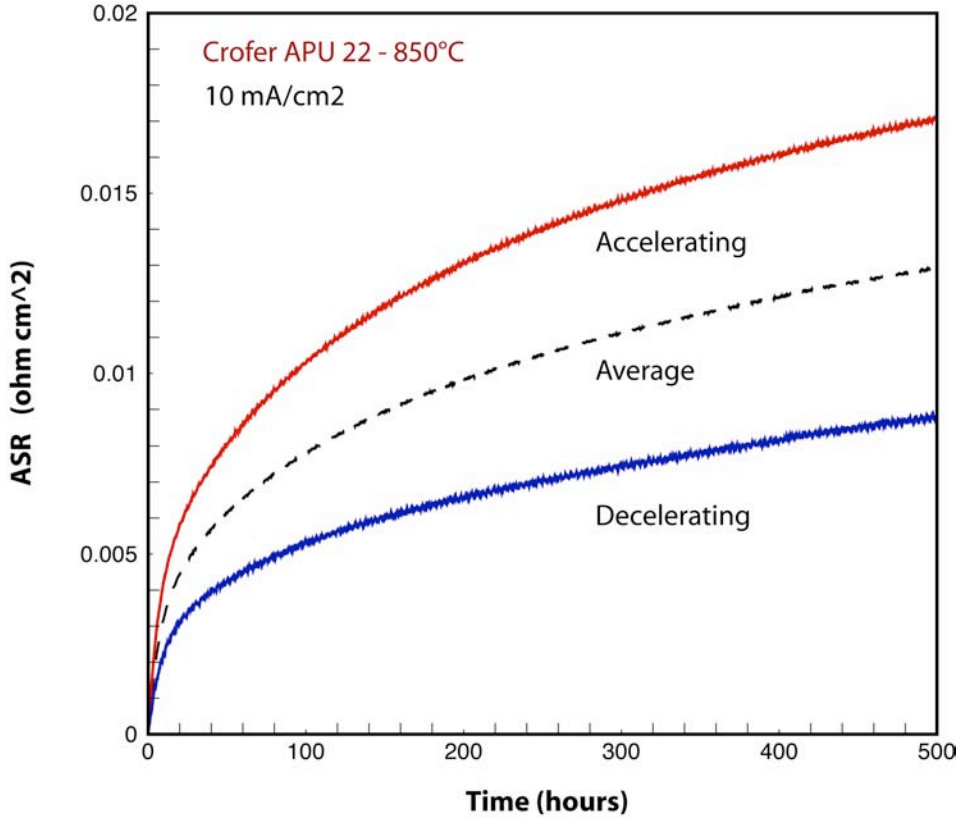

Thermo-Mechanical Damage Mechanisms

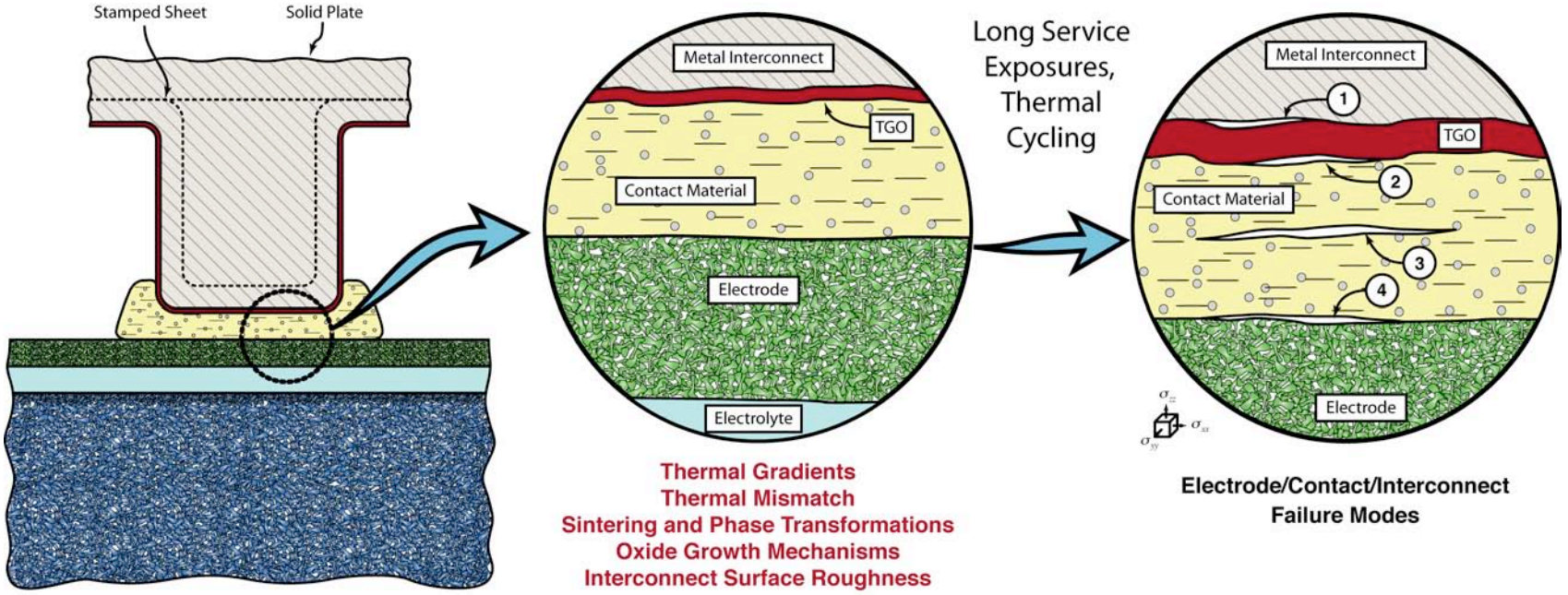

Need an Improved understanding of basic degradation mechanisms

Trilayer Mechanics and Stack Stability / Integrity

A. G. Evans (2002)

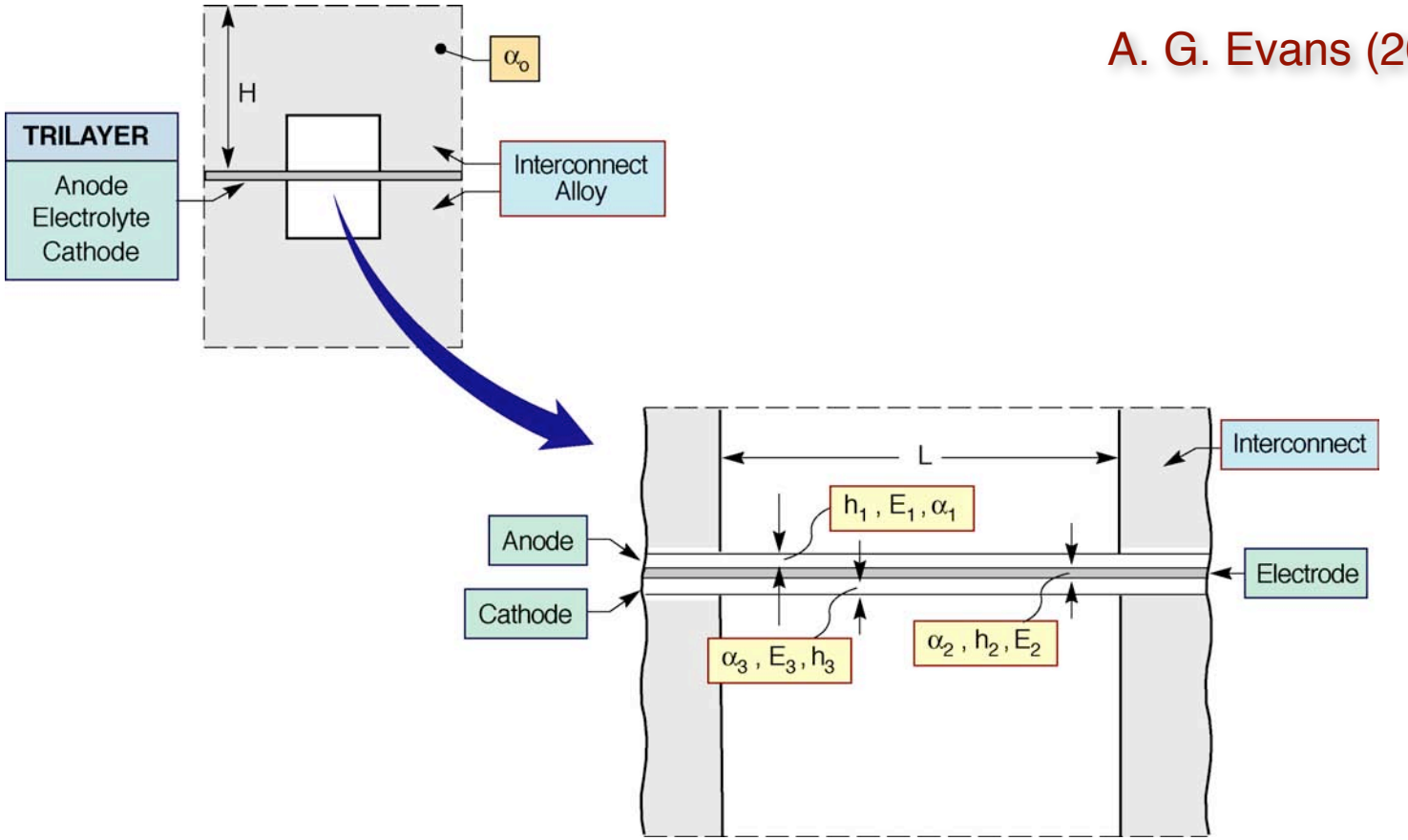

Assume the system is stress free at fabrication temperature
Assume CTE of each of the trilayer materials is lower than that of the interconnect
Primary problems arise at room temperature, when compressive stresses are maximum

Design Based on Mechanics

In Plane Compression

$$\sigma_2 = -\frac{\Delta\alpha_2 \Delta T E_2}{(1-\nu_2)}$$

Buckling Stress

$$\sigma_b = \left(\frac{\pi^2}{3}\right) E_2 \left(\frac{h_2}{L}\right)^2$$

Stress Due to Bending Moment

$$\sigma_{\max} = \frac{6M}{h_2^2}$$

Bending Moment

$$M = \frac{\Delta T}{2}\left\{E_1 \Delta\alpha_1 h_1 (h_1 + h_2) - E_3 \Delta\alpha_3 h_3 (h_3 + h_2)\right\}$$

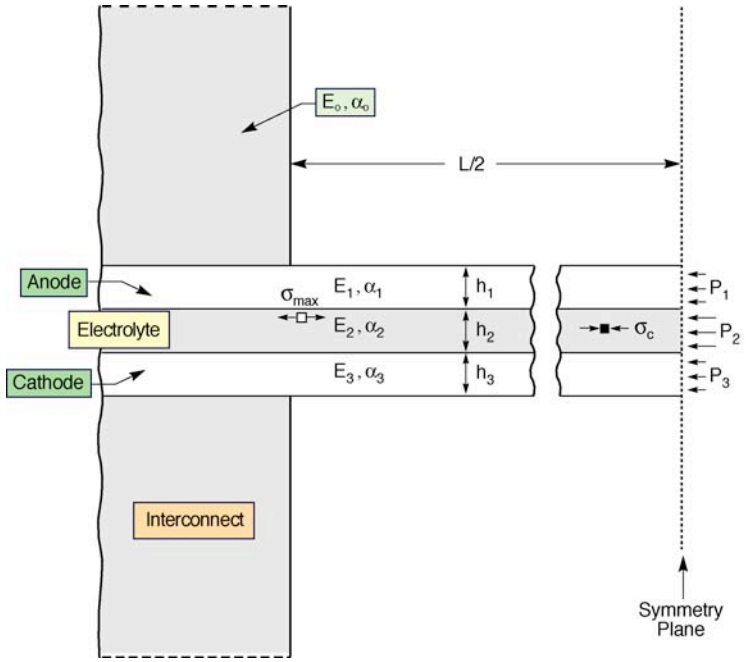

A. G. Evans (2002)

Criteria to Avoid Cracking Failure

Criteria based on Buckling

$$\frac{h_2}{L} \geq \left(\frac{1}{\pi}\right)\sqrt{\left(\frac{3\Delta\alpha_2\Delta T}{1-\nu_2}\right)}$$

Criteria based on Bending

$$h_2^2 + 3h_2\left\{\frac{E_3\Delta\alpha_3 h_3 - E_1\Delta\alpha_1 h_1}{E_2\Delta\alpha_2}\right\} - 3\left\{\frac{E_3\Delta\alpha_3 h_3^2 - E_1\Delta\alpha_1 h_1^2}{E_2\Delta\alpha_2}\right\} > 0$$

With Typical Values

$$h_2 / L \geq 3x10^{-2}$$

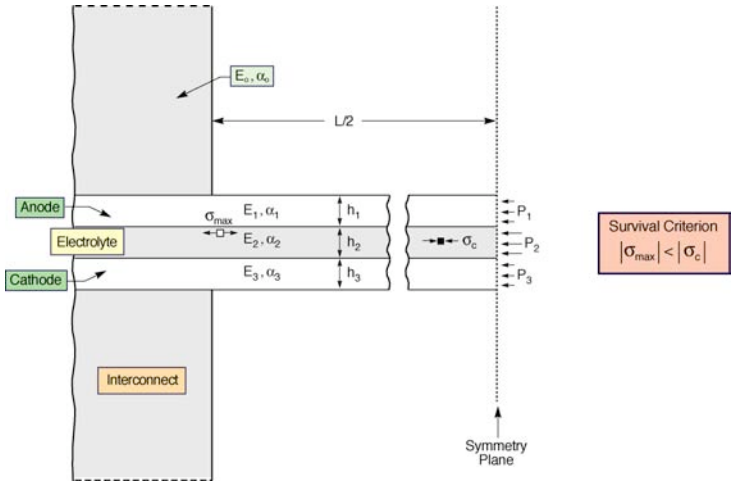

Among Other Parameters, Matching Thermal Expansion Coefficients Of Components is Key to Maximizing Durability

A. G. Evans (2002)

Tailoring Thermal Mismatch: Metal Interconnects and Ceramics

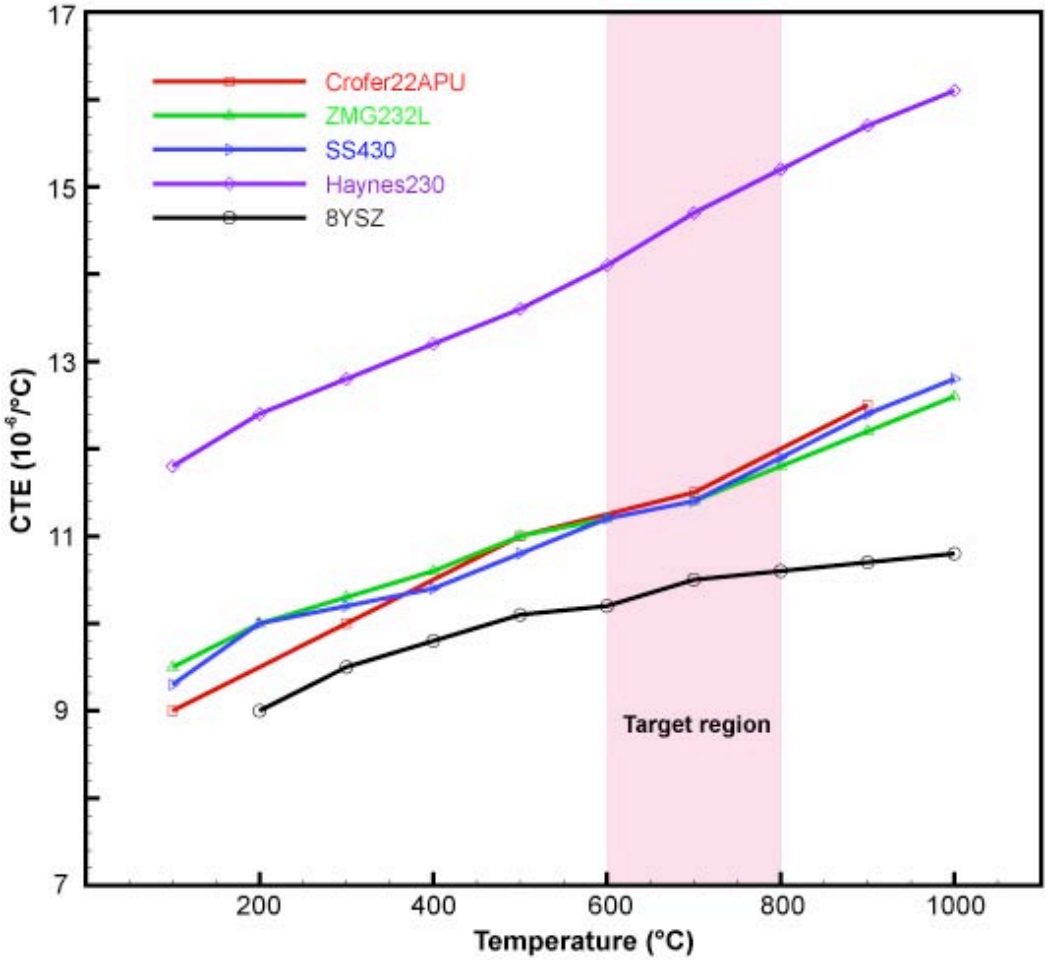

Ni alloys more difficult to work with Due to CTE mismatch

Degradation of Electrode/Electrolyte Interfaces Under Polarization

*M. Kuznecov, et al. (2003), Solid State Ionics, **157**, 371-378.*

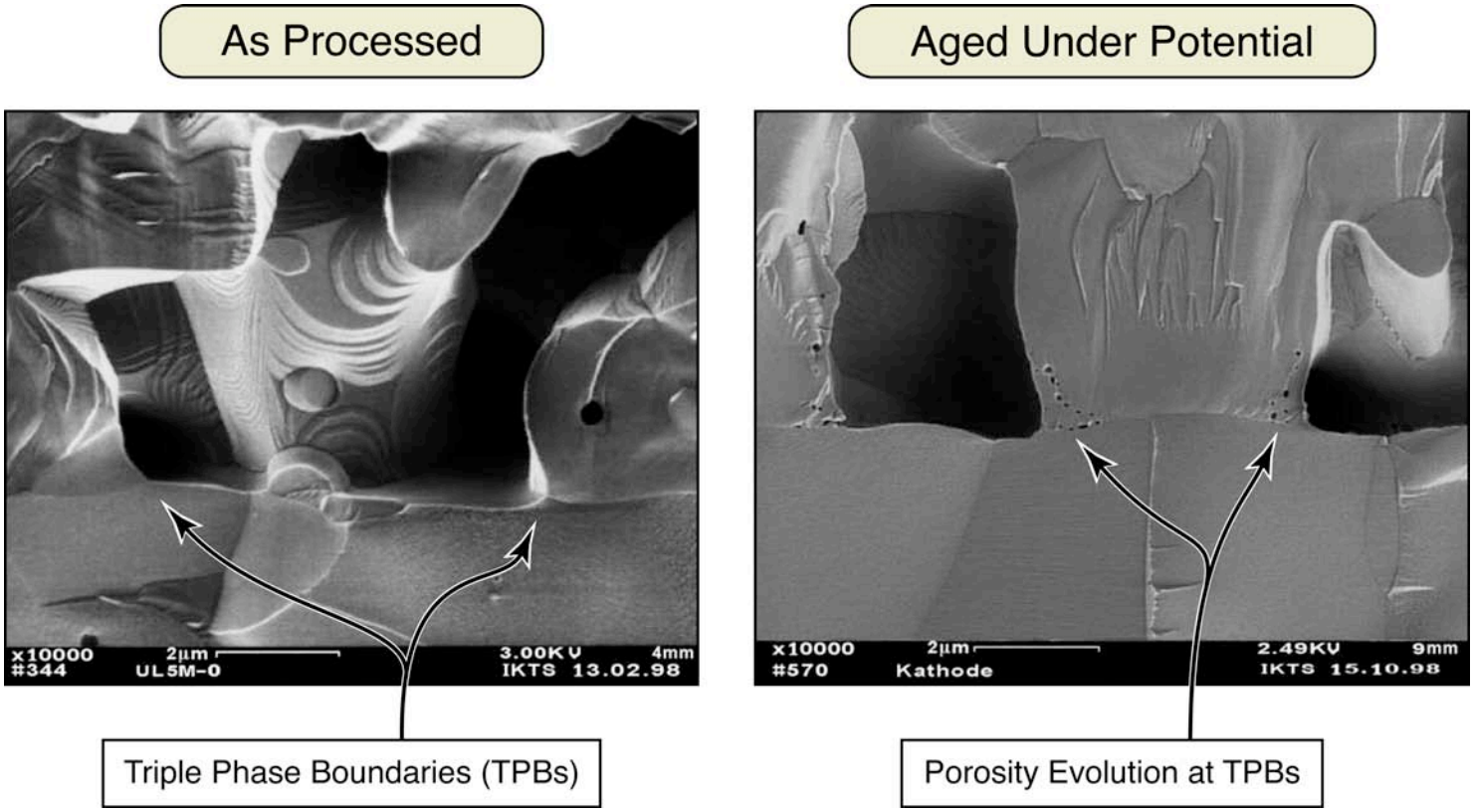

$$c_{V_{\ddot{o}}}^{\eta} = c_{V_{\ddot{o}}}^{0} \exp\left(\frac{z F \eta}{RT}\right)$$

Micropore formation is observed within LSM at $La_{0.8}Sr_{0.2}MnO_3/8YSZ$ interfaces held under high overpotential. The overpotential at the cathode/electrolyte interface generates additional oxygen vacancies and vacancy coalescence occurs.

Degradation of SSC/LSGMC Interfaces Under Polarization

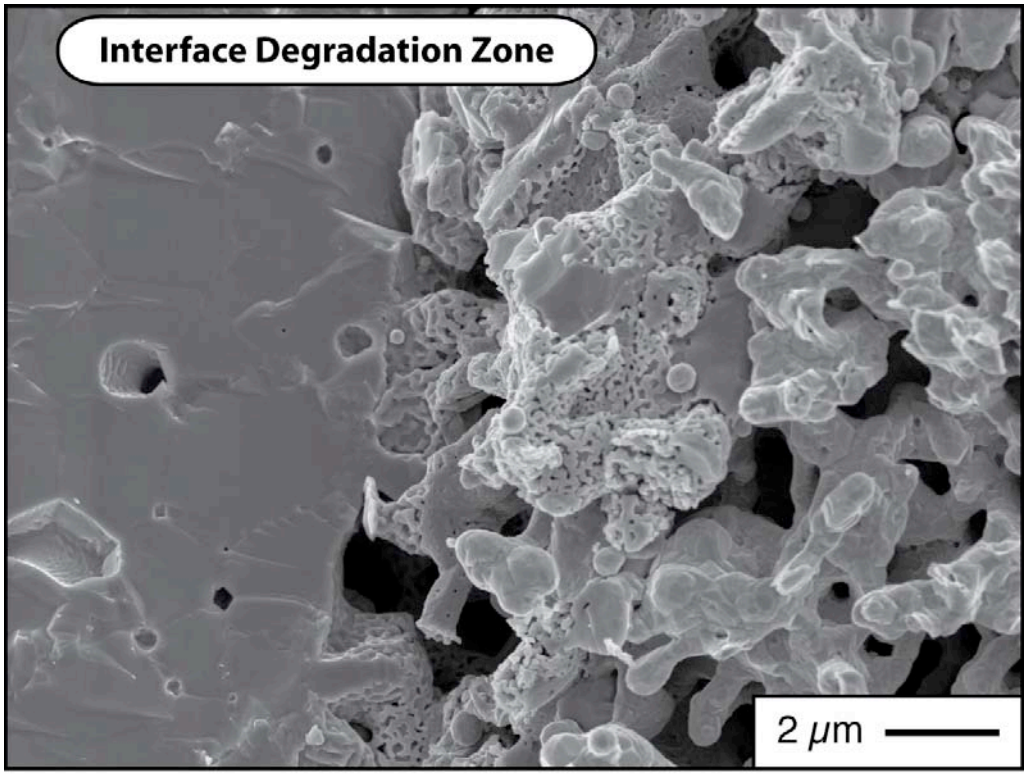

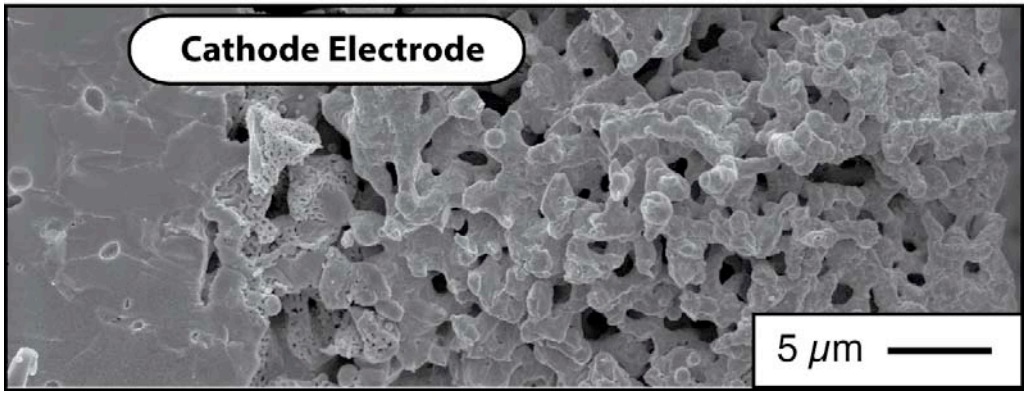

Similar effects are observed in testing SSC/LSGMC Interfaces held under high cathodic polarization.

$$c_{V_{\ddot{o}}}^{\eta} = c_{V_{\ddot{o}}}^{0} \exp\left(\frac{z F \eta}{RT}\right)$$

Interfacial Delamination and Loss of Conducting Pathway

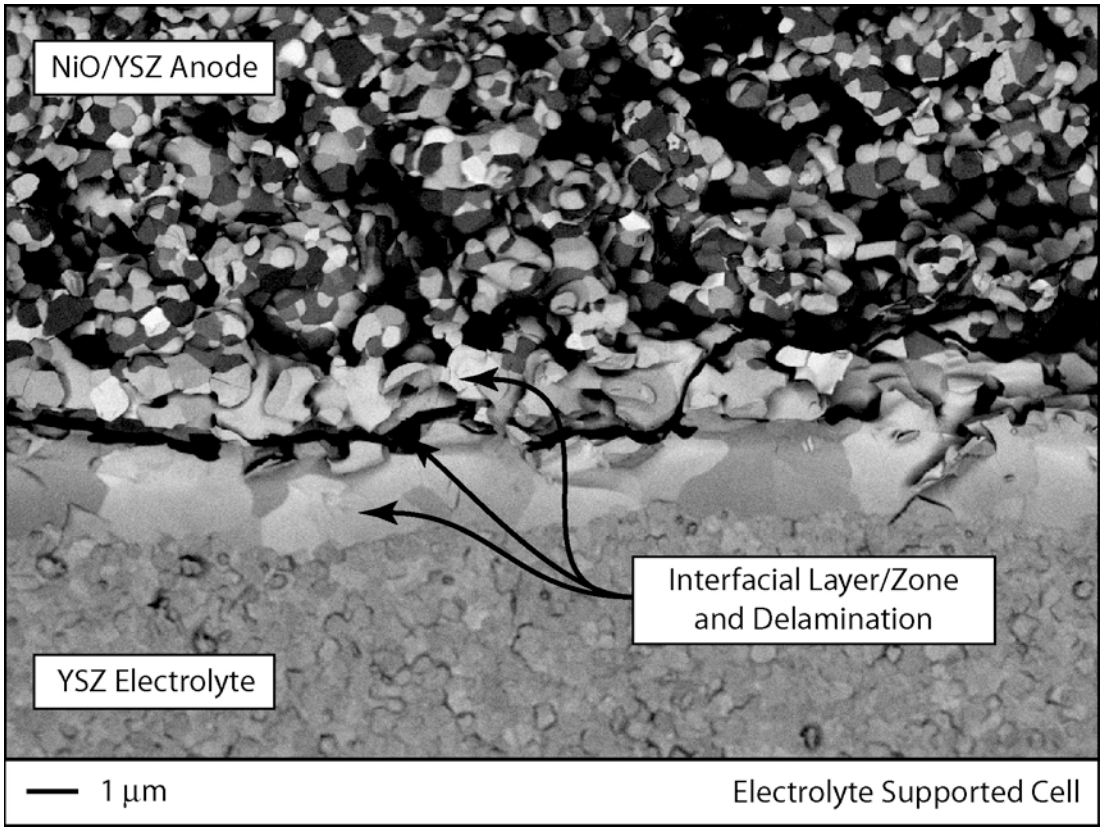

Unique Degradation Modes with Dual Environment Exposure – 304SS

Presented earlier - GH Meier

Air – Air Exposure

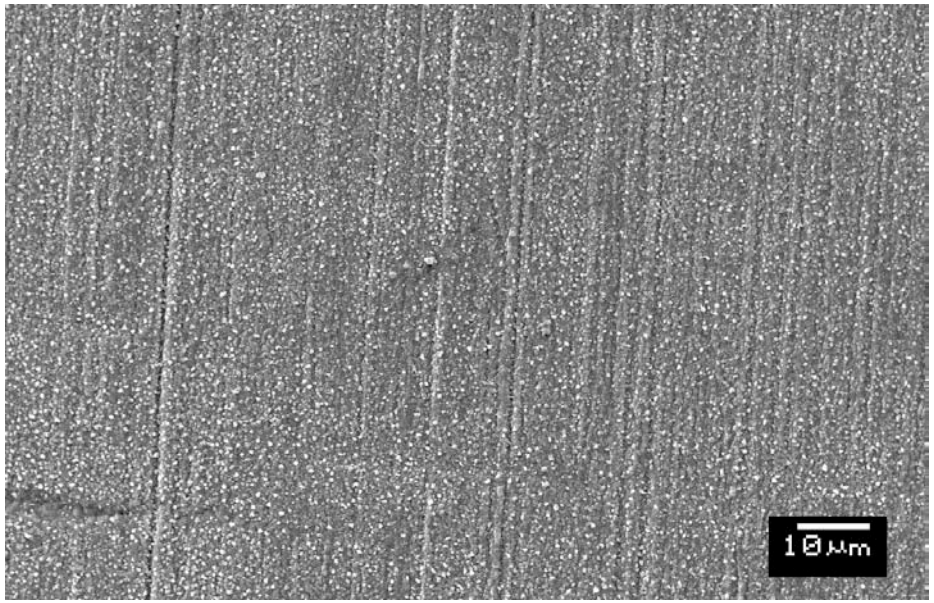

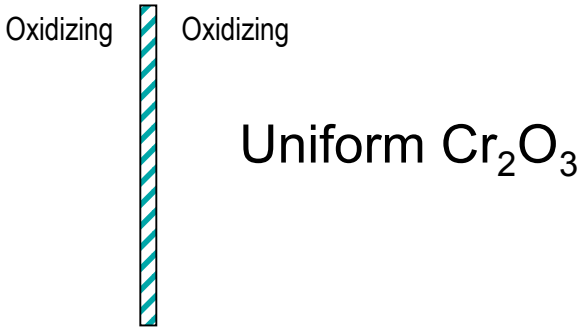

Uniform Cr_2O_3

Air Side – Dual Atmosphere Exposure

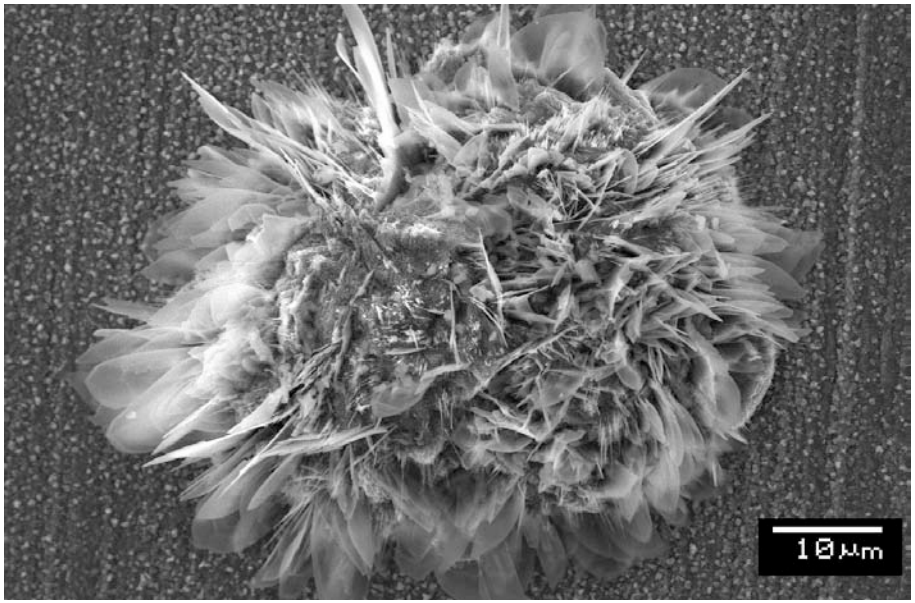

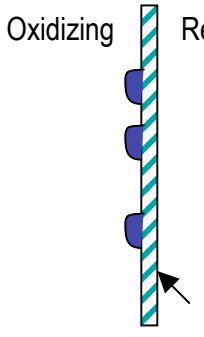

Fe-rich Oxide Nodules

Unique Degradation Modes with Dual Environment Exposures

Presented earlier - GH Meier

Silver Exposed Under Dual Atmosphere Conditions for 24 h at 800°C

Air Side

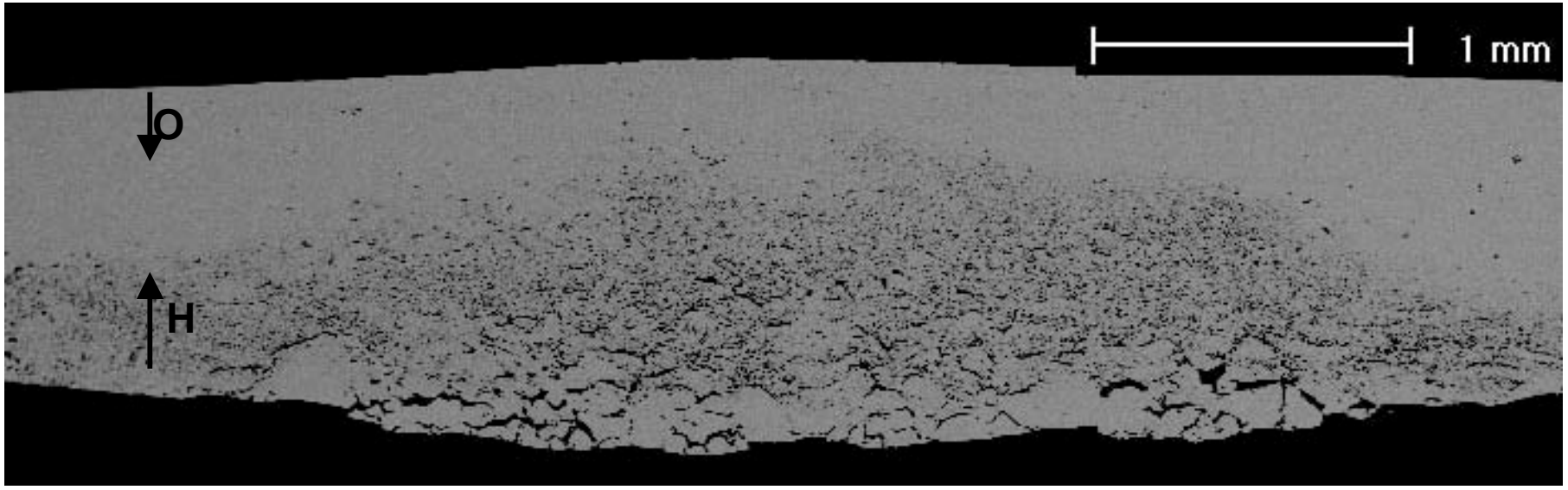

Ar- H_2 - H_2O Side

Variations of TEC and Conductivity with Doping Electronic Ceramics

Table 1
TECs and electrical conductivities of $LaCrO_3$-based solid solutions

Composition	Electrical conductivity (S cm^{-1})	Composition	Average TEC $\times 10^{-6}$/ °C
$LaCrO_3$	0.34 at 700 °C, 1 at 1000 °C	$LaCrO_3$	9.5
$LaCr_{0.9}Mg_{0.1}O_3$	3 at 1000 °C	$LaCr_{0.9}Ni_{0.1}O_3$	10.1
$La_{0.9}Sr_{0.1}CrO_3$	14 at 1000 °C	$LaCr_{0.8}Ni_{0.2}O_3$	11.2
$La_{0.95}Ca_{0.05}CrO_3$	2.3 at 700 °C	$LaCr_{0.7}Ni_{0.3}O_3$	11.8
		$LaCr_{0.9}Mg_{0.1}O_3$	9.5
$La_{0.95}Ca_{0.05}Cr_{0.5}Co_{0.5}O_3$	63 at 700 °C	$La_{0.9}Sr_{0.1}CrO_3$	10.7
$La_{0.8}Ca_{0.2}CrO_3$	7.1 at 700 °C, 35 at 1000 °C	$La_{0.65}Ca_{0.35}CrO_3$	10.8
$La_{0.8}Ca_{0.2}Cr_{0.8}Fe_{0.2}O_3$	9.2 at 700 °C	$La_{0.8}Ca_{0.2}Cr_{0.9}Co_{0.1}O_3$	11.1
$La_{0.8}Ca_{0.2}Cr_{0.8}Ni_{0.2}O_3$	18 at 700 °C	$LaCr_{0.9}Co_{0.1}O_3$	13.1
$La_{0.7}Ca_{0.3}CrO_3$	18 at 700 °C	$LaCr_{0.8}Co_{0.2}O_3$	14.6
$La_{0.7}Ca_{0.3}Cr_{0.8}Co_{0.2}O_3$	45 at 700 °C	$LaCr_{0.6}Co_{0.4}O_3$	18.7
$La_{0.7}Ca_{0.3}Cr_{0.5}Co_{0.5}O_3$	85 at 700 °C	$LaCr_{0.2}Co_{0.8}O_3$	20.9
$La_{0.7}Sr_{0.3}CrO_3$	15 at 700 °C	$La_{0.7}Sr_{0.3}Cr_{0.2}Co_{0.8}O_3$	19
$La_{0.7}Sr_{0.3}Cr_{0.5}Co_{0.5}O_3$	58 at 700 °C	$La_{0.7}Sr_{0.3}Cr_{0.5}Co_{0.5}O_3$	19
$LaCr_{0.6}Ni_{0.4}O_3$	26 at 700 °C	$La_{0.7}Sr_{0.3}Cr_{0.8}Co_{0.2}O_3$	14.5
$La_{0.85}Sr_{0.15}CrO_3$	21.8 at 1000 °C	$La_{0.87}Sr_{0.1}Cr_{0.95}Cu_{0.05}O_3$	9.81
$La_{0.87}Sr_{0.1}Cr_{0.95}Cu_{0.05}O_3$	23.9 at 1000 °C	$La_{0.85}Sr_{0.15}Cr_{0.98}Cu_{0.02}O_3$	9.91
$La_{0.85}Sr_{0.15}Cr_{0.98}Cu_{0.02}$	32.5 at 1000 °C	$La_{0.9}Sr_{0.1}Cr_{0.93}Mg_{0.05}Cu_{0.02}O_3$	9.61
$La0_{.9}Sr_{0.1}Cr_{0.95}V_{0.05}O_3$	9.7 at 1000 °C	$La_{0.9}Sr_{0.1}Cr_{0.95}V_{0.05}O_3$	9.87
$La_{0.85}Sr_{0.15}Cr_{0.95}V_{0.05}O_3$	19.9 at 1000 °C	$La_{0.9}Sr_{0.1}Cr_{0.92}V_{0.05}Co_{0.03}O_3$	10.4
$La_{0.9}Sr_{0.1}Cr_{0.9}Mg_{0.05}V_{0.05}O_3$	15.2 at 1000 °C	$La_{0.85}Sr_{0.15}Cr_{0.95}V_{0.05}O_3$	10
$La_{0.95}Sr_{0.05}Cr_{0.85}Mg_{0.1}V_{0.05}O_3$	12.9 at 1000 °C	$La_{0.9}Sr_{0.1}Cr_{0.9}Mg_{0.05}V_{0.05}O_3$	9.64
$La_{0.87}Sr_{0.1}Cr_{0.935}Cu_{0.05}Co_{0.015}O_3$	25.6 at 1000 °C	$La_{0.95}Sr_{0.05}Cr_{0.85}Mg_{0.1}V_{0.05}O_3$	9.22
$La_{0.85}Sr_{0.15}Cr_{0.935}V_{0.05}Co_{0.015}O_3$	22.9 at 1000 °C	$La_{0.87}Sr_{0.1}Cr_{0.935}Cu_{0.05}Co_{0.015}O_3$	10.4
$La_{0.9}Sr_{0.1}Cr_{0.92}V_{0.05}Co_{0.03}O_3$	12.8 at 1000 °C	$La_{0.85}Sr_{0.15}Cr_{0.935}V_{0.05}Co_{0.015}O_3$	10.5

What About Morphological Evolution at Metal/Oxide Interfaces?

Analogies to TBC systems….

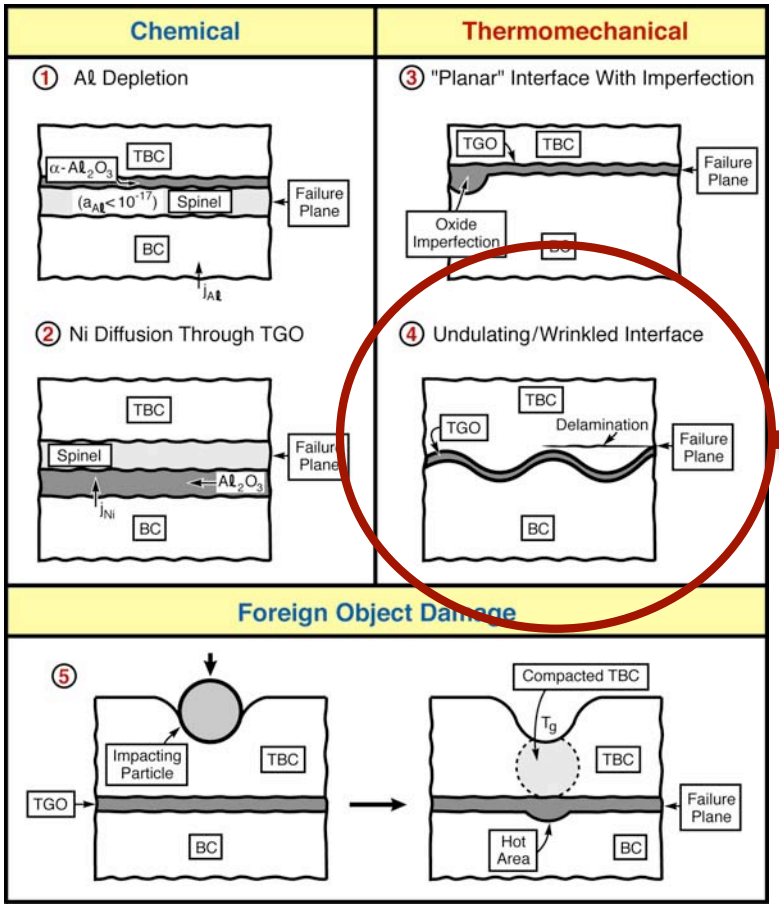

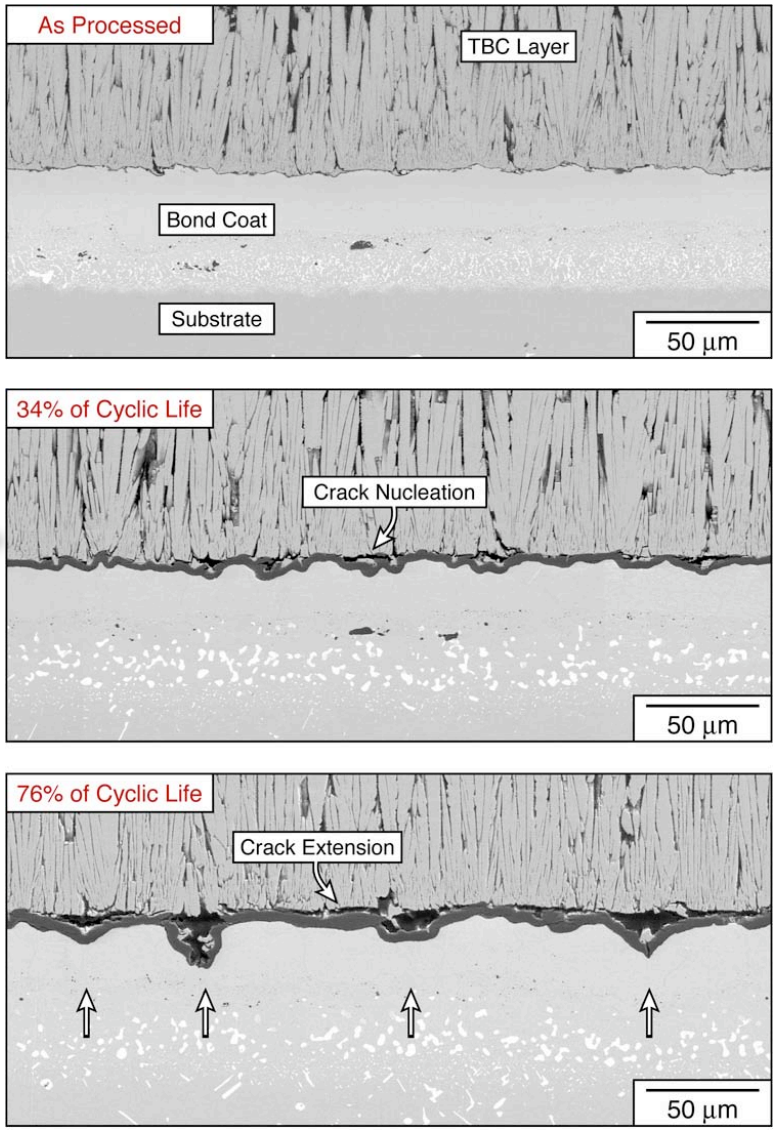

D.R. Mumm, A. G. Evans and I.T. Spitsberg (2001),
Acta Materialia, **49**, 2329-2340

Initial Imperfections and Crack Nucleation Sites

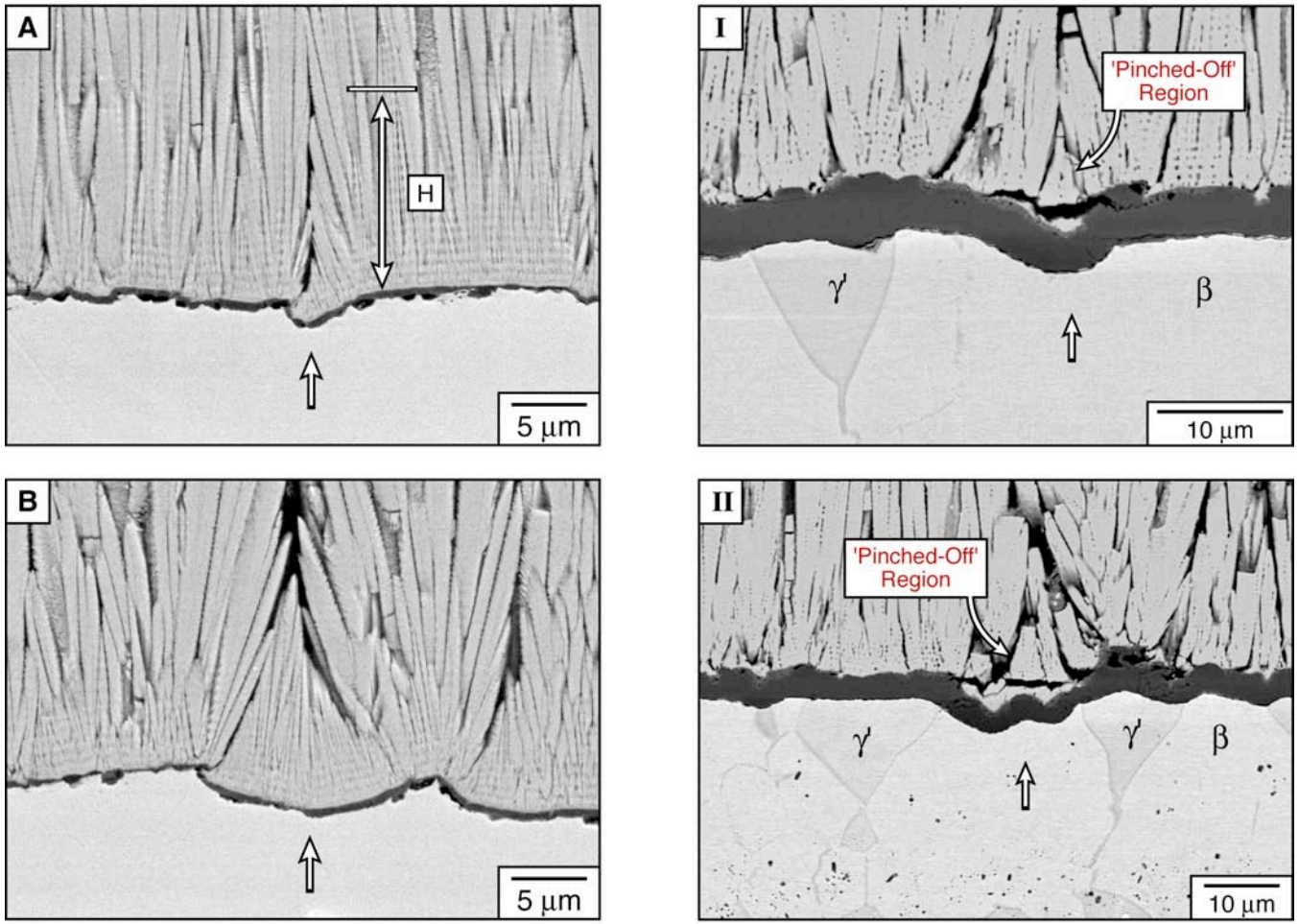

Cracking at interfaces between metals and porous ceramics initiates at pre-existing morphological features.

D.R. Mumm, A. G. Evans and I.T. Spitsberg (2001),
Acta Materialia, **49**, 2329-2340

Effects of Amplitude of Pre-Existing Defects

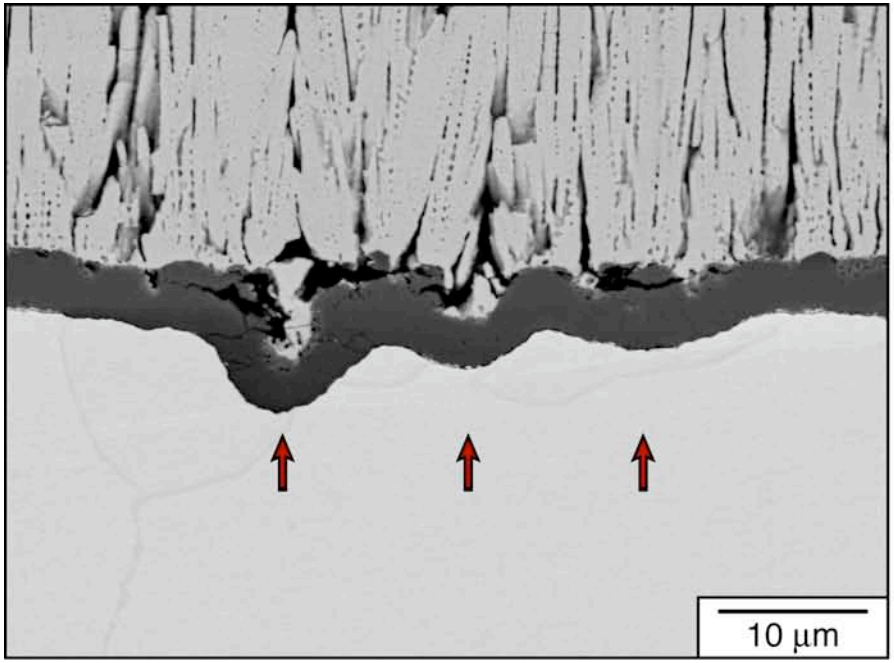

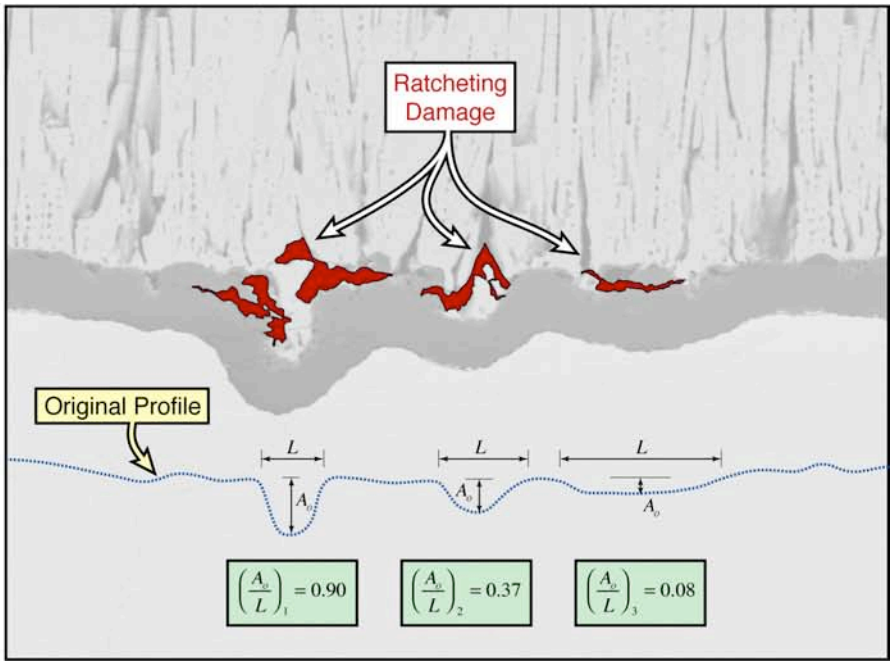

Damage that develops with oxidation and thermal cycling scales with the amplitude and aspect ratio of the pre-existing morphological defects.

D.R. Mumm, A. G. Evans and I.T. Spitsberg (2001),
Acta Materialia, **49**, 2329-2340

SOFC-Relevant Behavior – Morphological Effects

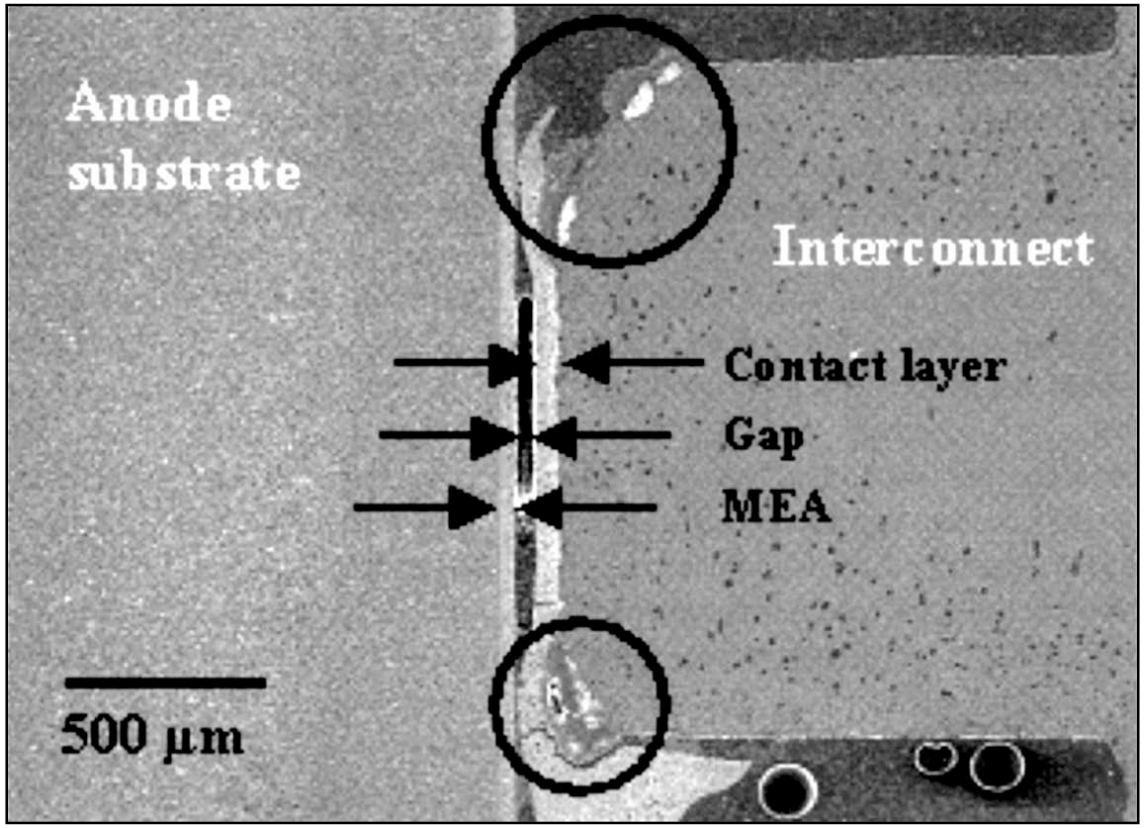

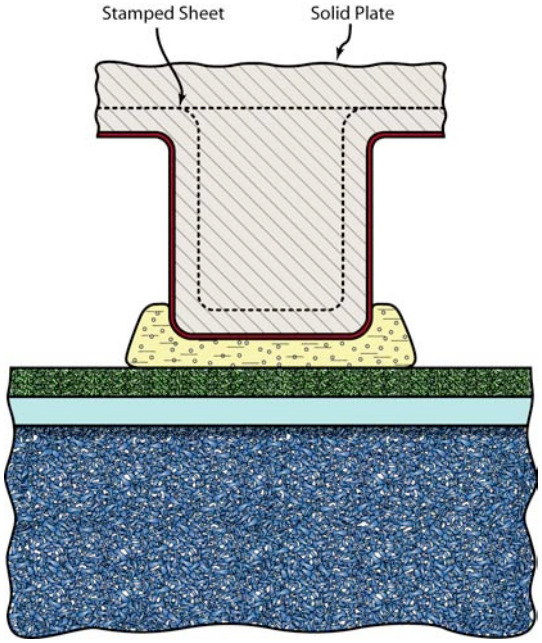

Interconnect alloy X10CrAl18, subjected to 3000 hr of 800°C operation at a constant power density of 0.22 W/cm^2 showed the growth of nodular corrosion products that led to partial delamination of the cathode contact layer interface.

S.P.S. Badwal, R. Bolden and K. Föger (1998),
Proceedings of the 3rd European SOFC Forum,
ed. P. Stevens , Oberrohrdorf, Switzerland, p. 105.

Metal Interconnect Oxidation and Spalling

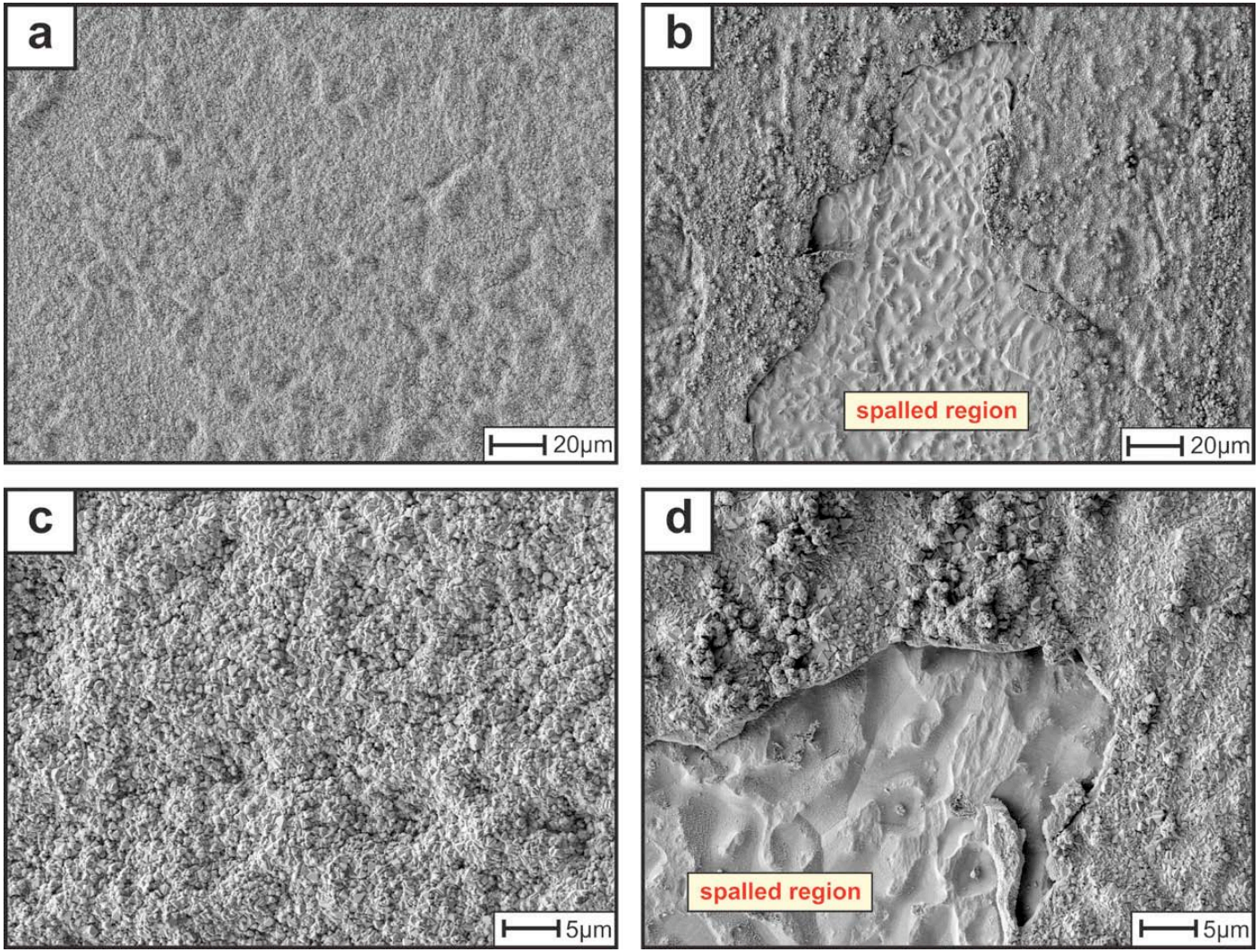

Thin Foil Morphological Effect – Another Example From G.H. Meier

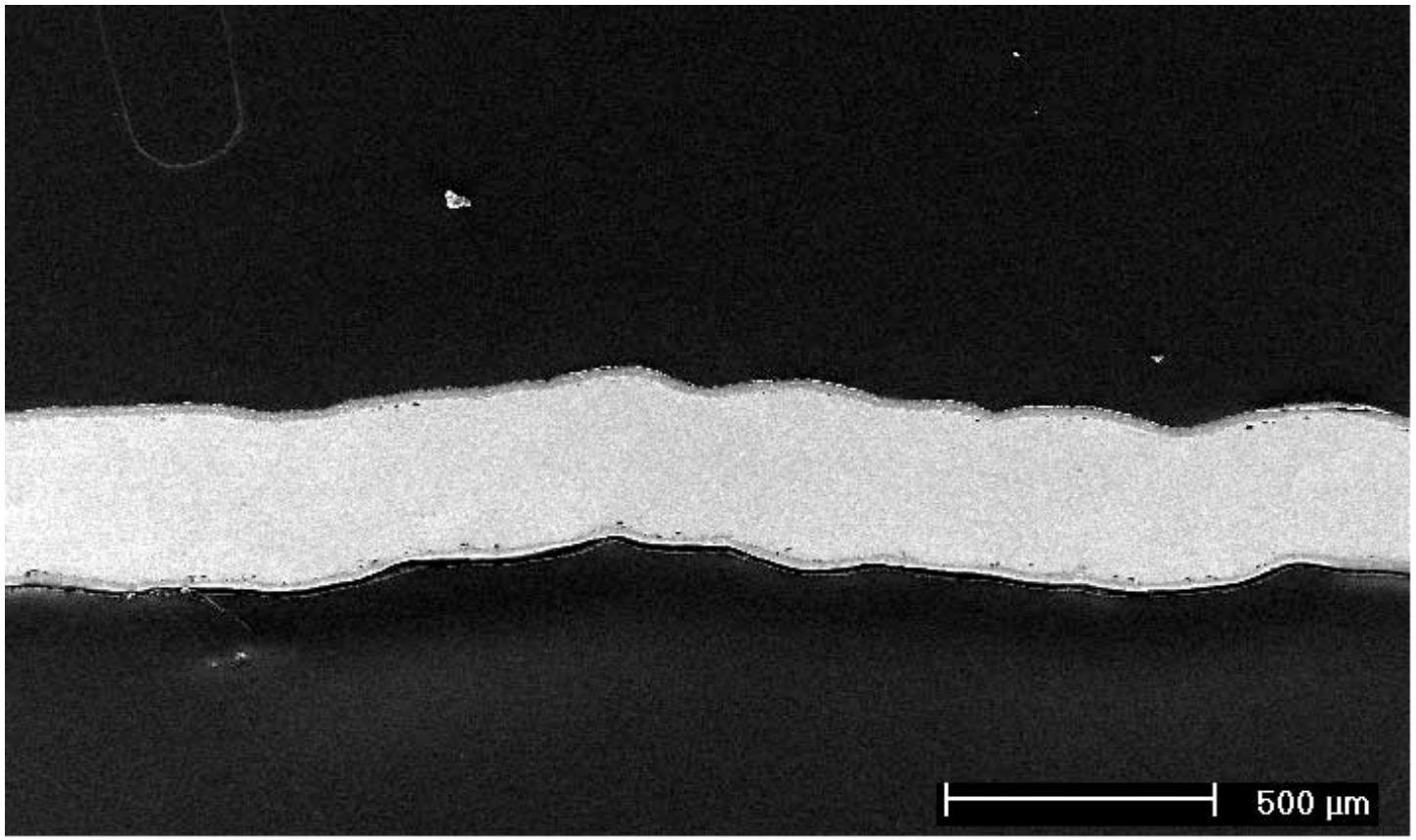

Deformation of 0.5 mm thick Crofer APU 22 Alloy (a leading Interconnect candidate) after exposure to cyclic oxidation conditions.

Challenges for Ferritic Steels – Studies at PNNL

- Oxidation: increasing scale thickness during lifetime may lead to excessively high ASR and cracking/spallation, both of which will lead to high stack power degradation rate
- Dual atmosphere effects on oxidation
- Chromia scale volatility: leading to degradation in cell performance.
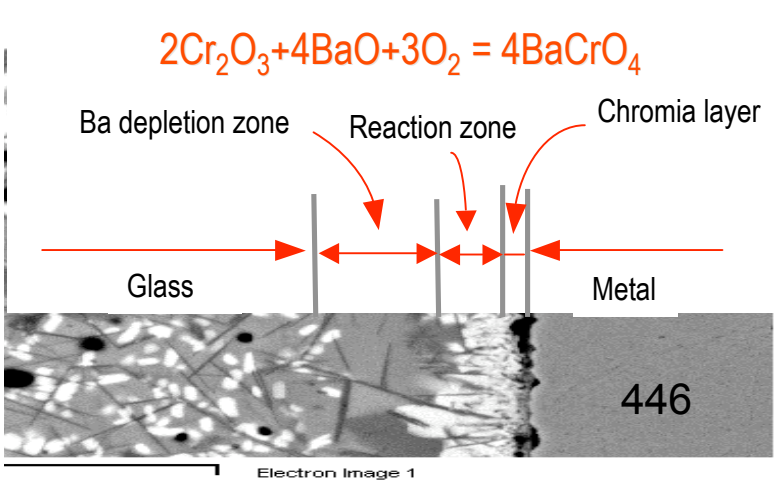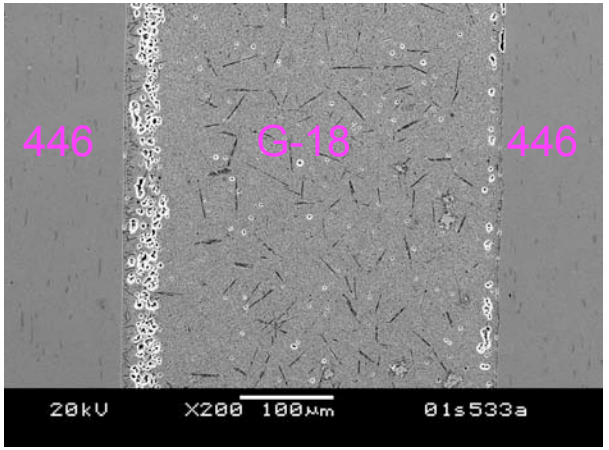
- Compatibility with adjacent components, e.g. a barium aluminosilicate base sealing glass: